GLOBAL DISTRIBUTIONS AND NATURAL SOURCES OF BROMINATED VERY SHORT-LIVED SUBSTANCES

A Dissertation

by

YINA LIU

Submitted to the Office of Graduate Studies of
Texas A&M University
in partial fulfillment of the requirements for the degree of

DOCTOR OF PHILOSOPHY

Chair of Committee,	Shari A. Yvon-Lewis
Co-Chair of Committee,	Daniel C.O. Thornton
Committee Members,	Thomas S. Bianchi
	Lisa Campbell
	John D. Kessler
	Gunnar W. Schade
Head of Department,	Piers Chapman

August 2013

Major Subject: Oceanography

ABSTRACT

Brominated very short-lived substances (BrVSLS) are atmospherically important trace gases that play an important role in stratospheric ozone destruction. Major BrVSLS including bromoform ($CHBr_3$), dibromomethane (CH_2Br_2), chlorodibromomethane ($CHClBr_2$), and bromodichloromethane ($CHBrCl_2$) are thought to be predominately formed naturally via vanadium bromoperoxidase (V-BrPO) mediated halogenation of organic matter (OM). The objective of this research was to couple field observations and laboratory experiments to understand global distributions, saturation anomalies, fluxes, and identify natural sources of BrVSLS. All the trace gases were measured with gas chromatography mass spectrometry (GC-MS).

Field observations were conducted in the Pacific and Atlantic Oceans. Results from field observations showed that BrVSLS tend to be elevated in biologically active waters, such as coastal waters, the productive surface open ocean, and at chlorophyll maximum depths. The production of natural BrVSLS is likely controlled by complex biogeochemical factors in the ecosystems. CH_2Br_2 was thought to be derived from the same source(s) as $CHBr_3$, but results presented in this dissertation suggest they may in fact be derived from disparate sources.

Screening for important BrVSLS producers was attempted in the laboratory. Only 2 out of 9 phytoplankton species screened show observable BrVSLS production. CH_2Br_2 production was only observed in 1 species screened. Chloroperoxidase-like

activity in diatom was observed for the first time, which provided evidence for biological production of chloroform ($CHCl_3$).

The role of dissolved organic matter (DOM) in controlling BrVSLS production was investigated in the laboratory. Production of BrVSLS varied significantly with different model DOM compounds upon V-BrPO mediated halogenation. Certain DOM enhanced BrVSLS production, but the majority of the model DOM compounds tested in this study either interfered with or had no observable effect on BrVSLS production. Further evidences showed that V-BrPO mediated halogenation can alter DOM chemical characteristics. Alteration of colored dissolved organic matter (CDOM) in terms of "bio-bleaching" was observed in model lignin phenol compounds and CDOM collected from two cyanobacterial cultures.

Results from this study suggest that the presence of V-BrPO producing phytoplankton is essential for enhanced BrVSLS production, as V-BrPO induced brominated reactive species, such as hypobromous acid ($HOBr_{enz}$), is required. However, BrVSLS production rates are largely controlled by other biogeochemical factors in seawater, such as DOM composition. Results from this study also suggest that V-BrPO activity not only plays an essential role in BrVSLS production, but it also plays a significant role in the transformation of DOM and may be a significant component of the marine carbon cycle.

ACKNOWLEDGEMENTS

I am especially grateful for having Drs. Shari Yvon-Lewis and Daniel Thornton as my advisers. Without them, this research would not be possible. I especially thank Shari for her support and allowing me to learn different skills from other labs. Her support is essential for such an interdisciplinary research. I thank Dan, who not only being a great adviser, but his insight also broadens my horizon of thinking. I would like to thank my committee members, Drs. Thomas Bianchi, Lisa Campbell, John Kessler, and Gunnar Schade, for their guidance and support throughout the course of this research.

I thank Dr. Steven Manley at California State University, Long Beach, who generously donated vanadium bromoperoxidases that were used in part of this study. I also thank his insight; which helped developed some of the hypotheses in my research. I sincerely thank Drs. François Primeau, Susan Trumbore, and Ellen Druffel at University of California, Irvine, for their guidance during my undergraduate researches. They not only provided me with opportunities to expose to research as an undergraduate student, the experiences gained when working with them also motivated me to pursued scientific research as my lifetime career.

I thank Drs. James Butler, Lei Hu, Joseph Salisbury, Richard Smith, and Julia O'Hern, for their contributions to my publications (Chapters II, II, and IV). Thanks also go to the department faculty and staff for making my time at Texas A&M University a great experience.

I thank my friends in College Station, Fenix, Jan, Ruifang, Brad, Eric, and Mike. I especially thank Fenix, who is being a great labmate and colleague. I thank my friends back in California, UK, and China, Yu, Shanlin, Mo, Hai-lun, Ka-Ki, Ka-Yan, Yuan-yuan, Wen-jun, and Yan-na. Their friendships and support mean a lot to me.

I thank my parents for their love and unconditional support for my whole life. Without their love, nothing is possible. I thank my other family members, especially my aunt and uncle, who took care of me in California. I would like to thank my cousins for their company back in California, especially Wei-qi.

This research is partially supported by National Oceanic and Atmospheric Administration (NOAA) grant NA06OAR4310049 and National Science Foundation (NSF) grant OCE 0927874 to S.A. Y-L.

NOMENCLATURE

BrVSLS	Brominated very short-lived substances
Br_y	Inorganic bromine
CDOM	Colored dissolved organic matter
$CHBr_3$	Bromoform
CH_2Br_2	Dibromomethane
$CHClBr_2$	Chlorodibromomethane
$CHBrCl_2$	Bromodichloromethane
CO	Carbon monoxide
CO_2	Carbon dioxide
COS	Carbonyl sulfide
DOC	Dissolved organic carbon
DOM	Dissolved organic matter
H_2O_2	Hydrogen peroxide
HAA	Haloacetic acid
ODSs	Ozone depleting substances
OM	Organic matter
ppt	Parts per trillion
patm	Pico atmosphere
PGI	Product gas injection
SGI	Source gas injection
V-BrPO	Vanadium bromoperoxidase

TABLE OF CONTENTS

Page

LIST OF FIGURES

Page

LIST OF TABLES

Page

CHAPTER I

INTRODUCTION

Bromoform ($CHBr_3$), dibromomethane (CH_2Br_2), chlorodibromomethane ($CHClBr_2$), and bromodichloromethane ($CHBrCl_2$) comprise the natural brominated very short-lived substances (BrVSLS). $CHBr_3$ and CH_2Br_2 account for ~80% of the very short-lived organic bromine in the marine boundary layer [*Law and Sturges*, 2007]. BrVSLS degrade into inorganic bromine (Br_y), which can catalytically destroy ozone, via photolysis and reaction with hydroxyl radicals (OH) in the atmosphere. These compounds are receiving increased interest, as the BrVSLS can supply significant amounts of Br_y to the stratosphere, in addition to the relatively longer-lived ozone depleting substances (ODSs), such as methyl bromide (CH_3Br) and halons. In addition, bromine is ~50 to 100% more effective in destroying ozone than chlorine, on an atom-by-atom basis [*Garcia and Solomon*, 1994; *Solomon et al.*, 1995].

Bromine atoms can enter the stratosphere via either source gas injection (SGI) or product gas injection (PGI). SGI is defined as the trace gases entering the stratosphere in their original forms as they were emitted. In regions experiencing strong atmospheric convection, such as the intertropical convergence zone (ITCZ), short-lived gases can be rapidly delivered to the stratosphere as source gases [*Montzka and Reimann*, 2011]. PGI on the other hand, is defined as delivering degradation products of trace gases to the stratosphere. Overall, relative contributions from SGI and PGI are mainly determined by the atmospheric lifetimes of the various trace gases and their product gases, and atmospheric transport [*Montzka and Reimann*, 2011].

Although BrVSLS tend to be degraded significantly in the troposphere, their degradation products are even less stable in the atmosphere allowing for substantial further degradation (*e.g.* chemical and physical scavenging) [*Hossaini et al.*, 2012b]. Hence, product gases of $CHBr_3$ and CH_2Br_2 may be removed rapidly from the atmosphere before they can reach the stratosphere via PGI. Therefore, SGI is thought to be the major delivery mechanism for Br $CHBr_3$ and CH_2Br_2 to the stratosphere [*Hossaini et al.*, 2012b].

These natural BrVSLS can contribute ~1 to 8 parts per trillion (ppt) of Br_y to the stratosphere, which is equivalent to ~4 to 36% of total stratospheric bromine, which included organic and inorganic bromine in the stratosphere [*Montzka and Reimann*, 2011]. This portion of Br_y is also known as VSLS supplied Br_y (Br_y^{VSLS}), where $CHBr_3$ and CH_2Br_2 together account for 76% of Br_y^{VSLS} [*Hossaini et al.*, 2012a]. As production of the anthropogenic ozone depleting substances (ODSs) has been phased out under the Montreal Protocol and their concentrations are continuing to decrease in the atmosphere, the naturally produced ODSs are becoming more important. As anthropogenic ODS concentrations decline, the relative contribution of BrVSLS to stratospheric bromine will increase. Ultimately, natural BrVSLS will become the key in controlling stratospheric ozone chemistry.

In a future climate scenario, the predicted stronger atmospheric convection is likely to enhance transport of $CHBr_3$ to the stratosphere as source gas injection (SGI) [*Hossaini et al.*, 2012b]. SGI for CH_2Br_2, $CHClBr_2$, and $CHBrCl_2$ is also likely to increase due to possible reduction in OH concentration, resulting from the predicted increase in atmospheric methane (CH_4) concentration [*Hossaini et al.*, 2012b].

Therefore, knowing where these natural BrVSLS are being produced and their emission strengths are essential for understanding ozone chemistry now and in the future. A fundamental question exists: how (why) are natural BrVSLS produced?

While enzyme-mediated halogenation by vanadium bromoperoxidase (V-BrPO) is a widely accepted mechanism for BrVSLS production, it has been largely neglected by the trace gas community. Little information is available on the factors controlling the production of BrVSLS. BrVSLS production is frequently related to photosynthetic biomass, such as macroalgae and phytoplankton [*Carpenter and Liss*, 2000; *Goodwin et al.*, 1997; *Manley et al.*, 1992; *Moore et al.*, 1996; *Sturges et al.*, 1992; *Sturges et al.*, 1993]. To produce $CHBr_3$, $CHClBr_2$, $CHBrCl_2$, and supposedly CH_2Br_2, three major components are required: (1) photosynthetic biomass that is capable of producing V-BrPO; (2) hydrogen peroxide (H_2O_2) to initiate the formation of hypobromous acid (HOBr); (3) suitable organic matter (OM) to be halogenated by HOBr. The V-BrPO induced HOBr ($HOBr_{enz}$) in the presence of H_2O_2 can halogenate a wide range of OM and form halogenated organic molecules. Finally, some of the unstable halogenated organic molecules can release BrVSLS via carbon-carbon bond cleavage in an alkaline environment, such as in seawater (pH ~8.1) [*Butler and Carter-Franklin*, 2004; *Theiler et al.*, 1978].

For a decade, researchers have been focusing on "who" are the BrVSLS producers [*Abrahamsson et al*., 2004; *Carpenter and Liss*, 2000; *Colomb et al.*, 2008; *Liu et al.,* 2013; *Liu et al.*, Submitted; *Mattson et al.*, 2012; *Quack et al.*, 2007a]. Only a few studies investigated the impact of H2O2 concentration and dissolved organic matter (DOM) on BrVSLS production [*Abrahamsson et al.*, 2003; *Lin and Manley*, 012; *Manley and Barbero*, 2001]. This dissertation focuses on two major aspects of BrVSLS biogeochemistry in the ocean: (1) describing how the BrVSLS are distributed in the global ocean, at the surface and in the water column (Chapters II, III, and IV); (2) determining what drives the observed distribution and variability (Chapters V and VI). Finally, I also present the significant implications of V-BrPO halogenation of DOM for the marine carbon cycle (Chapter VII). This research not only provides insight to marine source of BrVSLS, but also elucidates brominated organic matter biogeochemistry in seawater (Figure 1-1).

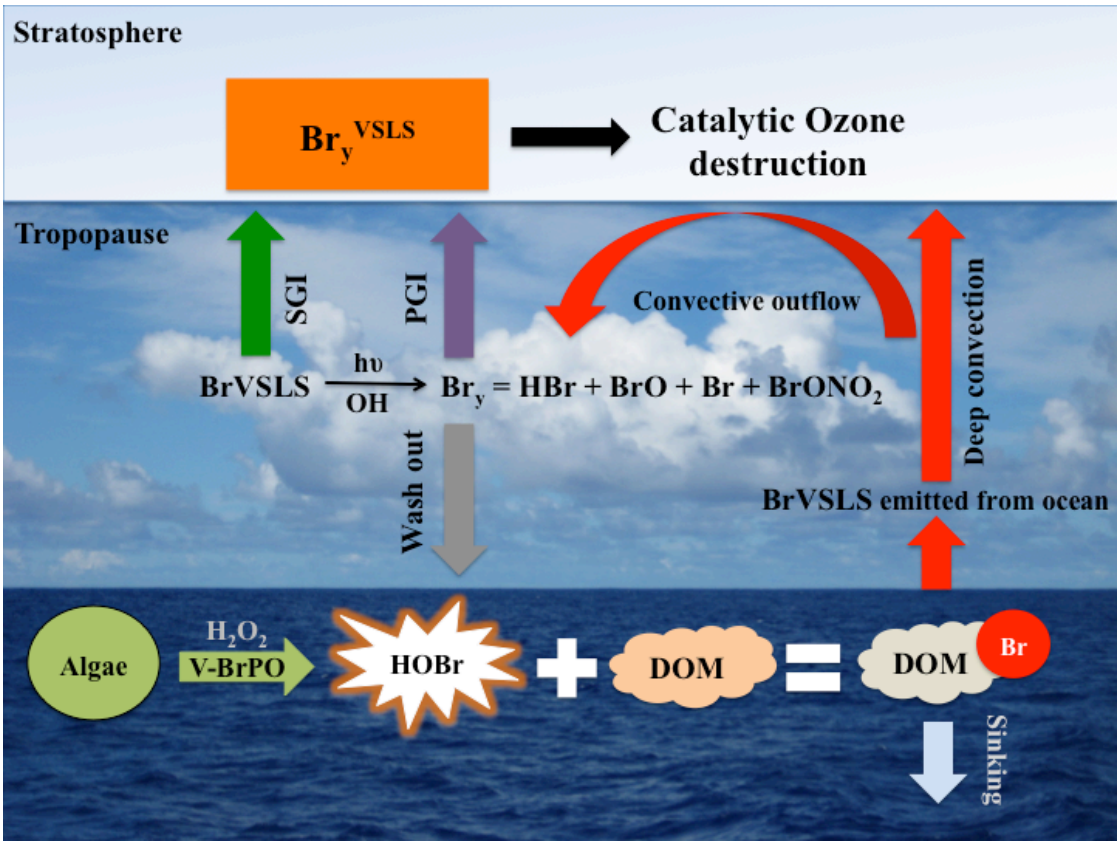

Figure 1-1. Brominated organic matter in marine and atmospheric environments derived from a conceptual model of V-BrPO enzyme-mediated BrVSLS formation mechanisms. Marine algae that produce V-BrPO can oxidize bromine to form reactive species such as hypobromous acid (HOBr), in the presence of H_2O_2. HOBr can react with a wide variety of DOM compounds and consequently form brominated DOM. Some brominated DOM may release BrVSLS and contribute to catalytic ozone destruction reactions; but some brominated DOM maybe stable enough and can potentially be sorbed to sinking particulates; hence being transported into deeper waters. Some of the brominated OM on the particulates may be stable enough to resist degradations in the water column and in the sediments. Atmospheric interactions shown in this figure is adapted from *Salawitch* [2006].

CHAPTER II

$CHBr_3$, CH_2Br_2 AND $CHClBr_2$ IN U.S. COASTAL WATERS DURING THE GULF OF MEXICO AND EAST COAST CARBON (GOMECC) CRUISE*

2.1 Introduction

Brominated very short live substances (VSLSs) such as bromoform ($CHBr_3$), dibromomethane (CH_2Br_2), chlorodibromomethane ($CHClBr_2$), *etc*. are important bromine carriers to the stratosphere in addition to the relatively more stable compounds such as halons and methyl bromide (CH_3Br) [*Kurylo and Rodriguez*, 1999]. These VSLSs degrade and release inorganic bromine (Br_y) via photolysis and reaction with hydroxyl radicals (OH) [*WMO*, 2007]. The resulting Br_y can participate in catalytic ozone destruction in the free troposphere [*von Glasow et al.*, 2004; *Yang et al.*, 2005] and the stratosphere (*e.g*. *Garcia and Solomon* [1994], *McElroy et al.* [1986], and *Solomon et al.* [1995]). Bromine is 40 to 100 times more efficient in O_3 destruction than chlorine (*Wamsley et al.* [1998] and references therein). The VSLSs are capable of supplying ~5.0 – 5.2 pptv of Br_y to the stratosphere [*Dorf et al.*, 2008; *Sinnhuber et al.*, 2002]. $CHBr_3$ and CH_2Br_2 are the most abundant VSLSs, which, when combined, account for > 80% of VSL organic bromine in the marine boundary layer and the upper troposphere [*WMO*, 2007]. $CHBr_3$ alone could contribute ~0.5 to

* Reprinted with permission from "$CHBr_3$, CH_2Br_2, and $CHClBr_2$ in U.S. coastal waters during the Gulf of Mexico and East Coast Carbon cruise" by Y. Liu et al., 2011. *Journal of Geophysical Research, Oceans,* 116, C10004, doi:10.1029/2010JC006729., Copyright [2011] by John Wiley and Sons.

1.8 pptv of Br_y to the stratosphere [*Dvortsov et al.*, 1999; *Nielsen and Douglass*, 2001; *Sinnhuber and Folkins*, 2006].

Current evidence suggests that marine $CHBr_3$, CH_2Br_2, and $CHClBr_2$ are primarily produced naturally, such as by macroalgae, ice algae and phytoplankton (*e.g. Carpenter and Liss* [2000]; *Gschwend and MacFarlane* [1986]; *Manley and Barbero* [2001]; *Manley et al.* [1992]; *Moore et al.* [1996]; *Sturges et al.* [1992]; *Sturges et al.* [1993]; and *Tokarczyk and Moore* [1994] *etc*.). $CHBr_3$ and $CHClBr_2$ also have anthropogenic sources as by-products of water disinfection (*e.g. Nieuwenhuijsen et al.* [2000]; *Quack and Wallace* [2003]; *Ram et al.* [1990]). Sea-to-air flux is the major source of atmospheric $CHBr_3$ in the marine environment [*Carpenter and Liss*, 2000; *Quack and Wallace*, 2003]. However, *Carpenter et al.* [2007b] also indicated sea-to-air flux of $CHBr_3$ alone could not account for the high atmospheric mixing ratios observed in the tropical Atlantic. The authors suggested non-localized sources, possibly terrestrial contributions for $CHBr_3$.

The temporal and spatial distributions of these compounds vary significantly, especially for $CHBr_3$, which has the shortest overall atmospheric lifetime (Table 2-1) (*WMO* [2003] and references therein). These variations are attributable to geographical distributions of source types, source strengths, gas-exchange coefficients, local degradation rates, and seasonality (*e.g. Carpenter et al.* [2009]; *Hughes et al.* [2009]; *Liang et al.* [2010]; *Quack and Wallace* [2003]; *Warwick et al.* [2006]; and *WMO* [2007] *etc*.). Such variations and the limited availability of paired seawater and atmospheric measurements of the VSLSs lead to large uncertainties for estimating their global fluxes. Attempts to estimate global coastal fluxes have even larger

uncertainties due to even more variability in the coastal environments. Coastal areas are important elements for VSLSs global fluxes. *Quack and Wallace* [2003] reported a $CHBr_3$ global coastal (shore regime) flux that accounts for ~23% of their estimated global flux. *Liang et al.* [2010] reported model stimulated $CHBr_3$ and CH_2Br_2 global fluxes of which 40% is from the coasts. *Carpenter et al.* [2009] also reported that their highest $CHBr_3$ and CH_2Br_2 fluxes were observed in the coastal waters in the northeast Atlantic, and tropical eastern Atlantic. In this study, we present the first $CHBr_3$, CH_2Br_2, and $CHClBr_2$ data over an extensive area of the coastal United States (24° – 43° N). This is the first brominated VSLSs data set collected from large area of urbanized coastline.

Table 2-1. Global annual averaged atmospheric lifetimes for $CHBr_3$, CH_2Br_2, and $CHClBr_2$ (*WMO* [2003] and references therein).

	τ_{OH} (day)	τ_J (day)	τ_{total} (day)
CH_2Br_2	120	5000	120
$CHClBr_2$	120	161	69
$CHBr_3$	100	36	26

2.2 Methods

For the Gulf of Mexico and East Coast Carbon (GOMECC) cruise, the NOAA ship, R/V Ronald H. Brown, departed from Galveston, TX on July 10 and arrived in Boston, MA on August 4, 2007 (Figure 2-1). Surface air and water samples were collected and analyzed for $CHBr_3$, CH_2Br_2, $CHClBr_2$, and a suite of other halocarbons.

Continuous air and surface water samples were collected from Year Day (YD) ~196 onward.

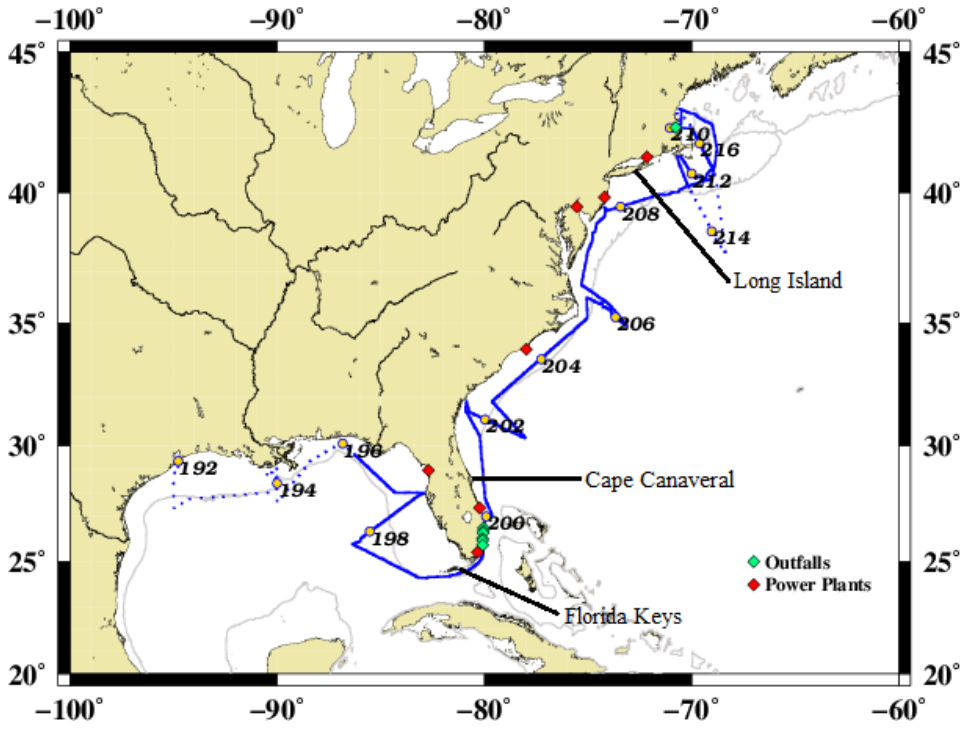

Figure 2-1. Map showing the Gulf of Mexico and East Coast Carbon (GOMECC) cruise with track (—), 200m isobath (—), yearday (●), treated water outfalls (♦), and seawater-cooled nuclear power plants (♦).

Air was continuously pumped (~6 L min^{-1}) through a 0.63-cm ID SynFlex tubing (Motion Industries, Dallas, TX), which was mounted on the mast at the bow of the ship. Seawater from the ship's pumping system flowed through a Weiss equilibrator [*Butler et al.*, 1988; *Johnson*, 1999]. Samples are periodically drawn from the equilibrated headspace of the Weiss equilibrator and from the air pumped from the

bow. Air and equilibrator headspace samples were collected alternately every ~56, or 112 minutes if the calibration gas standard is in sequence. Each sample was drawn through a Nafion dryer, and preconcentrated on one cryotrap and focused on a second cryotrap. The sample is then injected into a ~60 m, 0.25mm DB – VRX (J & W) column and analyzed by Gas Chromatography and Mass Spectrometry (GC-MS) [*Yvon-Lewis et al.*, 2004]. The equilibrium partial pressure (p_w) of each gas is corrected for any warming effects induced by the ship's pumping system. Calibration standards, run every fifth injection, are whole air working standards calibrated against gravimetric standards prepared at NOAA Earth System Research Laboratory (ESRL). For $CHClBr_2$, the working standards were calibrated against liquid standards dissolved in ~35 salinity synthetic seawater in the lab. The analytical system performance was determined by working standard analysis results. The detection limits for $CHBr_3$, CH_2Br_2, and $CHClBr_2$ were 0.02 ppt, 0.04 ppt, and 0.01 ppt respectively. The total measurement uncertainties for $CHBr_3$, CH_2Br_2, and $CHClBr_2$ were 7.31%, 6.34% and 8.79% respectively.

Chlorophyll-*a* (chl-*a*) and colored dissolved organic matter (CDOM) were measured with a Wetlab "ECO" triplet sensor, which was calibrated in the manufacture before the GOMECC cruise. The instrument with factory calibration settings was submerged in an 80 L black tank supplied with seawater from the ship's pumping system at a rate of 4 to 7 L min^{-1}. The sensors measured the stimulated fluorescence of chlorophyll-a (μg L^{-1}, optical configuration: ex470/em685) and CDOM (quinine sulfate units, optical configuration: ex370/em460) at a rate of 1 Hz, and the signal was averaged over 1 minute.

2.3 Results and discussions

2.3.1 Oceanic and atmospheric conditions

Our data cover the eastern Gulf of Mexico and the western Atlantic coastlines of the United States of America. Much of the cruise track is located in water shallower than 200 m (Figure 2-1). Three major oceanic currents in the study region are the Loop Current in the Gulf of Mexico, the northward Gulf Stream as a continuation of the Loop Current, and the Labrador Current moving south along the coast at higher latitudes. Most of the data collected in the Gulf of Mexico are under the influence of coastal seawater, while some of the offshore data were collected in the Loop Current. Most of the data from the Florida Straits to just south of Cape Hatteras (Lat ~ 35.7°N) could experience influence from the Gulf Stream. Abrupt changes in sea surface temperature (SST) and salinity were observed around YD 207 (Lat ~ 36.8°N) (Figure 2-2a). This distinct feature indicated the influence of the Labrador Current, which brought colder and fresher water southward along the coastline.

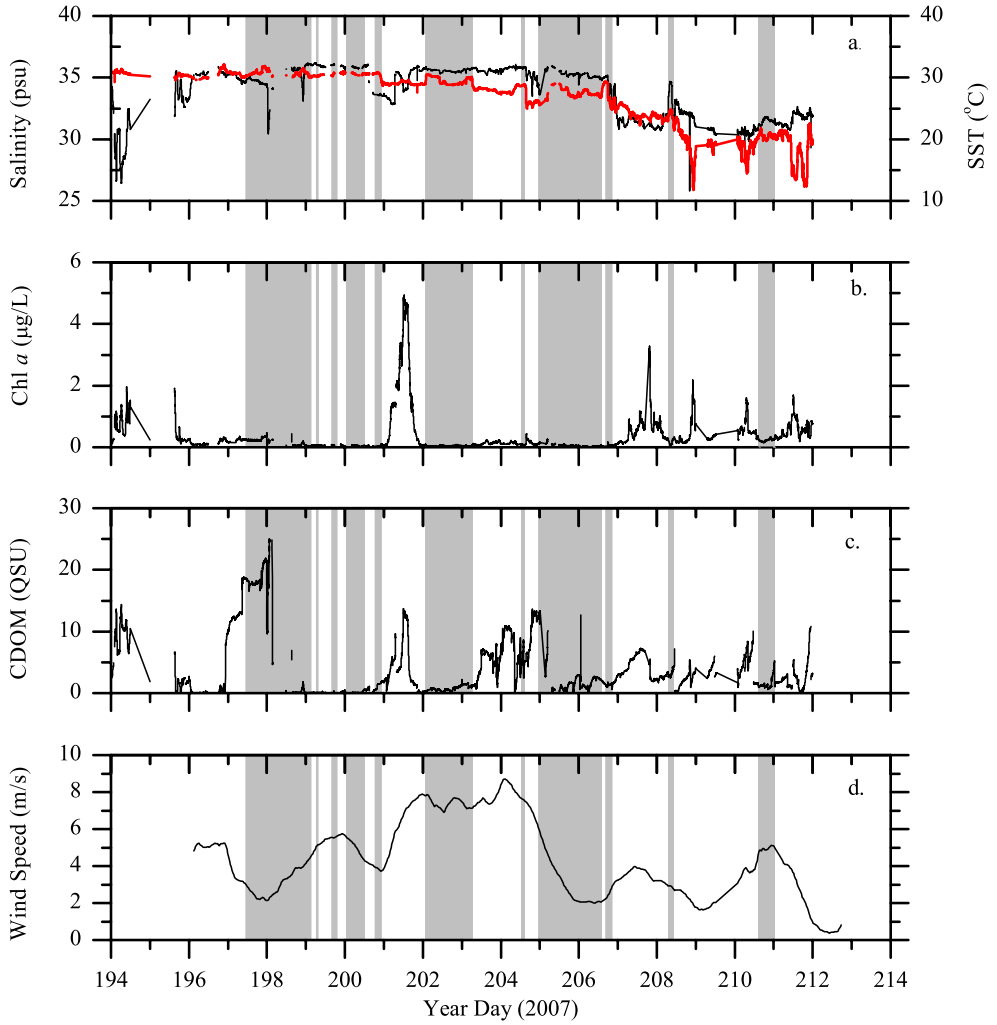

Figure 2-2. Time series of salinity (—) and sea-surface temperature (—) (a), chlorophyll *a* concentrations (—) (b), CDOM concentrations (—) (c), and wind speed (—) (d) for the GOMECC cruise. The gray shadings highlight open ocean data.

In the atmosphere, the subtropical high pressure over the Atlantic basin was governing the general atmospheric circulation in our study area. This atmospheric feature led to mostly onshore winds along the eastern Florida coast, and alongshore winds north of Cape Canaveral, Florida until YD 202. On YD 202 and onward, the

coastal atmospheric circulation patterns were more variable with occasional offshore winds, which could bring continental air masses into the study region (Figure 2-3).

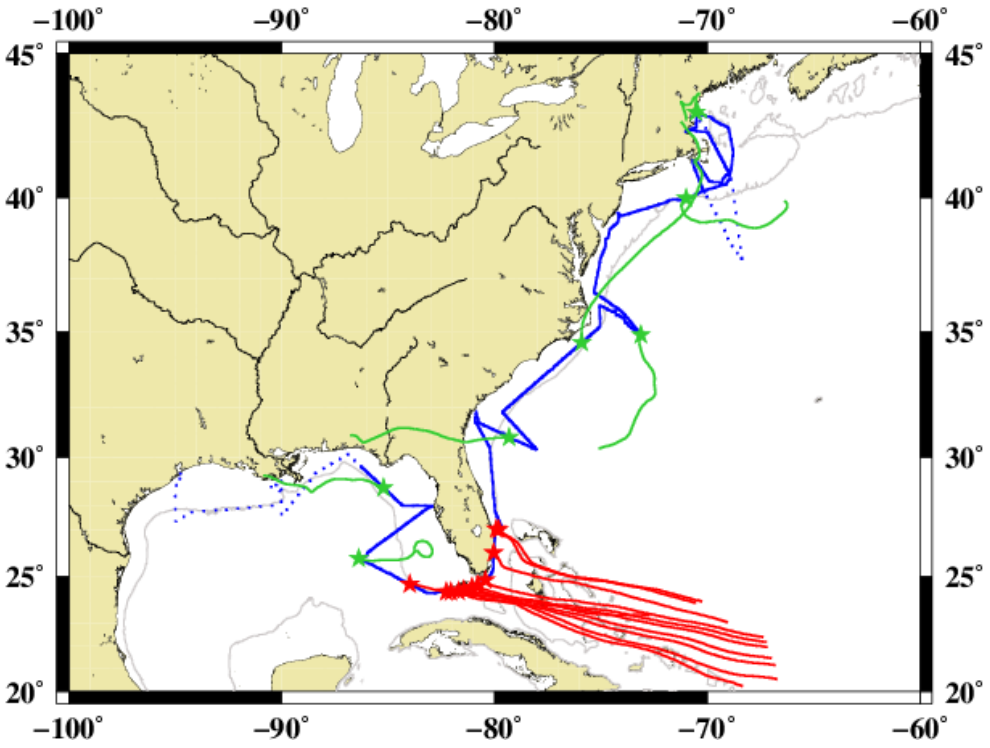

Figure 2-3. Daily 48 hr 100m above sea surface Hysplit air mass back trajectories for selected points (—) along the GOMECC cruise track (—), and back trajectories for selected points with negative saturation anomalies (YD 199 – 200) (—). (★) indicated the starting point of the back trajectories.

2.3.2 Atmospheric mixing ratios, seawater concentrations and saturation anomalies

The continuously alternating air and equilibrator headspace sampling allows us to examine the relationship between the VSLS water concentrations and the mixing ratios in the adjacent air. The mean atmospheric mixing ratios for $CHBr_3$, CH_2Br_2, and $CHClBr_2$ were 14.6 (0.7 to 138.3) ppt, 2.8 (0.5 to 13.2) ppt, and 0.5 (0.03 to 3.2) ppt, respectively. The mean water concentrations for the entire GOMECC cruise were 66.0 (4.4 – 1724.8) pmol L^{-1}, 10.6 (1.9 – 153.8) pmol L^{-1}, and 1.0 (0.1 – 17.2) pmol L^{-1}, for $CHBr_3$, CH_2Br_2 and $CHClBr_2$, respectively. The VSLSs have strong correlations with each other in the seawater for the entire cruise (Table 2-2). This suggests they may share common sources, which is consistent with previous studies (*e.g. Carpenter* [2003]; *Laturnus* [1996]; and *Yokouchi et al.* [2005]). However, these VSLSs are less correlated with each other in the atmosphere than in seawater (Table 2-2). This may be due to atmospheric mixing and differences in atmospheric lifetimes (Table 2-1).

Table 2-2. R^2 ($p < 0.01$) for correlations between $CHBr_3$, CH_2Br_2, and $CHClBr_2$ seawater concentrations and atmospheric mixing ratios during the GOMECC cruise.

	Seawater		Air	
R^2	CH_2Br_2	$CHClBr_2$	CH_2Br_2	$CHClBr_2$
$CHBr_3$	0.93 (n = 280)	0.95 (n = 276)	0.78 (n = 279)	0.63 (n = 275)
CH_2Br_2	-	0.96 (n = 275)	-	0.37 (n = 274)

Atmospheric mixing ratios and surface water concentrations for $CHBr_3$, CH_2Br_2, and $CHClBr_2$ generally exhibit similar trends (Figures 2-4a and b), except the data collected during YD ~199 to 200. During this period, atmospheric mixing ratios were significantly elevated (up to 56.6 ppt for $CHBr_3$), with no corresponding elevation in the water concentrations resulting in negative saturation anomalies in some locations along the transit (Figure 2-5a). The Saturation anomaly (SA; %) of a gas indicates the deviation from equilibrium between the ocean and the atmosphere, and is calculated with the following equation:

$$SA = \frac{P_w - P_a}{P_a} \times 100\% \qquad \text{(Equation. 2.1)}$$

where p_w (atm) is the equilibrium partial pressure of the gas dissolved in surface seawater, and p_a (atm) is the partial pressure of the gas in the air.

The 48 hour 100 m above sea surface HYSPLIT (*http://www.arl.noaa.gov/HYSPLIT.php*) back trajectories for YD 199 to 200 indicate that the high atmospheric mixing ratios near the Florida Straits and the east coast of Florida that led to negative saturation anomalies may be the result of air mass transport from the southeast of the ship, whereas the back trajectories for locations before and after the elevated atmospheric mixing ratios (YD 198 and 201) indicate different air mass source regions (Figure 2-3). The seawater was supersaturated and served as a source of the VSLSs to the atmosphere everywhere else during the GOMECC cruise.

2.3.3 Coastal sources and sinks

Data that were collected when the water depth was less than or equal to 200 meters are extracted and are considered as coastal data. This is similar to the combined coastal and coastally influenced region defined by *Carpenter et al.* [2009] and the shelf region defined by *Quack and Wallace* [2003]. The mean coastal water concentrations are higher than the averages for the open ocean concentrations (Table 2-3). These findings suggest there are significant sources of VSLSs to the coastal ocean, which agrees with earlier findings for $CHBr_3$ and CH_2Br_2 [*Carpenter et al.*, 2009; *Quack and Wallace*, 2003].

2.3.3.1 Anthropogenic sources

The Gulf of Mexico and east coast United States of America are highly urbanized regions. Human inputs could influence the VSLS budgets in various ways, such as treated water outfalls and seawater-cooled nuclear or conventional power plants. These facilities discharge significant amounts of chlorinated (for disinfection) fresh water or seawater; and it is well known that the chlorine disinfection processes in either fresh water or seawater could produce a wide range of byproducts, such as the trihalomethanes (*e.g. Nieuwenhuijsen et al.* [2000]; *Quack and Wallace* [2003]; *Ram et al.* [1990]). Massive nutrient inputs from the outfalls could stimulate microalgal or macroalgal blooms [*Lapointe et al.*, 2004; *Lapointe et al.*, 2005], which may, in turn, produce the VSLSs.

During the GOMECC cruise, we encountered two nuclear power plant cooling water discharge areas and a series of treated water outfalls along the east coast of Florida, and the treated water outfall in Boston Harbor. Elevated VSLS concentrations were observed in the seawater when the ship passed these locations. Two spikes in surface water concentrations (Figure 2-4b), one just before YD 200 and one after that day coincide with the time when the ship passed near a series of nuclear power plants and treated-water outfalls along the Florida coast. The highest water concentrations for the VSLSs were seen near the Boston Harbor (on YD ~210). These findings suggest anthropogenic inputs. However, it is impossible to estimate the magnitude of the contribution from these facilities for several reasons. First, we do not have tracers that allow us to identify waters discharged from these facilities. Nutrient data might have been a good tracer for treated water outfalls plumes. Unfortunately, these data are not available for the locations of interest during the GOMECC cruise. Therefore, it would be difficult for us to estimate the extent of treated water outfall influence to the water mass that we sampled. The features that we observed in these areas are likely to be mixtures of anthropogenic sources, and co-existing natural sources as describe below.

Table 2-3. Air mixing ratios, surface water concentrations, saturation anomalies, fluxes and calculated production rates for $CHBr_3$, CH_2Br_2, and $CHClBr_2$ for the GOMECC cruise.

	Air Mixing Ratio (ppt)	Surface Water Conc. (pmol L^{-1})	Saturation Anomaly (%)	Calculated Production Rates (nmol m^{-3} d^{-1})
Open Ocean				
	14.9	39.7	282.5	2.4 ± 1.1*
$CHBr_3$	(0.8 - 47.4)	(4.4 - 125.2)	(-14.7 - 1201.8)	(-1.0 - 22.5)
	2.7	6.6	301.5	3.4 ± 1.1*
CH_2Br_2	(0.5 - 9.2)	(1.9 - 17.7)	(-12.0 - 775.5)	(1.1 - 12.5)
	0.5	0.7	252.0	0.03 ± 0.003*
$CHClBr_2$	(0.04 - 3.2)	(0.1 - 2.1)	(-48.1 - 1129.0)	(-0.1 - 0.6)
Coastal (≤ 200m) South of 40°N				
	15.4	41.0	281.9	6.1 ± 1.1*
$CHBr_3$	(0.9 - 138.3)	(6.0 - 366.8)	(-27.7 - 1274.7)	(-2.6 - 36.4)
	2.8	7.5	326.1	4.8 ± 1.1*
CH_2Br_2	(0.6 - 13.2)	(2.3 - 37.3)	(25.6 - 1317.4)	(1.4 - 21.8)
	0.5	0.8	303.1	0.1 ± 0.003*
$CHClBr_2$	(0.05 - 2.6)	(0.2 - 3.9)	(-25.0 - 1141.6)	(-0.04 - 0.8)
North of 40°N				
	12.5	162.5	390.4	31.2 ± 1.1*
$CHBr_3$	(0.7 - 90.7)	(4.7 - 1724.8)	(76.5 - 1536.3)	(0.4 - 395.0)
	3.0	23.9	428.4	14.2 ± 1.1*
CH_2Br_2	(0.5 - 10.8)	(1.9 - 153.8)	(61.7 - 2002.1)	(1.1 - 101.7)
	0.3	2.1	505.6	0.3 ± 0.003*
$CHClBr_2$	(0.03 - 1.3)	(0.1 - 17.2)	(-83.3 - 2329.7)	(-0.1 - 3.6)

* Uncertainties for calculated production rates for $CHBr_3$, CH_2Br_2, and $CHClBr_2$ calculated using error propagating method with uncertainties given for each degradation rate constant.

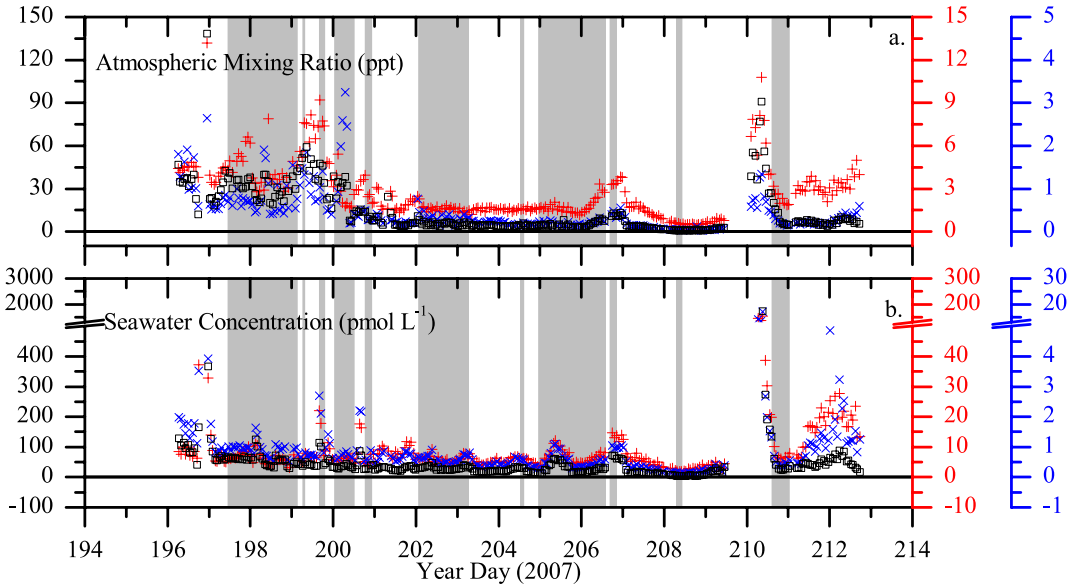

Figure 2-4. Time series of atmospheric mixing ratios (a) and water concentrations (b) for $CHBr_3$ (□), CH_2Br_2 (+), and $CHClBr_2$ (×). The gray shadings highlight open ocean data.

2.3.3.2 Natural sources

Several studies reported that seawater $CHBr_3$ concentrations are generally positively correlated with chlorophyll *a* (*Carpenter et al.* [2009]; and *Schall et al.* [1997] *etc*.). *Manley and Barbero* [2001] suggested the presence of certain types of dissolved organic matter (DOM) may result in $CHBr_3$ production. However, our results found that the VSLS concentrations over the whole study region show no clear relationships with chlorophyll *a* ($R^2 < 0.1$) or colored dissolved organic matter (CDOM) ($R^2 < 0.05$) (Figures 2-2 b and c).

Low correlation between $CHBr_3$ concentrations in seawater and CDOM may be attributable to the complicated coastal DOM components, as the type of DOM

required for trihalomethane formations may be very specific. For example, *Theiler et al.* [1978] suggested ketones are better substrates for $CHBr_3$ formations than phenols. The low correlation between $CHBr_3$ concentrations in seawater and chlorophyll *a* is in agreement with *Hughes et al.* [2009], in which observations were made in coastal Antarctica during the summer. However, the R^2 values reported by the referenced study for $CHBr_3$ and CH_2Br_2 ($R^2 < 0.4$) with chlorophyll *a* were still much higher than those observed in this study. Chlorophyll *a* analysis is not species specific or able to detect the presence of macroalgae in the surrounding area. Hence, such a relationship could be altered by co-existing non-bromoalkane producing species or differences in bromoalkane productivities between each species that were present in the water. *Hughes et al.* [2009] also suggested the effects of sea-to-air gas exchange could alter the correlation. Other explanations for the lack of correlation could also be anthropogenic inputs and potential macroalgal contributions in some areas.

The area north of 40ºN in our study region is known to support numerous macroalgae species [*Lüning*, 1990]. Elevated VSLS concentrations in this area may be attributed to macroalgal production, in addition to the anthropogenic sources discussed above. Macroalgal influence south of this area is uncertain. Rocky bottoms that are favorable for macroalgae growth are almost entirely absent from south of Long Island until the Florida Keys (Figure 2-1), where the lime stone bottom could provide anchorage for the rootless macroalgae [*Searles*, 1984]. Between these areas, macroalgae growth is dependent on outcrops and near shore human-made structures, which could restrict macroalgae growth in places very close to the coastline in a

patchy pattern. Therefore, during the transit between 30ºN to 40ºN, we may not have been close enough to the macroalgal habitats.

2.3.3.3 $CH_2Br_2/CHBr_3$ ratios

In previous studies, $CH_2Br_2/CHBr_3$ concentration ratios in seawater and in air were lower in coastal regions than in open ocean regions [*Carpenter et al.*, 2009; *Quack et al.*, 2007b]. The drivers of these ratios could be related to the first order decay of $CHBr_3$ and CH_2Br_2 in the atmosphere and seawater, and emission ratios which themselves differ from source to source [*Carpenter et al.*, 2009]. However, we did not see significant differences between the ratios of $CH_2Br_2/CHBr_3$ in the coastal waters and the open ocean for either seawater concentrations or atmospheric mixing ratios (Table 2-4). This may be due to the fact that we have limited data to represent open ocean characteristics, and hence, could not make legitimate comparisons with other studies in the open ocean. The wide ranges of air and seawater concentration ratios shown in Table 2-4 suggest there are substantial heterogeneities in the sources and sinks in this extensive study area. The highest water and air concentration ratios observed during this cruise are in the coastal region north of 40ºN, which is likely to have the most macroalgal influence. This is contrary to the results from earlier studies suggesting lower ratios in areas of macroalgal influence [*Carpenter et al*., 2009].

Table 2-4. $CH_2Br_2/CHBr_3$ air and seawater concentration ratios.

	Water	Air
Open Ocean	0.2 (0.1 - 0.4)	0.3 (0.05 - 0.7)
Coastal		
South of 40°N	0.2 (0.06 - 0.4)	0.3 (0.07 - 0.7)
North of 40°N	0.3 (0.08 - 0.7)	0.4 (0.1 - 0.8)

2.3.3.4 $CHBr_3$ photodegradation in surface seawater

Different degradation rates in seawater may also contribute to the different $CH_2Br_2/CHBr_3$ concentration ratios observed in our study. Photolysis of $CHBr_3$ in the mixed layer could lead to a higher $CH_2Br_2/CHBr_3$ ratio in water concentrations in the area north of 40°N.

Carpenter and Liss [2000] and *Hense and Quack* [2009] briefly discussed the role of photolytic loss of $CHBr_3$ in surface seawater. *Carpenter and Liss* [2000] estimated the mixed layer $CHBr_3$ 1/*e* lifetime due to photolysis is ~9 years in a 100 m mixed layer, assuming that all of the photochemical reactions occur only in the top 1 m, and assuming a photolysis lifetime of ~30 days in the top layer. Their findings suggested that $CHBr_3$ photolysis loss is negligible in situations with deep mixed layers, such as in the open ocean.

However, photolysis of $CHBr_3$ may be a significant sink in this study region. For the GOMECC cruise, the mean mixed layer depth in the region north of 40ºN is only ~3.6 (2.0 – 7.0) m, while the mean mixed layer depth in the region south of 40ºN is ~ 13.2 (2.0 to 50.0) m. Therefore, the photodegradation rate constant for $CHBr_3$ (J_z)

is calculated to assess the significance of the photolytic loss of $CHBr_3$ to its overall budget in coastal waters during the GOMECC cruise.

The modeled lifetime for the top 1 m layer is ~ 25 days, which is relatively close to the referenced study [*Carpenter and Liss*, 2000]. However, the COART [*Jin et al.*, 2004] model used for determining percentage of light attenuation at each layer relative to the atmosphere indicated that the wavelengths that are capable of photolytically degrading $CHBr_3$ can penetrate down to 5 m for conditions experienced during the GOMECC cruise. The $CHBr_3$ mean integrated lifetime for the top 5 m of the mixed layer is ~ 34 days. Applying such rate constant to the open ocean and assuming a mixed layer depth of 100 m, the total mixed layer lifetime is shortened to ~ 2 years.

The mean mixed layer depth during this cruise is almost ten times shallower than the typical open ocean mixed layer depth. The mean mixed layer photolysis lifetime calculated for the GOMECC data is ~82 days, which is much shorter than the lifetime in the open ocean. Since 34% of our data were collected in locations with mixed layer depths less than 5 m, where the whole mixed layer experienced photodegration of the compound, photolytic loss is an important component of the budget for seawater $CHBr_3$ during the GOMECC cruise. Although this modeled photolysis loss in seawater is rather crude, it indicates the importance of this degradation path in coastal environments.

2.3.4 Net fluxes

The net sea-to-air fluxes (F, nmol m^{-2} d^{-1}) for the bromoalkanes are calculated with the following equation:

$$F = k_w(C_w - \frac{p_a}{H}) \quad \text{(Equation 2.2)}$$

where k_w (m d^{-1}) is the wind speed dependent gas exchange coefficient *Sweeney et al.* [2007] corrected for the Schmidt number of the gas of interest; H (m^3 atm mol^{-1}) is the Henry's law constant [*Moore et al.*, 1995a]; C_w (mol m^{-3}) is the concentration of the gas of interest in the surface seawater; and p_a (atm) is the partial pressure in the air. Wind speeds were measured at ~19 m and were corrected to 10m above the sea surface [*Erickson*, 1993] for the flux calculations. The Schmidt numbers for the VSLSs were calculated from the kinematic viscosity of seawater and diffusivities of the gases [*Hayduk and Laudie*, 1974].

The sea-to-air fluxes of $CHBr_3$, CH_2Br_2 and $CHClBr_2$ reflect the effects of wind speeds (Figure 2-2d) and concentration gradients between water and air. For the entire cruise, the mean fluxes for $CHBr_3$, CH_2Br_2, and $CHClBr_2$ were 47.6 (-25.4 to 1056.3) nmol m^{-2} d^{-1}, 9.7 (-0.5 to 112.3) nmol m^{-2} d^{-1}, and 0.8 (-1.2 to 10.8) nmol m^{-2} d^{-1}, respectively, assuming the *Sweeney et al.* [2007] parameterization for the gas exchange coefficient as our best estimate (Figure 2-5b). The coastal mean net fluxes for these bromoalkanes were significantly higher than the open ocean net fluxes (Table 2-5). The overall coastal net fluxes for $CHBr_3$, CH_2Br_2, and $CHClBr_2$ were 59.0 (-25.4 to 1056.3) nmol m^{-2} d^{-1}, 11.5 (0.3 to 112.3) nmol m^{-2} d^{-1}, and 1.0 (-0.4 to 10.8) nmol m^{-2} d^{-1}, respectively.

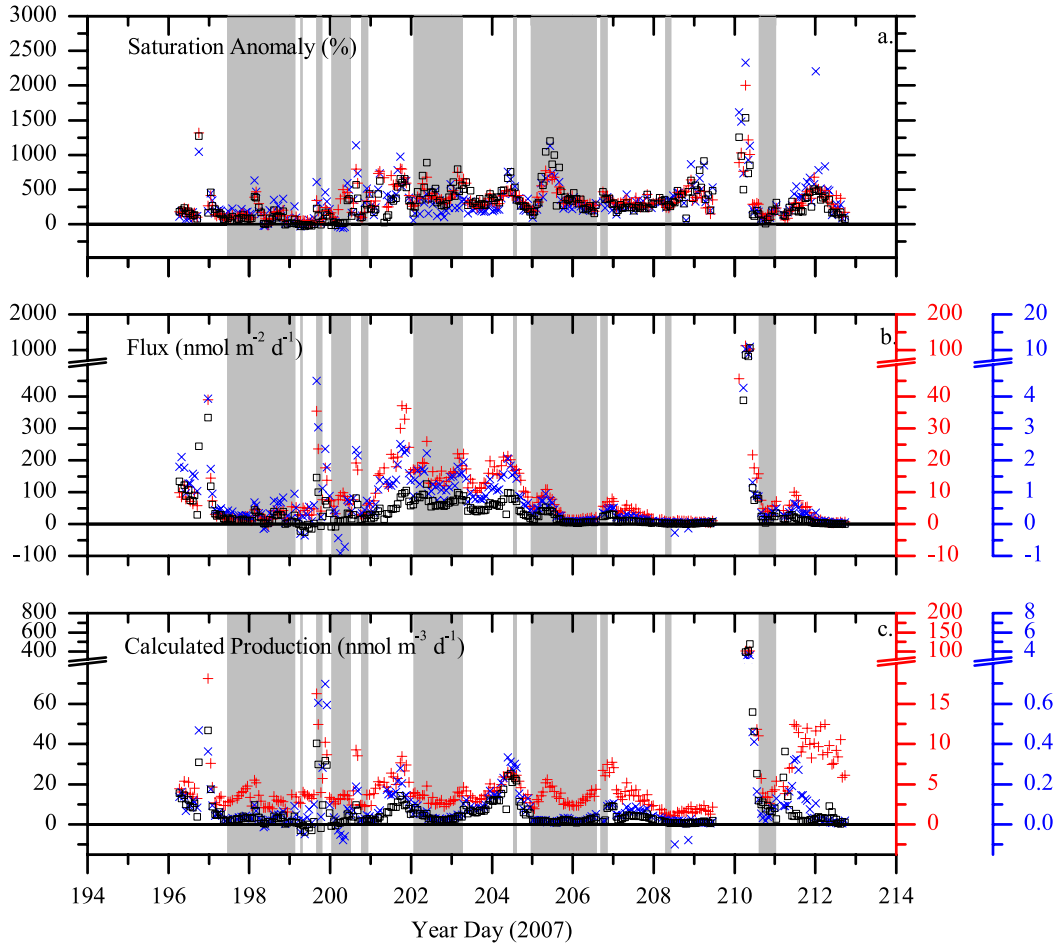

Figure 2-5. Time series of saturation anomalies (a), fluxes (b), and calculated production (c) for $CHBr_3$ (□), CH_2Br_2 (+), and $CHClBr_2$ (×). The gray shadings highlight open ocean data.

As discussed above, we consider the area north of 40º N as predominantly influenced by macroalgal and anthropogenic inputs. The maxima for the sea-to-air fluxes of the gases were observed in this region. The mean coastal net fluxes in the area north of 40ºN were 85.1 (0.6 to 1056.3) nmol m^{-2} d^{-1} for $CHBr_3$, 11.2 (0.3 – 112.3) nmol m^{-2} d^{-1} for CH_2Br_2, and 1.0 (-0.3 to 10.8) nmol m^{-2} d^{-1} for $CHClBr_2$. The mean sea-to-air fluxes for $CHBr_3$ and CH_2Br_2 in this area were significantly lower

than the mean fluxes reported by *Jones et al.* [2009] and *Zhou et al*. ([2005] and [2008]) (Table 2-5), where measurements were made in locations that may have been influenced by macroalgal production. The area south of 40º N is not thought to be macroalgae dominated, and it is more likely to be influenced by phytoplankton and anthropogenic sources. The coastal net fluxes for the VSLSs in this region were 45.7 (-25.4 to 334.3) nmol m^{-2} d^{-1}, 11.6 (1.0 to 62.0) nmol m^{-2} d^{-1}, and 1.0 (-0.4 to 5.4) nmol m^{-2} d^{-1}, for $CHBr_3$, CH_2Br_2, and $CHClBr_2$, respectively. $CHBr_3$ and CH_2Br_2 coastal net fluxes in this region are approximately half of those reported by *Hughes et al.* [2009] during the Antarctic summer at locations dominated by ice algae. These fluxes are also significantly lower than fluxes observed by *Carpenter et al.* [2009] along the tropical Atlantic coast (Table 2-5).

Table 2-5. A comparison of the VSLS fluxes (nmol m^{-2} d^{-1}) from this study with *Sweeney et al.* [2007] (S07), *Nightingale et al.* [2000] (N00) and *Wanninkhof* [1992] (W92) parameterizations and previous studies.

	k_w	$CHBr_3$	CH_2Br_2	$CHClBr_3$
GOMECC Open Ocean	S07	28.5 (-8.7 - 126.1)	6.6 (-0.5 - 26.0)	0.5 (-1.2 - 3.0)
	N00	26.7 (-8.3 - 126.9)	6.2 (-0.4 - 26.0)	0.5 (-1.2 - 2.9)
	W92	38.5 (-11.9 - 183.3)	9.0 (-0.6 - 37.6)	0.7 (-1.7 - 4.2)
GOMECC Coastal South of 40°N	S07	45.7 (-25.4 - 334.3)	11.6 (1.0 - 62.0)	1.0 (-0.4 - 5.4)
	N00	44.1 (-24.0 - 310.9)	11.3 (0.8 - 58.4)	1.0 (-0.3 - 5.1)
	W92	63.7 (-34.6 - 449.1)	16.3 (1.2 - 84.4)	1.4 (-0.5 - 7.3)
GOMECC Coastal North of 40°N	S07	85.1 (0.6 - 1056.3)	11.2 (0.3 - 112.3)	1.0 (-0.3 - 10.8)
	N00	72.8 (0.2 - 909.5)	9.5 (0.1 - 98.4)	0.8 (-0.2 - 9.3)
	W92	105.2 (0.3 - 1313.7)	13.7 (0.1 - 142.2)	1.2 (-0.3 - 13.5)
Jones et al. [2009] (Macroalgae dominant coast, Sept 2006)	N00	mean 1800	mean 18.0	-
Zhou et al. [2005] (Great Bay, NH, Aug 2003)	-	624.0 ± 1368.0	112.8 ± 129.6	-
Zhou et al. [2005] (Gulf of Maine, Aug 2002)	W92	median 465.6 (33.6 – 4392.0)	-	-
Zhou et al. [2008] (Coastal region of New Hampshire, summer 2002 - 2004)	-	453.6 ± 295.2	62.4 ± 45.6	-
Hughes et al. [2009] (Antarctica, summer 2006/2007)	N00	84.0 (-13.0 - 275.0)	21.0 (2.0- 70.0)	-
Carpenter et al. [2009] (Tropical Atlantic Coastal, summer 2006 and 2007)	N00	236.0 (127.0 - 322.0)	72.2 (62.7 - 84.5)	-

As shown in Table 2-5, coastal net fluxes differ significantly between locations, even when comparisons were made in the same season to attempt to eliminate the effects of seasonality. This variability is likely due to spatial and temporal variations in productivity, coastal mixing, factors that affect gas exchange, such as temperature and wind speed. Variations in the parameterization of the gas exchange coefficient are also important. Moreover, inter study comparisons also need to be treated with caution. The subsets of coastal sea-to-air fluxes of $CHBr_3$ and CH_2Br_2 measured during the GOMECC cruise are lower than those observed in other coastal regions. This is partly attributable to the differences in coastal coverage. Most

of the referenced studies were conducted in relatively confined coastal regions. Therefore, the source types of VSLSs should be relatively constant for the duration of each of those studies. The GOMECC cruise covered more than 5000 km of coastline. The sampling time and data density for each environmental regime encountered during the GOMECC cruise varied substantially. Therefore, global coastal extrapolations using limited coastal data which may be dominated by certain sources may not be appropriate. The extrapolated global coastal net fluxes for the VSLSs using the GOMECC cruise values are not presented in this paper, as the coastal environmental regimes in this region may not be globally representative.

2.3.5 Calculated production rates

Production rates (P, nmol m^{-3} d^{-1}) (Table 2-3, Figure 2-5c) are calculated as described by *Yvon-Lewis et al.* [2004], assuming steady state, where mixed layer production equals total mixed layer loss:

$$P = \frac{k_w}{z}\frac{(SA - SA_{cfc\text{-}11})p_a}{100}\frac{1}{H} + k_{loss}(Cw) \qquad \text{(Equation 2.3)}$$

$k_{loss} = k_h + J_z + k_{hs}$ for $CHBr_3$;

$k_{loss} = k_h + k_B$ for CH_2Br_2;

$k_{loss} = k_h$ for $CHClBr_2$;

where $SA_{cfc\text{-}11}$ (%) is the saturation anomaly for CFC-11; k_{loss} (d^{-1}) is the total pseudo first order loss rate constant for all the possible loss terms; k_h (d^{-1}) is the hydrolysis rate constant [*Mabey and Mill*, 1978; *Washington*, 1995]; k_{hs} (d^{-1}) is the halide substitution pseudo first order rate constant [*Geen*, 1992]; J_z (d^{-1}) is the photolysis loss

rate constant in the mixed layer; and k_B (d^{-1}) is the pseudo first order biological degradation rate constant for CH_2Br_2 [*Goodwin et al.*, 1998]. The chlorofluorocarbons (CFCs) are conservative tracers, and the $SA_{cfc\text{-}11}$ correction accounts for any physical forcing (e.g. warming or cooling of surface seawater) that may create disequilibrium between the ocean and the atmosphere. The calculated production rates should be interpreted only as "apparent" production rates. Some of the apparent production may be the result of water mass transport in the complex coastal environment that is not captured by variations in CFC concentrations.

The calculated production rates for the entire GOMECC cruise for $CHBr_3$, CH_2Br_2, and $CHClBr_2$ are 10.0 (-2.6 to 395.0) nmol m^{-3} d^{-1}, 6.2 (1.1 to 101.7) nmol m^{-3} d^{-1}, and 0.1 (-0.1 to 3.6) nmol m^{-3} d^{-1}, respectively. The coastal "hot spot" for VSLSs production during the GOMECC cruise is located north of 40°N (Table 2-3, Figure 2-5c), which may be due to existence of macroalgae or proximity to the Boston outfall. These rates are meant to provide some general idea of production rate distributions of the VSLSs with the assumption of steady state.

2.4 Conclusion

The GOMECC cruise data provided $CHBr_3$, CH_2Br_2, and $CHClBr_2$ concentration, saturation anomaly, flux and production rate distributions in an extensively urbanized coastal area. These compounds were supersaturated almost everywhere in the study region, indicating waters of the east coast of United States are sources of the VSLSs to the atmosphere. Significant correlations between the VSLS

seawater concentrations suggest they could share common sources in our study area during the cruise. Maximum values for seawater concentrations, saturation anomalies, fluxes and calculated production rates for the VSLSs are observed north of 40°N, where human influences and macroalgal production are implicated. $CHBr_3$ seawater concentrations and coastal net fluxes in this region were significantly higher than in the area south of 40°N, where the co-existence of phytoplankton and anthropogenic sources is implicated.

These results suggest a few possibilities. First, anthropogenic input such as treated water outfalls and nuclear power plants may only have a significant impact on the local scale. Second, the phytoplankton species presented during this study may not be prolific sources of VSLSs. Third, the maxima observed in the north are partly the result of macroalgal sources.

While the saturation anomalies suggest that the gulf and the eastern coasts of the United States are sources of VSLSs to the atmosphere, both the $CHBr_3$ and CH_2Br_2 mean coastal net fluxes lie at the low ends of the ranges of fluxes that were observed in other regions. However, these differences could be due to the different spatial resolutions of the various studies. The photolytic loss of $CHBr_3$, under the conditions observed during this study, is not negligible and should be considered in future studies of $CHBr_3$. Environmental parameters such as chlorophyll *a*, CDOM, and CH_2Br_2 to $CHBr_3$ concentration ratio characteristics observed from other natural environments are not good proxies for determining the sources of these VSLSs during the GOMECC cruise. More work is needed in order to distinguish VSLS contributions from different sources in complex urbanized coastal environments. Since coastal

environments are complicated and many features are regionally specific, global extrapolation should be treated with caution.

CHAPTER III

SPATIAL DISTRIBUTION OF BROMINATED VERY SHORT-LIVED SUBSTANCES IN THE EASTERN PACIFIC*

3.1 Introduction

Bromoform ($CHBr_3$), dibromomethane (CH_2Br_2), bromodichloromethane ($CHBrCl_2$), chlorodibromomethane ($CHClBr_2$), along with bromochloromethane (CH_2BrCl), are the most abundant brominated very short-lived substances (BrVSLS) in the atmosphere [*Montzka and Reimann*, 2011]. These compounds are important sources of inorganic bromine (Br_y) to the troposphere and lower stratosphere, in addition to the longer-lived compounds such as halons and methyl bromide. Thus, these BrVSLS play an important role in catalytic ozone destruction in the atmosphere. BrVSLS mainly originate from natural sources in seawater and enter the marine boundary layer via sea-to-air fluxes [*Quack and Wallace*, 2003]. Anthropogenic sources, such as seawater-cooled power plants, also contribute to elevated concentrations of $CHBr_3$, $CHClBr_2$, and $CHBrCl_2$ observed in coastal waters; however, these sources may only be significant on a local scale [*Quack and Wallace*, 2003].

Elevated concentrations of brominated BrVSLS in seawater and the adjacent atmosphere are thought to be affected by macroalgae and phytoplankton production [*Carpenter and Liss*, 2000; *Goodwin et al.*, 1997; *Karlsson et al.*, 2008; *Manley et al.*,

* Reprinted with permission from "Spatial distribution of brominated very short-lived substances in the Eastern Pacific" by Y. Liu et al., 2013. *Journal of Geophysical Research, Oceans,* DOI: 10.1002/jgrc.20183., Copyright [2013] by John Wiley and Sons.

1992; *Moore et al.*, 1996; *Moore et al.*, 1995b; *Quack et al.*, 2007a; *Sturges et al.*, 1992; *Sturges et al.*, 1993]. For example, elevated BrVSLS concentrations in surface seawater have been observed near regions where surface chlorophyll *a* concentrations were also elevated [*Carpenter et al.*, 2009; *Schall et al.*, 1997]. Although phytoplankton production has been suggested as a possible source, poor correlation between chlorophyll *a* and BrVSLS concentrations observed in different regions have raised questions regarding the sources and mechanisms of formation and degradation of these compounds in seawater. Therefore, many uncertainties remain concerning environmental factors that influence production and distributions of BrVSLS and the role of phytoplankton in BrVSLS production.

The enzyme bromoperoxidase is thought to be responsible for the production of some poly-brominated compounds, such as $CHBr_3$ and CH_2Br_2, in the presence of hydrogen peroxide (H_2O_2) and dissolved organic matter (DOM) as the substrate [*Hill and Manley*, 2009; *Lin and Manley*, 2012; *Manley*, 2002; *Manley and Barbero*, 2001; *Moore et al.*, 1996; *Theiler et al.*, 1978; *Wever et al.*, 1993]. The presence of bromoperoxidase in macroalgae and microalgae appears to be class and species-specific, which may partly explain the observed weak correlations between BrVSLS and chlorophyll *a* concentrations. Several studies have used pigment biomarkers to identify specific taxa of phytoplankton that may be significant BrVSLS sources in seawater [*Abrahamsson et al.*, 2004; *Karlsson et al.*, 2008; *Mattson et al.*, 2012; *Quack et al.*, 2007a; *Raimund et al.*, 2011; *Roy*, 2010]. For example, *Quack et al.* [2007a] showed significant correlations between $CHBr_3$ seawater concentrations with the abundances of cyanobacteria (*Synechococcus* spp.) and diatoms in the Mauritanian

upwelling region. *Karlsson et al.* [2008] also suggested that some species of cyanobacteria in the Baltic Sea were possible sources of $CHBr_3$. Other phytoplankton groups, such as prymnesiophytes, green algae, and prochlorophytes, may have also contributed to the production of BrVSLS, as observed by *Raimund et al.* [2011] near the Iberian upwelling system. However, in certain regions, such as the Antarctic, elevated diatom abundances may, in part, have contributed to the observed brominated BrVSLS concentrations in seawater; yet, no significant correlations were found between the BrVSLS and phytoplankton pigments [*Abrahamsson et al.*, 2004; *Mattson et al.*, 2012].

In this study, depth-profiles of $CHBr_3$ (219 samples), CH_2Br_2 (236 samples), $CHClBr_2$ (238 samples), and $CHBrCl_2$ (238 samples) were measured during the Halocarbon Air-Sea Transect – Pacific (HalocAST-P) cruise. Phytoplankton pigment concentrations, picoplankton abundance, and inorganic nutrient concentrations were measured to determine relationships between phytoplankton abundance and BrVSLS concentrations over the large spatial range covered by this cruise.

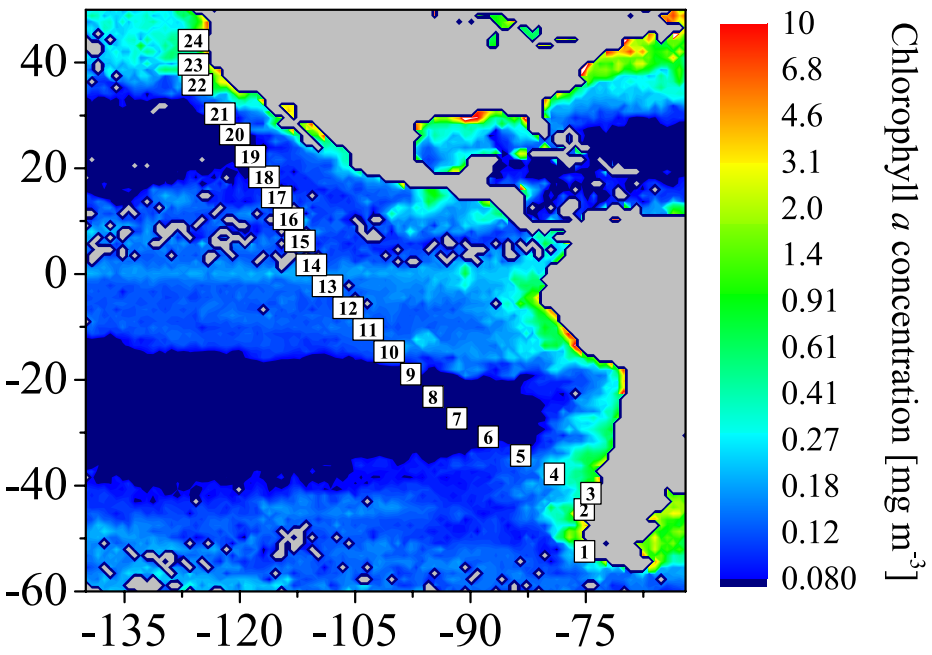

Figure 3-1. Sampling station map for the Halocarbon Air-Sea Transect – Pacific cruise, superimposed on March – April 2010 monthly averaged SeaWiFs chlorophyll *a* concentrations [*Acker and Leptoukh*, 2007].

3.2 Sampling and analyses methods

The Halocarbon Air-Sea Transect – Pacific (HalocAST-P) cruise, conducted onboard the *R/V Thomas G. Thomson,* departed from Punta Arenas, Chile on March 31, 2010 and arrived in Seattle, WA, United States on April 28, 2010 (Figure 3-1). The cruise track was designed to observe oceanic and atmospheric latitudinal distributions of a suite of halocarbon compounds including $CHBr_3$, CH_2Br_2, $CHBrCl_2$, and $CHClBr_2$. A total of 24 CTD/rosette casts were conducted along the cruise track (one cast per day at local noon) and water was collected from 12 depths ranging from

~5 m to 750 m. Here onwards, we refer the "surface" values to measurements made at ~5 m. For stations with water depths less than 750 m, *i.e.* casts 1, 2, and 3, the water columns were sampled from the surface to just above the sediment. Data collected from casts 1 and 2, where water depths were less than 200 m, are considered as coastal data. These definitions are approximately equivalent to "coastal and coastally influenced waters" defined by *Carpenter et al.* [2009] and "shelf regime" defined by *Quack et al.* [2004]. Cast 3 with water depth less than 400 m, although not coastal by our definition, was located on the continental shelf. Seawater samples were collected using a CTD/rosette sampler with 24 10-L Niskin bottles. The CTD/rosette package was also equipped with an oxygen sensor, a fluorescence sensor, and a transmissometer.

3.2.1 Halocarbons

Samples for halocarbon analysis were collected using 100 mL gas tight ground glass syringes immediately after the rosette unit was on deck. The samples were immediately transferred to a purge-and-trap sample storage module. The purge-and-trap sample storage module is a compact thermoelectric refrigerator held at ~ 6 ºC. Inside, sixteen 70 mL glass bulbs were connected to a 16-position loop selection valve (Valco Instrument Co.), which was connected to the purge-and-trap system. This configuration allowed seawater samples to be stored in a cold, dark and gas tight environment until analysis [*Yvon-Lewis et al.*, 2004]. Each seawater sample was

gently injected into the appropriate bulb through a 0.2 μm membrane filter to remove microorganisms. All of the samples were analyzed within 12 hours of collection.

For gas analysis, each seawater sample in the glass bulb was sequentially transferred into a glass sparger with an ultra-pure helium gas stream, and purged at 144 mL min^{-1} at 40ºC. The whole sample line was then flushed with the same ultra-pure helium gas stream until it was time for the next sample to ensure no residue from the previous sample was left in the line. The sample purge stream was dried with two in-line Nafion driers (Perma Pure, NJ), and the analytes were pre-concentrated on one cryotrap and focused on a second cryotrap that were both held at -75°C, and then desorbed at 200ºC. The analytes were desorbed from the focusing trap and transfered by chromatography grade helium carrier gas into the gas chromatograph – mass spectrometer (GC-MS) for quantification (Agilent GC 6890N and MS 5973N; DB-VRX 0.180 ID column with 10 m pre-column and 30 m main column). Detailed analytical method was described in *Yvon-Lewis et al.* [2004] and references therein.

Moist whole air gas calibration standards used in the field were calibrated before and after the cruise against gas standards obtained from the National Oceanic and Atmospheric Administration Global Monitoring Division (NOAA GMD). The field calibration standard was run after every fourth injection. The ultra-pure helium gas stream was run as a blank after every three samples to monitor flushing efficiency. The detection limit for $CHBr_3$ and CH_2Br_2 were 1.00×10^{-3} pmol L^{-1}. For $CHClBr_2$ and $CHBrCl_2$, the detection limits were 5.00×10^{-3} pmol L^{-1}. The averaged analytical uncertainty was 7.00 % for $CHBr_3$, 6.00 % for CH_2Br_2 , and 9.00 % for $CHClBr_2$ and $CHBrCl_2$. Purge efficiency was determined by re-stripping seawater samples three

times, and the percentage in total concentration for the first stripping was 72.3 % for $CHBr_3$, 72.4 % for CH_2Br_2, 77.0 % for $CHClBr_2$, and 93.7 % for $CHBrCl_2$. BrVSLS concentrations reported here were corrected for purge efficiencies.

3.2.2 Pigment, picoplankton counts, and nutrients

Pigment samples were collected from designated Niskin bottles at 5 m, the chlorophyll maximum depth, and at 750 m. For each cast, 5 to 10 L of seawater at each depth were filtered through a pre-combusted 0.7 μm nominal pore size GF/F filter until color was visible on the filter. The filters were frozen immediately at -80 °C and kept frozen until analysis back in the laboratory. The phytoplankton pigment extraction procedure was followed as described in *Wright et al.* [1991]. Briefly, filters were extracted ultrasonically with acetone, centrifuged, and the supernatant blown to dryness under a nitrogen stream at room temperature in the dark. The concentrated residue was re-dissolved in 150 μL of acetone prior to the analysis by high-performance liquid chromatography (HPLC). Pigments were analyzed using a Waters HPLC coupled to an on-line 996 photodiode array detector (PDA), a fluorescence detector (Shimadzu RF535) (ex: 440 nm; em: 660 nm), on a reversed-phase Grace Adsorbosphere C_{18} column (5 μm, 250 mm x 4.6 mm i.d.), using the gradient flow described by *Chen et al.* [2003]. A total of 18 pigment biomarkers were analyzed, which included total chlorophyll *a* (chlorophyll *a* + divinylchlorophyll *a*), chlorophyll *b*, c_2 and c_3, total carotene (α + β), peridinin, 19-butanoyloxyfucoxanthin, fucoxanthin, 19-hexanoyloxyfucoxanthin, prasinoxanthin, pheophorbide *a*, violaxanthin,

diadinoxanthin, alloxanthin, diatoxanthin, lutein, pheophytin *a*, and zeaxanthin. Pigment standards were purchased from DHI Water and Environment, Denmark. The pigment standards were run individually and as a mixed standard to determine retention times, spectra, and the response factors.

The pigment biomarker zeaxanthin can provide information about the presence of cyanobacteria [*Jeffrey et al.*, 2011; *Wright and Jeffrey*, 2006]. However, this pigment is common in both *Prochlorococcus* and *Synechococcus*, two genera of cyanobacteria that often dominate the picoplankton. To gain specific information on the potential picoplankton contribution to the BrVSLS seawater concentrations, these two genera were distinguished and enumerated using flow cytometry. In addition, flow cytometry counts were used to provide abundance information on picoeukaryotes (< 3 μm algae including chlorophytes, pelagophytes, and haptophytes) and heterotrophic bacteria. Picoplankton samples were collected from the Niskin bottles, 1 mL of the sample was filtered through a 35 μm mesh cell strainer and fixed with 20 μL 10% paraformaldehyde for 10 minutes (final concentration 0.2%) and then quickly frozen at -80 °C and kept frozen until analysis. Enumeration of picoplankton and heterotrophic bacteria was performed using a Becton Dickinson FACSCalibur flow cytometer [*Campbell*, 2001]. For the non-pigmented heterotrophic bacteria, the cells were stained with SYBR Green (Molecular Probes) prior to introduction into the flow cytometer. Data were analyzed using CytoWIN [*Vaulot*, 1989].

Inorganic nutrient samples, nitrate (NO_3^-), nitrite (NO_2^-), orthophosphate (HPO_4^{2-}), and silicate (SiO_4^{4-}), were sent to the Geochemical and Environmental Research Group (GERG) at Texas A & M University for analysis. Inorganic nutrient

concentrations were determined using the Astoria-Pacific auto-analyzer following the methodologies of *Armstrong et al.* [1967] and *Bernhardt and Wilhelms* [1967].

3.2.3 Data handling and statistical methods

All data were checked for quality. Exceptionally high or low concentrations measured due to occasional instrumental error, which were determined from CFC-11 concentration as an inert tracer in the same sample, were removed. Subsequently, the data were tested for normality to determine the most appropriate statistical method used for data interpretation. Spearman's rank correlation was chosen to assess the association between parameters, due to the non-normal distributions of the data. Spearman's rank correlation analyses were evaluated at 95% confidence level. Significance of the correlation was determined using a two-tailed test. Significant differences in means between data groups were determined by one-way ANOVA test at 95% confidence level. All statistical analyses were performed using the OriginLab® version 9.0 statistic module.

3.3 Results and discussion

3.3.1 Hydrography and water column layers during the HalocAST-P cruise

Based on profiles of salinity, temperature, potential density (σ_θ), dissolved oxygen, and CFC-11 (Figures 3-2, 3-3 and 3-4), there were four main hydrographic

features observed during the HalocAST-P cruise: (1) freshwater discharged from the coasts, (2) the entrainment of surface waters into deeper water column, (3) the Antarctic intermediate water (AAIW) in the southern hemisphere, and (4) the North Pacific intermediate water (NPIW) in the northern hemisphere. There was apparent entrainment of surface waters into the deeper water column, which was probably due to seasonal fluctuation of thermocline depths and mixing. Based on the dissolved oxygen profile, surface water entrainment reached down to ~ 300 m in the southern temperate waters and to ~ 500 m in the northern temperate waters. Lower salinity and elevated CFC-11 concentrations were also observed in these regions. The AAIW is characterized as low salinity (~34.2) [*Pickard*, 1990] located at $26.98 < \sigma_\theta < 27.80$ isopycnal [*Schmidtko and Johnson*, 2011] in the southern hemisphere, which was ~ 500 m and below in the temperate waters during the HalocAST-P cruise (Figure 3-2, and 3 - 3a). Near the Chilean shelf, the top of AAIW can be as shallow as ~ 300 m [*Palma et al.*, 2005]. The AAIW is also characterized as enriched in NO_3^- and HPO_4^{2-} and low in $HSiO_3^-$ concentrations (Figure 3-5) [*Sarmiento and Gruber*, 2006], and enriched in oxygen and CFC-11 [*Hartin et al.*, 2011] (Figure 3-4). The NPIW is characterized as low salinity located at $26.60 < \sigma_\theta < 27.40$ isopynal [*Talley*, 1997] in the north Pacific, which was ~ 300 m and below in the temperate waters during the HalocAST-P cruise (Figure 3-2 and 3-3b). This water mass is enriched in nutrients such as NO_3^-, HPO_4^{2-}, and $HSiO_3^-$ [*Sarmiento and Gruber*, 2006] (Figure 3-5), and depleted in CFC-11, with an apparent age of a few decades in the eastern boundary of the Pacific ocean [*Watanabe et al.*, 1994] (Figure 3-4).

To better understand BrVSLS distributions in the water column, the water column was divided into three layers: mixed layer, below mixed layer within euphotic zone, and below euphotic zone. The bottom of the mixed layer was defined following *Brainerd and Gregg* [1995]. The bottom of the euphotic was defined as depths where photosynthetic active radiation (PAR) is 1% of surface value, as measured at ~ 5 m [*Kirk*, 1994].

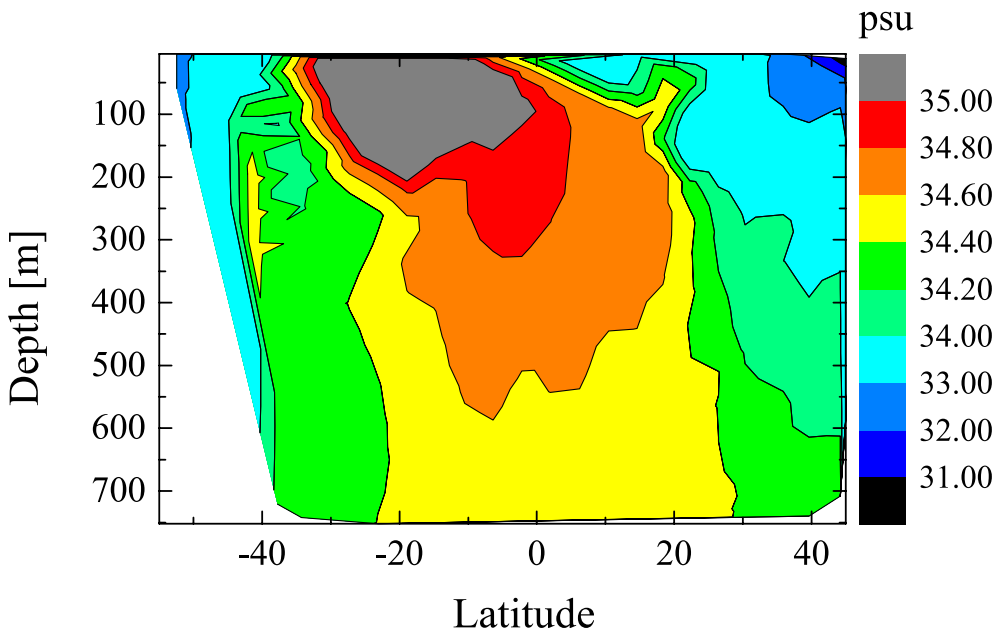

Figure 3-2. Salinity profile for the HalocAST-P cruise.

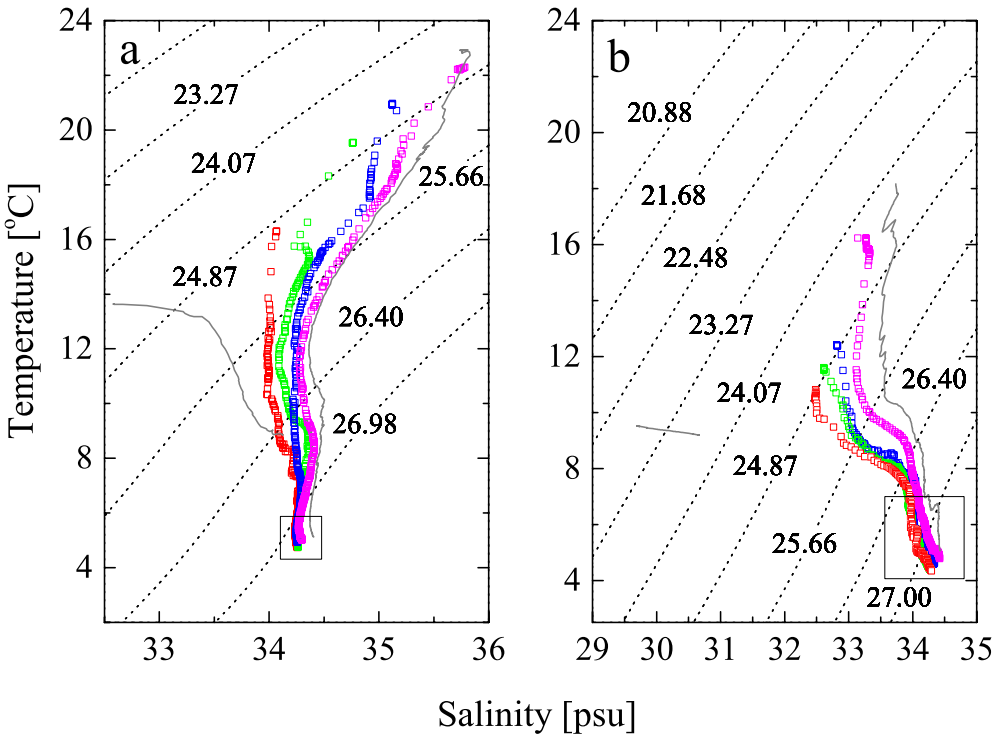

Figure 3-3. Temperature-salinity (TS) diagram. (a) Below ~ 500 m of casts 4 (red), 5 (green), 6 (blue), and 7 (magenta) were the Antarctic intermediate water (AAIW; marked with black square). Casts 2 and 8 were plotted in grey lines as reference of water masses not in the AAIW. (b) Below ~300 m of casts 21(red), 22 (green), 23 (blue), and 24 (magenta) were the North Pacific intermediate water (NPIW; marked with black square). Casts 22 and 25 (TS only, no BrVSLS data collected for Cast 25, conducted in Puget Sound, Seattle, USA) were plotted in grey lines as reference of water masses not in the NPIW.

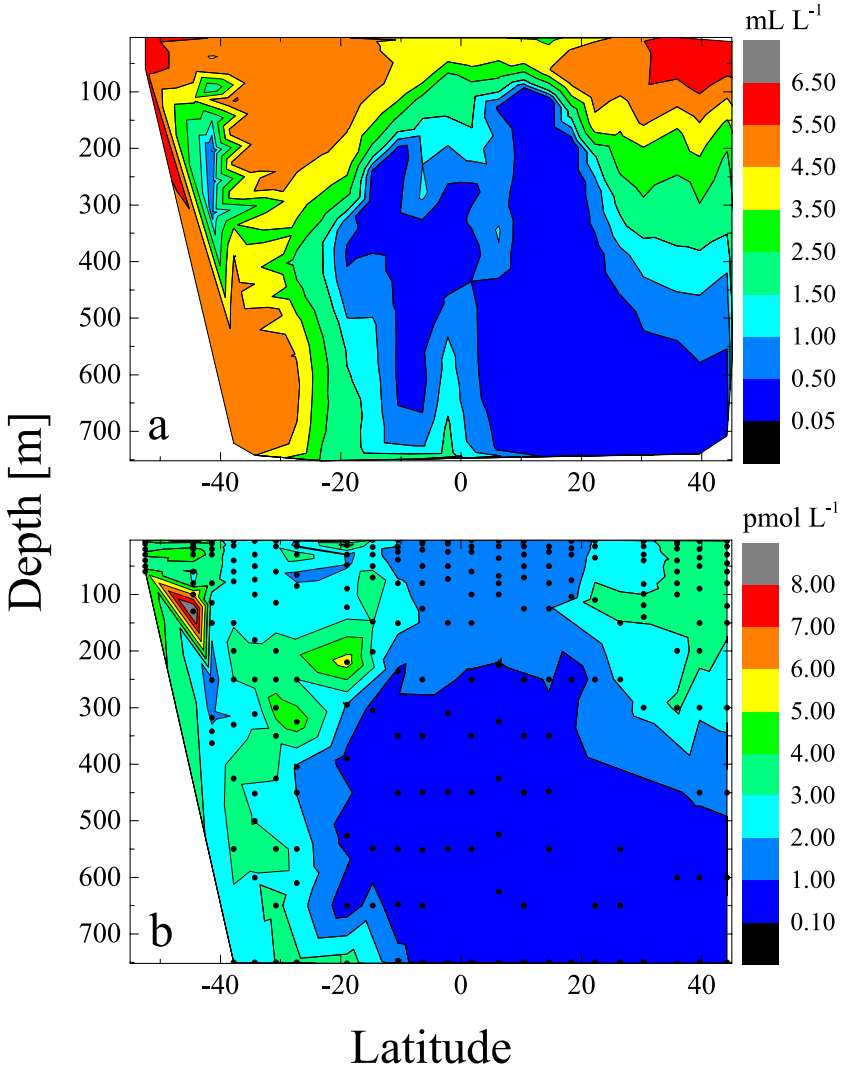

Figure 3-4. (a) Dissolved oxygen profile and (b) CFC-11 profile during the HalocAST-P cruise.

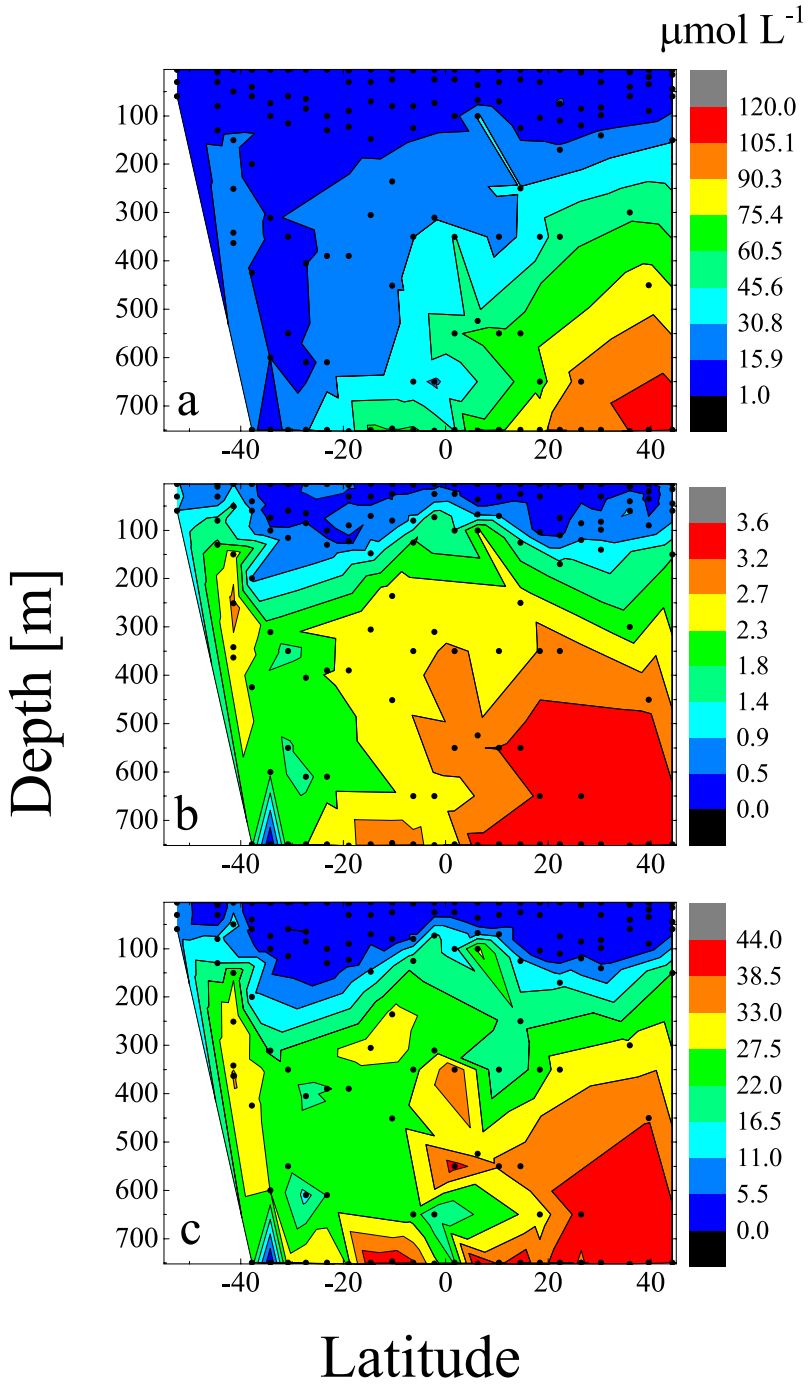

Figure 3-5. (a) Silicate ($HSiO_3^-$), (b) orthophosphate (HPO_4^{2-}), and (c) nitrate (NO_3^-) profile during the HalocAST-P cruise.

3.3.2 Spatial distributions of $CHBr_3$, CH_2Br_2, $CHClBr_2$, and $CHBrCl_2$

In the mixed layer, $CHBr_3$, CH_2Br_2, $CHClBr_2$, and $CHBrCl_2$ concentrations were in general higher in the coastal ocean (depth ≤ 200 m) and the tropics (~ 20° S to 20° N) (Table 3-1; Figure 3-6). Such a general trend is consistent with that observed in other regions [*Butler et al.*, 2007; *Carpenter et al.*, 2007b; *Class and Ballschmiter*, 1988; *Liu et al.*, 2011; *Quack and Wallace*, 2003]. $CHBr_3$ and CH_2Br_2 concentrations were higher below the mixed layer within the euphotic zone than those observed in the mixed layer and below euphotic zone (Table 3-1; Figures 3-7 and 3-8). The maximum seawater concentrations for $CHBr_3$, CH_2Br_2, and $CHClBr_2$ were observed near the depths of subsurface chlorophyll *a* maxima in subtropical waters (Table 3-1; Figure 3-7), which suggests that the production of these compounds is likely related to photosynthetic biomass production and associated biochemical processes. Such features were consistent with the report by *Quack et al.* [2004], who also found that $CHBr_3$ concentration maxima in the Atlantic tropical ocean were located below the mixed layer, near the chlorophyll *a* maxima. The authors reported subsurface $CHBr_3$ concentration maxima ranged from 14 to 60 pmol L^{-1}. Subsurface $CHBr_3$ concentration maxima in the Pacific tropical ocean (~ 20° S to 20° N) were within the range reported by *Quack et al.* [2004] (Figure 3-7). Patches of elevated $CHBr_3$, CH_2Br_2, and $CHClBr_2$ below the bottom of tropical euphotic zone (~ 20° S to 20° N) were likely due to entrainment of water from the euphotic zone, where high concentrations of BrVSLS were produced.

Table 3-1. Mean (range; number of samples) BrVSLS concentrations (pmol L^{-1}) in coastal and open ocean water column. Bold text highlighted the minimum and maximum of the data.

$CHBr_3$	CH_2Br_2	$CHClBr_2$	$CHBrCl_2$
Coastal ocean			
Mixed Layer			
17.46	4.79	2.59	1.69
(13.80 - 20.67; 13)	(3.36 - 6.51; 13)	(2.00 - 3.11; 13)	(1.28 - 2.10; 13)
Below Mixed layer, within euphotic zone			
	2.19	0.29	0.15
-	(1.78 - 2.59; 2)	(0.10 - 0.49; 2)	(0.11 - 0.19; 2)
Below euphotic zone			
	1.79	0.49	0.31
-	(1.62 - 1.96; 2)	(0.46 - 0.52; 2)	(0.11 - 0.52; 2)
Open ocean			
Mixed Layer			
2.47	1.61	0.51	0.24
(0.15 - 11.32; 65)	(0.70 - 3.91; 69)	(0.14 - 1.39; 69)	(**0.01** - 0.95; 69)
Below Mixed layer, within euphotic zone			
6.32	6.00	1.11	0.40
(0.08 - **31.77**; 35)	(1.25 - **24.97**; 37)	(0.29 - **3.72**; 37)	(0.04 - **2.26**; 37)
Below euphotic zone			
2.78	1.99	0.63	0.64
(**0.01** - 19.44; 106)	(**0.04** - 17.23; 113)	(**0.05** - 2.76; 115)	(0.03 - 4.23; 115)

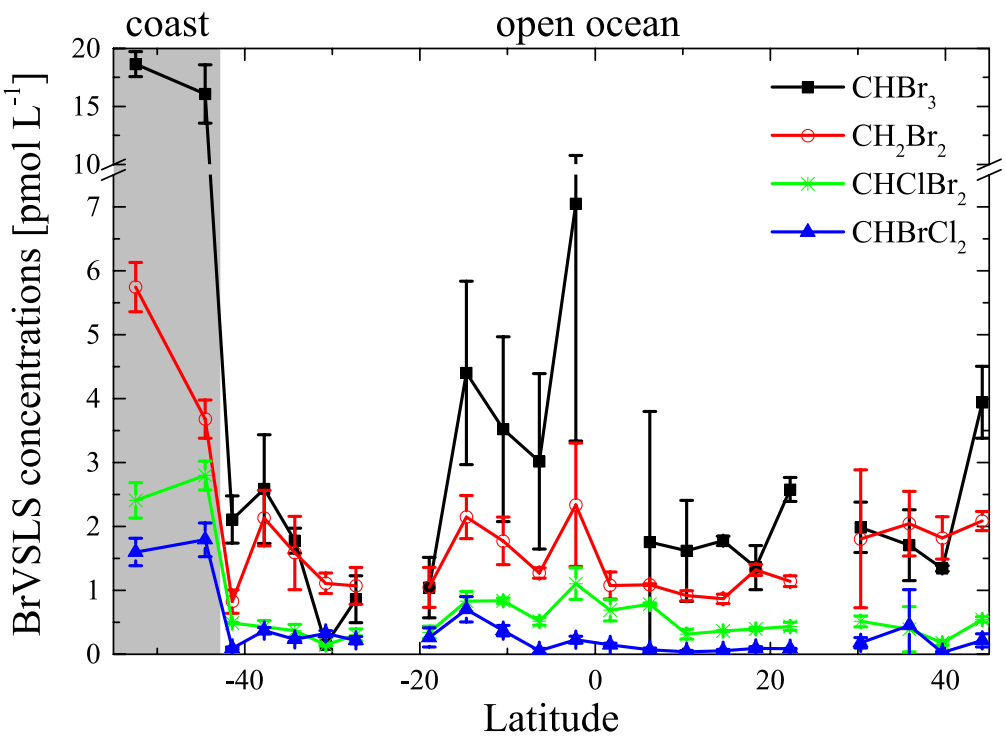

Figure 3-6. Latitudinal distributions of mean mixed layer $CHBr_3$, CH_2Br_2, $CHClBr_2$, and $CHBrCl_2$ concentrations, error bars indicate ±1 standard deviation of the mixed layer concentrations.

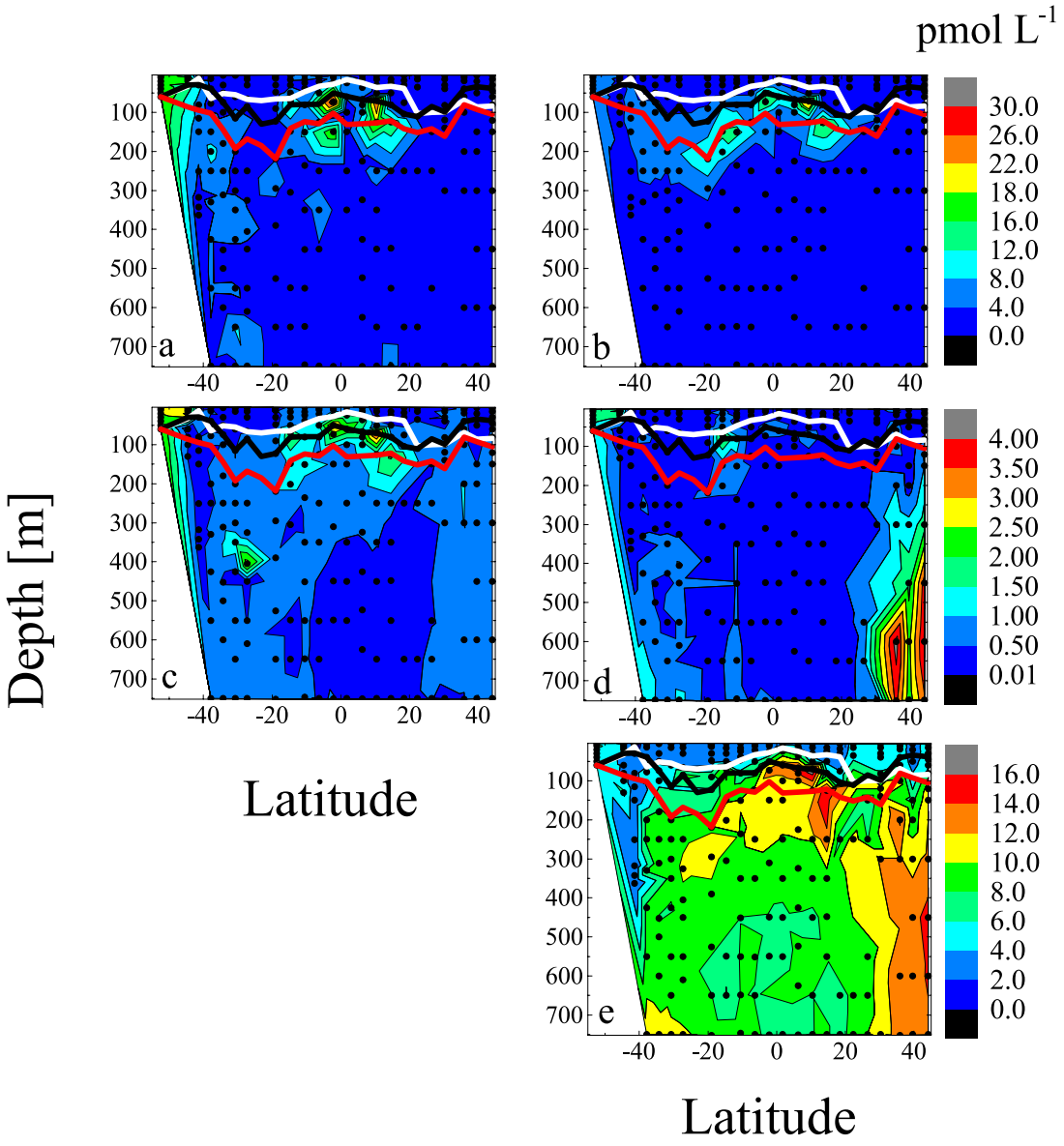

Figure 3-7. Depth profiles of (a) $CHBr_3$, (b) CH_2Br_2, (c) $CHClBr_2$, (d) $CHBrCl_2$ and (e) $CHCl_3$. White line marks the bottom of mixed layer, black line marks the depths of chlorophyll *a* maxima, and red line marks the bottom of the euphotic zone.

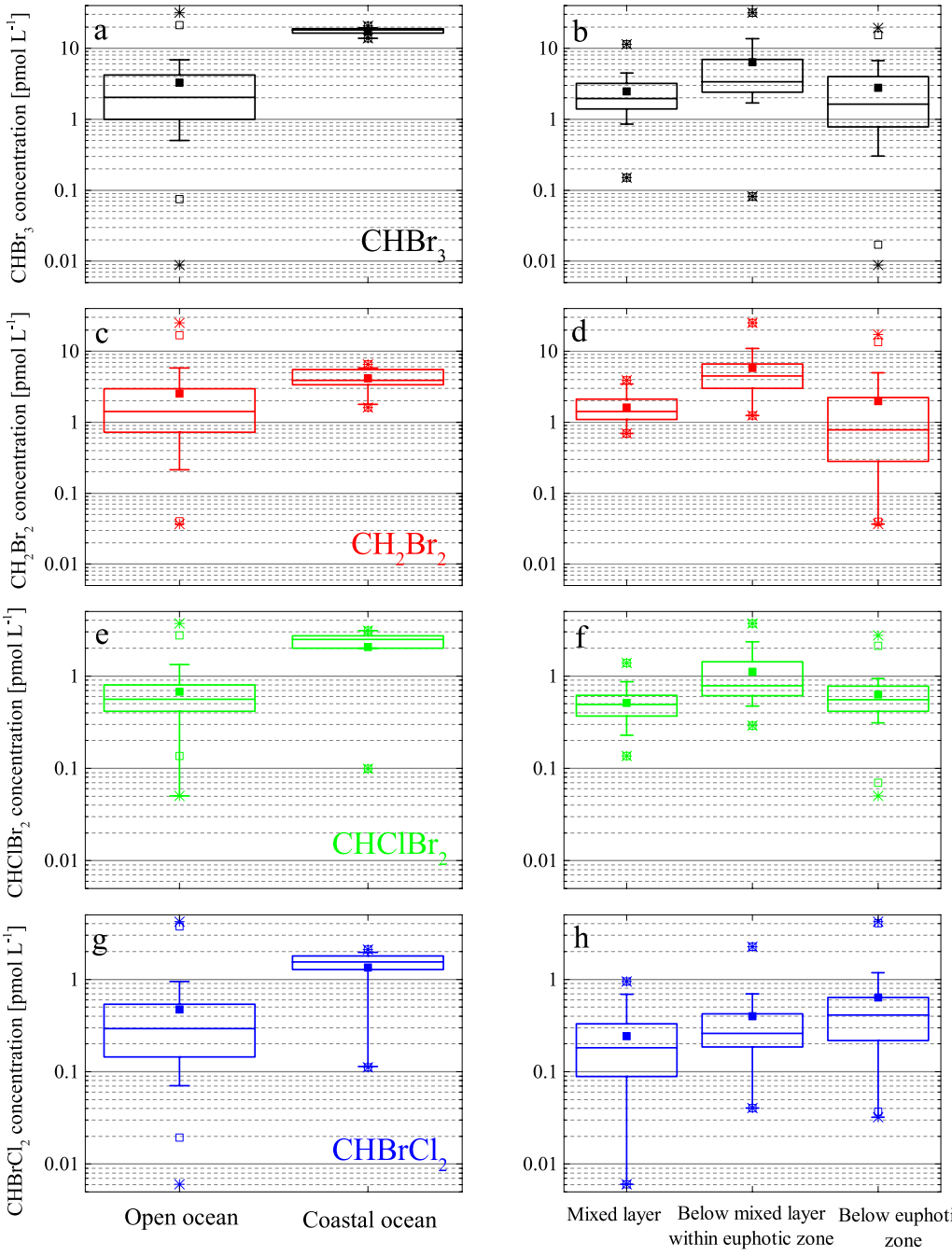

Figure 3-8. Boxplots of data grouped based on geographical setting (open ocean *vs*. coastal ocean), and data grouped based on water column layers (mixed layer, below mixed layer within euphotic zone, and below euphotic zone), for $CHBr_3$ (a and b), CH_2Br_2 (c and d), $CHClBr_2$ (e and f), and $CHBrCl_2$ (g and h). Vertical line in the box indicates median of data, filled square indicates mean of data, box range indicates 25th to 75th percentile of data, whisker indicates 10th to 90th percentile of data, open box indicates 5th to 95th percentile of data. Stars indicate minimum and maximum of data. Note that the y-axis is a log-scale.

$CHClBr_2$ and $CHBrCl_2$ concentrations were higher below the euphotic zone than in the mixed layer (Figures 3-7 and 3-8), which suggest there were sources of these two BrVSLS in deeper waters. In fact, the $CHBrCl_2$ concentration range below the euphotic zone was even higher than near the chlorophyll *a* maxima. $CHBrCl_2$ concentration was greatest below the euphotic zone in the northern temperate water column (Figure 3-7), which suggests source strengths of $CHBrCl_2$ in deeper waters could be higher than in the euphotic zone in certain regions (Figure 3-8). Our results were consistent with the observations of *Moore and Tokarczyk* [1993] in the Northwest Atlantic Ocean, where $CHClBr_2$ and $CHBrCl_2$ concentrations were higher in deeper waters compared to surface waters. The authors suggested slow successive $CHBr_3$ chlorine substitutions to $CHClBr_2$, then $CHBrCl_2$ [*Class and Ballschmiter*, 1988; *Geen*, 1992], may in part explained such features, as $CHBr_3$ produced at the upper water columns mixed and/or diffused into deeper waters.

Patches of elevated $CHBr_3$, $CHClBr_2$, and $CHBrCl_2$ were observed below the euphotic zone, particularly in the AAIW and NPIW (Figure 3-7). Other studies have reported high concentrations of BrVSLS in surface Antarctic waters. For example, concentration ranges from 5.25 to 280 pmol L^{-1} and 2.99 to 30.0 pmol L^{-1} were observed in Antarctic surface seawater for $CHBr_3$ and CH_2Br_2, respectively, depending on the location of observations [*Abrahamsson et al.*, 2004; *Butler et al.*, 2007; *Carpenter et al.*, 2007a; *Hughes et al.*, 2011; *Mattson et al.*, 2012]. As suggested by these studies, the high $CHBr_3$ and CH_2Br_2 concentrations may be attributed to sources like phytoplankton blooms and sea ice. Hydrolysis half-lives of $CHBr_3$, CH_2Br_2, $CHClBr_2$, and $CHBrCl_2$ at 20°C are 686, 183, 137, and 274 years,

respectively [*Vogel et al.*, 1987]. Chlorine substitution half-life of $CHBr_3$ is ~ 5 to 74 years depending on seawater temperature [*Geen*, 1992]. With such long half-lives of these BrVSLS in seawater, it is not surprising that low concentrations of these BrVSLS were retained in the AAIW, as the water mass subsided from the surface where prolific sources of these BrVSLS existed. While elevated $CHClBr_2$ and $CHBrCl_2$ concentrations in the AAIW may be partially attributed to successive chlorine substitution of $CHBr_3$, it is difficult to assess the magnitude of the contributions of this process to the features observed in this study.

Nonetheless, it would be reasonable to speculate that the $CHBrCl_2$ maxima and elevated $CHClBr_2$ located in the NPIW were, at least partially, the result of successive chlorine substitution of $CHBr_3$. The apparent age of NPIW (few decades) in this location was old enough relative to chlorine substation half-life of $CHBr_3$ to result in such a feature. In this water mass, $CHBr_3$ concentrations were not elevated, which may potentially suggest conversions to $CHClBr_2$ and then $CHBrCl_2$. Although chloroform ($CHCl_3$) is not discussed in detail in this study, it is worth noting that $CHCl_3$ concentrations were also elevated in the NPIW (Figure 3-7e), probably due to further chlorine substitution of $CHBrCl_2$. Such features of $CHCl_3$ in NPIW further support the hypothesis of successive chlorine substitution of $CHBr_3$.

3.3.3 Sources of $CHBr_3$, CH_2Br_2, $CHClBr_2$, and $CHBrCl_2$ in the euphotic zone

3.3.3.1 Sources of $CHBr_3$, CH_2Br_2, $CHClBr_2$, and $CHBrCl_2$ in the coast

Elevated $CHBr_3$, CH_2Br_2, $CHClBr_2$, and $CHBrCl_2$ concentrations were observed in Chilean coastal waters (*i.e.* Cast 1 and 2; Figures 3-6, 3-7, and 3-8). Distinctly lower salinity in this region implies freshwater input from the continent (Figure 3-2). The southern Chilean coast, where Cast 1 and 2 were collected, is characterized as a fjord coast, dominated by islands, channels, and fjords [*Fariña et al.*, 2008]. The subtidal kelp *Macrocystis pyryfera* and the intertidal kelp *Durvillea antarctica* are the most representative macroalgae in this region [*Fariña et al.*, 2008; *Lüning*, 1990; *Ríos et al.*, 2007]. In this region, phytoplankton assemblages have heterogeneous spatial and temporal distribution patterns, with diatoms being the most abundant phytoplankton group year-round [*Alves-de-Souza et al.*, 2008]. The giant kelp *Macrocystis pyryfera* has been shown to produce considerable amounts of $CHBr_3$ and CH_2Br_2 [*Manley et al.*, 1992]. Numerous laboratory studies also showed production of $CHBr_3$ and CH_2Br_2 from certain diatoms, which are likely associated with bromoperoxidase activity [*Hill and Manley*, 2009; *Moore et al.*, 1996; *Moore et al.*, 1995b; *Tokarczyk and Moore*, 1994]. Therefore, it is not surprising that the maximum mixed layer concentrations of $CHBr_3$, CH_2Br_2, $CHClBr_2$, and $CHBrCl_2$ were observed in this region (Table 3-1, Figure 3-6), which may be explained either due to *in situ* biologically mediated production or transport from the channels.

During the BLAST-I cruise conducted in 1994, high $CHBr_3$ and CH_2Br_2 concentrations, up to 90.23 and 25.83 pmol L^{-1}, respectively, were observed in the inland passage [*Butler et al.*, 2007], which supports the role of channels on the Chilean coast as significant sources of BrVSLS to the atmosphere. The HalocAST-P cruise track followed the coast outside of the inland passage and mixed layer $CHBr_3$ and CH_2Br_2 concentrations were much lower than those observed during the BLAST I cruise (Table 3-1, Figure 3-6). Such a substantial differences in $CHBr_3$ and CH_2Br_2 concentrations may suggest significant spatial variability in their concentrations, if we assume inter-annual differences in $CHBr_3$ and CH_2Br_2 production was not significant. The fact that $CHBr_3$ and CH_2Br_2 concentrations were higher inside the inland passage may suggest more prolific sources. Moreover, unlike outside the inland passage, the restricted water circulations in the inland passage may also allow $CHBr_3$ and CH_2Br_2 to accumulate. Despite the fact that the $CHBr_3$ and CH_2Br_2 mixed layer concentration maxima observed in this study were lower than other studies in macroalgal-dominated regions, where extremely high concentrations of BrVSLS were observed in surface waters above macroalgal beds, the concentration patterns observed in the Chilean coast were consistent with other studies [*Carpenter and Liss*, 2000; *Fogelqvist and Krysell*, 1991; *Goodwin et al.*, 1997; *Gschwend and MacFarlane*, 1986; *Jones and Carpenter*, 2005; *Laturnus*, 1996, 2001; *Laturnus et al.*, 1996; *Liu et al.*, 2011; *Moore and Tokarczyk*, 1993; *Yokouchi et al.*, 2005]. *Lin and Manley* [2012] found that $CHBr_3$ and CH_2Br_2 production is a function of coastal dissolved organic matter (DOM) characteristics (*i.e.* size fraction and source). Therefore, terrestrial-derived DOM

carried by the channels may also influence $CHBr_3$ and CH_2Br_2 concentrations observed in this region.

Flow cytometry cell counts of picoplankton, which have the same sampling resolution as the BrVSLS, allowed us to examine BrVSLS biological sources in further detail. In the Chilean coastal region, CH_2Br_2 was significantly correlated with *Synechococcus* spp. and picoeukaryotes (< 3 μm algae including chlorophytes, pelagophytes, haptophytes), and $CHClBr_2$ was significantly correlated with heterotrophic bacteria (Table 3-2). However, $CHBr_3$ and $CHBrCl_2$ did not show any association with any of the picoplankton groups. Relationship between BrVSLS with phytoplankton taxonomic group derived from pigment analysis was not considered in the coastal region due to small sample size (n = 5).

Table 3-2. Spearman's rank correlation coefficient (ρ) of BrVSLS with picoplankton, *p*-value and number of samples (*n*) are presented in the parentheses. Relationships between the BrVSLS with photosynthetic picoplanktons were not considered below the euphotic zone. Below the euphotic zone, only relationships between BrVSLS and heterotrophic bacteria were considered. "ns" indicates not significant correlation.

	Heterotrophic bacteria	*Prochlorococcus*	*Synechococcus*	Picoeukaryotes
Coastal euphotic zone				
$CHBr_3$	ns	ns	ns	ns
CH_2Br_2	ns	ns	0.92 (<< 0.001; 13)	0.90 (<< 0.001; 13)
$CHClBr_2$	0.59 (<< 0.03; 13)	ns	ns	ns
$CHBrCl_2$	ns	ns	ns	ns
Open Ocean				
Mixed Layer				
$CHBr_3$	ns	ns	0.27 (0.03; 65)	ns
CH_2Br_2	0.36 (<< 0.003; 65)	-0.25 (0.04; 67)	0.46 (<< 0.001; 68)	ns
$CHClBr_2$	0.24 (<< 0.05; 65)	ns	0.27 (0.02; 68)	ns
$CHBrCl_2$	ns	ns	ns	ns
Below Mixed layer, within euphotic zone				
$CHBr_3$	ns	ns	ns	ns
CH_2Br_2	ns	ns	ns	ns
$CHClBr_2$	ns	0.36 (0.03; 36)	ns	ns
$CHBrCl_2$	ns	ns	ns	0.37 (0.03; 36)
Below euphotic zone				
$CHBr_3$	ns	-	-	-
CH_2Br_2	0.29 (0.003; 109)	-	-	-
$CHClBr_2$	ns	-	-	-
$CHBrCl_2$	ns	-	-	-

3.3.3.2 Sources of $CHBr_3$, CH_2Br_2, $CHClBr_2$, and $CHBrCl_2$ in the open ocean

In the surface open ocean, CH_2Br_2 was significantly correlated with 19'-hexanoyloxyfucoxanthin (ρ = 0.52, p = 0.03, n = 17), which is the pigment biomarker for prymnesiophytes [*Jeffrey et al.*, 2011; *Wright and Jeffrey*, 2006]. In the open ocean chlorophyll *a* maximum depths, $CHClBr_2$ was significantly correlated with violaxanthin (ρ = 0.54, p = 0.03, n = 19), which is the pigment biomarker for green

algae [*Jeffrey et al.*, 2011; *Wright and Jeffrey*, 2006]. $CHBr_3$ and $CHBrCl_2$ were not significantly correlated with any of the pigment biomarkers. While some studies have observed correlations between $CHBr_3$ and pigment biomarkers [*Quack et al.*, 2007a; *Raimund et al.*, 2011], the lack of correlation between $CHBr_3$ and pigment biomarkers is not uncommon. *Abrahamsson et al.* [2004] and *Mattson et al.* [2012] consistently found that $CHBr_3$ did not yield significant correlations with any of the pigment biomarkers in Antarctic seawater. Such a lack of correlation between $CHBr_3$ and pigment biomarkers may be due to differences in their turnover times in the water column [*Mattson et al.*, 2012], short term (diurnal) variability in $CHBr_3$ production rate [*Ekdahl et al.*, 1998], species specificity to $CHBr_3$ production (which cannot be resolved by using pigment biomarkers), and/or the interplay between different phytoplankton and bacterioplankton groups.

Zeaxanthin is a pigment biomarker commonly used for assessing the presence of cyanobacteria [*Jeffrey et al.*, 2011; *Wright and Jeffrey*, 2006]. However, unlike the flow cytometry data, information from zeaxanthin distributions cannot distinguish important cyanobacteria taxa such as *Synechococcus* and *Prochlorococcus*. Several studies have indicated cyanobacteria as a possible source of $CHBr_3$ [*Karlsson et al.*, 2008; *Quack et al.*, 2007a]. Therefore, data from flow cytometry were employed to examine the relationship between the BrVSLS and picoplankton in greater detail. In addition, heterotrophic bacteria counts were also obtained, which allowed us to examine the potential influence of heterotrophic bacteria in BrVSLS biogeochemistry. However, it should be noted that heterotrophic bacteria abundance does not necessarily correlate with bacterial activity. We found that the BrVSLS were

correlated with various picoplankton groups at different layers of the water column (Table 3-2). For example, $CHBr_3$, CH_2Br_2, and $CHBrCl_2$ were significantly correlated with *Synechococcus* spp. in the open ocean mixed layer (Table 3-2). Despite the fact that $CHBr_3$ was only weakly correlated with *Synechococcus*, more detailed phytoplankton assemblage analyses could reveal relationships between $CHBr_3$ and specific groups of phytoplankton.

CH_2Br_2 was significantly correlated with heterotrophic bacteria in the mixed layer and below the euphotic zone (Table 3-2), which may indicate bacterial production. While bacterial degradation of CH_2Br_2 has been observed [*Goodwin et al.*, 1998; *Hughes et al.*, 2013], to date, no information is available on bacterial production of CH_2Br_2. In the open ocean mixed layer, $CHClBr_2$ was also correlated with heterotrophic bacteria. *Moore* [2003] indicated bacteria are unlikely to affect $CHBr_3$ production, which supports our observations of a lack of correlation of $CHBr_3$ with bacteria. Our results suggest that heterotrophic bacteria may also contribute to BrVSLS biogeochemistry in terms of their destruction and production.

In the open ocean water column, mean $CHBr_3$ and CH_2Br_2 concentrations were comparable in the mixed layer, below the mixed layer within the euphotic zone, and below the euphotic zone. In contrast, $CHBr_3$ concentrations in the coastal ocean mixed layer were more than three times higher than CH_2Br_2. While these observations may suggest differences in their formation and degradation rates in the coastal ocean and open ocean, it is also possible that different DOM characteristics were influencing such trends. *Lin and Manley* [2012] found that CH_2Br_2 was not always formed when different DOM size fractions collected from various locations in California were

exposed to bromoperoxidase. This finding may indicate terrestrially derived DOM is potentially more reactive for $CHBr_3$ formation, compared to DOM derived in the marine environment.

3.3.4 Correlations between $CHBr_3$ and CH_2Br_2, $CHClBr_2$, and $CHBrCl_2$

Despite the differences in the degree of correlations, $CHBr_3$ was significantly correlated with CH_2Br_2 and $CHClBr_2$ throughout the water column for the entire HalocAST-P cruise (Table 3-3). Significant correlation between $CHBr_3$ and CH_2Br_2 has been frequently interpreted as the two are derived from common sources. However, $CHBr_3$ and CH_2Br_2 significantly correlated with different biological parameters during the HalocAST-P cruise. For example, heterotrophic bacteria abundance only significantly correlated with CH_2Br_2 but not with $CHBr_3$. Such a pattern suggests different biogeochemical factors within the ecosystem can affect the concentrations of these compounds separately. This finding is consistent with observations by [*Quack et al.*, 2007a] in the Mauritanian upwelling system. A recent laboratory study by *Hughes et al.* [2013] found that $CHBr_3$ and CH_2Br_2 concentrations in seawater were controlled by different processes. The authors hypothesized that CH_2Br_2 is transformed from $CHBr_3$ via biologically mediated processes. Such a hypothesis was supported by their experimental results and other lines of evidence previously observed in the laboratory and field [*Hughes et al.*, 2009; *Tokarczyk and Moore*, 1994]. Therefore, the co-occurrence of $CHBr_3$ and CH_2Br_2 is potentially due to

processes occurring in a common type of ecosystem and controlled by different factors, rather than their being derived from a common biological source.

$CHBr_3$ was only significantly correlated with $CHBrCl_2$ in the mixed layer (Table 3-3). It is interesting to consider $CHBrCl_2$ below the euphotic zone, where successive chlorine substitution of $CHBr_3$ was proposed. $CHBrCl_2$ was significantly correlated with $CHClBr_2$ ($\rho = 0.55$, $p << 0.001$, $n = 106$) but not associated with $CHBr_3$ below the euphotic zone, which may further support the idea of chlorine substitution, as $CHBrCl_2$ is not directly linked to $CHBr_3$ in such a chemical process.

Table 3-3. Spearman's rank correlation coefficient (ρ) of $CHBr_3$ with CH_2Br_2, $CHClBr_2$, and $CHBrCl_2$, p-value and number of samples (n) are presented in the parentheses. "ns" indicates not significant correlation.

	CH_2Br_2	$CHClBr_2$	$CHBrCl_2$
Mixed Layer			
$CHBr_3$	0.67 (<< 0.001; 78)	0.81 (<< 0.001; 78)	0.57 (<< 0.001; 78)
Below mixed layer within the euphotic zone			
$CHBr_3$	0.56 (<< 0.001; 35)	0.66 (<< 0.001; 35)	0.30^{ns} (0.08; 35)
Below euphotic zone			
$CHBr_3$	0.70 (<< 0.001; 106)	0.29 (0.003; 106)	0.06^{ns} (0.56; 106)

3.4 Conclusions

Our findings suggest BrVSLS production is in general related to photosynthetic biomass production, and heterotrophic bacteria may be sources for certain BrVSLS, for example, CH_2Br_2. However, the relationship between BrVSLS production and photosynthetic biomass production is not straight forward, and likely involves complex factors, such as phytoplankton species composition, interactions

between phytoplankton groups and/or bacterioplankton, and enzymatic reactions with specific DOM moieties. Our results also suggest $CHBr_3$ and CH_2Br_2 may be derived from disparate sources and are controlled by difference biogeochemical processes in certain regions. Finally, $CHBrCl_2$ may have more significant sources in deeper waters than biochemical sources found in the euphotic zone, and successive chlorine substitution of $CHBr_3$ may be one of them. To better understand source of the BrVSLS and their feedbacks under climate change, fundamental studies concerning their formation and degradation mechanisms are required. A better understanding of these mechanisms is important as most of the anthropogenic ozone depleting substances (ODS) were controlled by the Montreal Protocols, and the naturally derived ODS will be more important in controlling ozone chemistry in the future atmosphere.

CHAPTER IV

SPATIAL AND TEMPORAL DISTRIBUTIONS OF BROMOFORM AND DIBROMOMETHANE IN THE ATLANTIC OCEAN AND THEIR RELATIONSHIP WITH PHOTOSYNTHETIC BIOMASS

4.1 Introduction

Brominated very short-lived substances (BrVSLS), thought of as brominated trace gases with atmospheric lifetimes of 0.5 year or less, are potentially significant contributors to catalytic ozone loss in the troposphere and lower stratosphere [*Montzka and Reimann*, 2011]. BrVSLS have received considerable attention because bromine is more effective in depleting ozone than chlorine on a per atom basis [*Garcia and Solomon*, 1994; *Solomon et al.*, 1995]. Once emitted to the atmosphere, BrVSLS are degraded either via reactions with hydroxyl radicals or photolysis in the atmosphere resulting in inorganic bromine (Br_y), which may then participate in catalytic ozone destruction. Bromoform ($CHBr_3$) and dibromomethane (CH_2Br_2) are the most abundant BrVSLS accounting for ~ 80% of the very short-lived organic bromine in the marine boundary layer [*Law and Sturges*, 2007]. Mean local atmospheric lifetimes for $CHBr_3$ and CH_2Br_2 are 24 days and 123 days, respectively [*Montzka and Reimann*, 2011]. Along with the minor VSLS constituents such as bromodichloromethane ($CHBrCl_2$), chlorodibromomethane ($CHClBr_2$), and bromochloromethane (CH_2BrCl), these trace gases are capable of supplying 1 to 8 parts per trillion (ppt) of Br_y to the

stratosphere, which is equivalent to ~ 4 to 36% of the total stratospheric bromine [*Montzka and Reimann*, 2011].

$CHBr_3$ and CH_2Br_2 are predominantly produced naturally in seawater and are believed to be associated with phytoplankton and macroalgae [*Carpenter and Liss*, 2000; *Goodwin et al.*, 1997; *Manley et al.*, 1992; *Moore et al.*, 1996; *Sturges et al.*, 1992; *Sturges et al.*, 1993]. However, biological proxies, such as chlorophyll *a*, usually do not significantly correlate with these BrVSLS. Currently, we do not have an adequate conceptual model of the sources and formation mechanisms of the BrVSLS, and the environmental forcing that influences BrVSLS production in the ocean. To date, no prolific terrestrial natural sources for these two BrVSLS have been identified, although small amounts of $CHBr_3$ emissions were observed in a flooded rice paddy [*Redeker et al.*, 2003]. $CHBr_3$ also has anthropogenic sources, as it is one of the by-products of water disinfection [*Quack and Wallace*, 2003; *Rook*, 1974, 1976]. Despite the significant amount of $CHBr_3$ released from such a process, it only accounts for less than 1 % of the total global emission [*Quack and Wallace*, 2003].

A number of recent studies reported $CHBr_3$ and CH_2Br_2 sources, atmospheric mixing ratios, seawater concentrations, and sea-to-air fluxes in different regions of the world [*Butler et al.*, 2007; *Carpenter and Liss*, 2000; *Carpenter et al.*, 2009; *Carpenter et al.*, 2007b; *Quack and Wallace*, 2003; *Quack et al.*, 2007a; *Quack et al.*, 2007b; *Quack et al.*, 2004; *Raimund et al.*, 2011]. However, large uncertainties remain in estimating their global budgets because of the significant spatial and temporal variations of $CHBr_3$ and CH_2Br_2. This is especially true for $CHBr_3$, which is not well-mixed in the atmosphere owing to its short local lifetime [*Montzka and Reimann*,

2011]. Therefore, elevated $CHBr_3$ atmospheric mixing ratios are usually confined to their source regions. A model study showed that altering $CHBr_3$ emission source distribution scenarios from only the tropical open ocean to the tropical coastal and open oceans combined would significantly alter the estimated annual global sea-to-air flux from 5.0 to 7.4 Gmol Br yr^{-1} [*Warwick et al.*, 2006]. While this finding highlights the importance of the coastal ocean as a significant contributor to atmospheric $CHBr_3$, it also clearly shows that the global $CHBr_3$ emission budget is sensitive to varying source types and emission regions.

Quack and Wallace [2003] combined large amounts of data from different studies conducted in different regions of the ocean to provide an estimate of the $CHBr_3$ global annual net sea-to-air flux. The authors noted, however, that different measurement techniques and calibration methods used in the various studies may have resulted in large discrepancies in their estimate. The authors also suggested that the uncertainty in their global estimate largely depends on uncertainties in the saturation anomalies. Moreover, extrapolation with relatively sparse and variable data, as well as choice of different gas exchange coefficient parameterizations (k_w) in different studies, may also introduce large discrepancies in estimating global budget of $CHBr_3$ and CH_2Br_2. Finally, in the data compiled by *Quack and Wallace* [2003], atmospheric and seawater measurements were not always paired, which highlighted the importance of measuring atmospheric and seawater concentrations simultaneously in order to minimize such uncertainties.

Here, we present air and seawater measurements of $CHBr_3$ and CH_2Br_2 over a large spatial extent and over a period of almost two decades. Importantly, $CHBr_3$ and

CH_2Br_2 were measured using the same analytical technique during all of the cruises discussed. Measurements of boundary layer air and of seawater were made simultaneously and were calibrated against the National Oceanic and Atmospheric Administration (NOAA) scale. The objective of this study is to employ datasets with less variation in analytical and calibration techniques, which should reduce uncertainty and improve our understanding of global distributions of $CHBr_3$ and CH_2Br_2, their marine sources, and their global annual net fluxes. BrVSLS data were collected from five cruises from 1994 to 2010 (Figure 4-1; Table 4-1) in the Atlantic basin. A16 north (A16N) and A16 south (A16S), which occurred in 2003 and 2005, are both part of the Climate Variability and Predictability (CLIVAR) repeat hydrography project onboard *R/V Ronald H. Brown*. The Halocarbon Air-Sea Transect – Atlantic (HalocAST-A) cruise in 2010, onboard the *FS Polarstern,* was conducted in an attempt to repeat the Bromine Latitudinal Air-Sea Transect II (BLAST-II) cruise conducted in 1994 [*Butler et al.*, 2007; *Lobert et al.*, 1996], along similar latitudinal bands within a similar region and season. BrVSLS data for the BLAST-II and Gas Exchange Experiment 98 (GaxEx98) cruises were obtained from the NOAA Earth System Research Laboratory Global Monitoring Division database (http://www.esrl.noaa.gov/gmd/hats/ocean/) [*Butler et al.*, 2007; *King et al.*, 2000; *Lobert et al.*, 1996] and are also identified in the HalOcAt database.

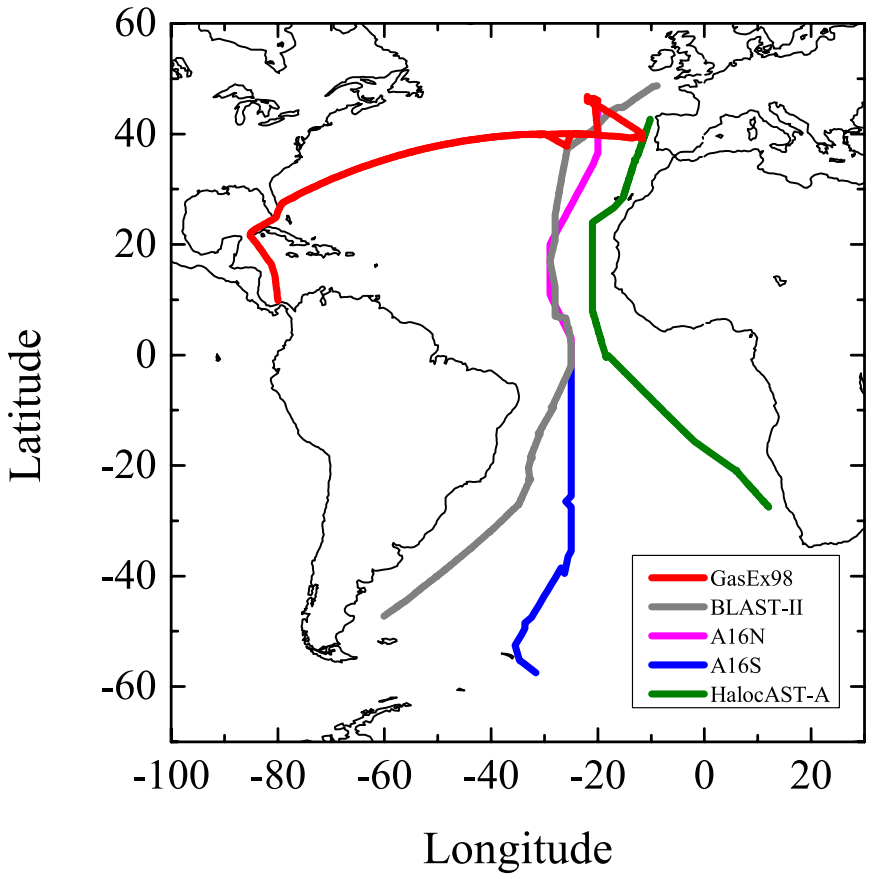

Figure 4-1. Ship tracks for the GasEx98 (red line), BLAST-II (grey line), A16N (magenta line), A16S (blue line), and HalocAST-A (green line) cruises.

Table 4-1. List of cruises presented in this study.

Expedition	Start/End Points	Season	Research Vessel
CLIVAR A16N			
Leg B	Reykjavik, Iceland (June 19, 2003) - Funchal, Madeira (July 10, 2003)	Summer	*R/V Ron Brown* (US)
Leg C	Funchal, Maeria (July 15, 2003) - Natal, Brazil (August 10, 2003)	Summer	*R/V Ron Brown* (US)
CLIVAR A16S			
Leg 2	Punta Arenas, Chile (Jan 11, 2005) - Fortaleza, Brazil (Feb 22, 2005)	Fall	*R/V Ron Brown* (US)
HalocAST-A	Bremerhaven, Germany (October 25, 2010) - Cape Town, South Africa (November 24, 2010)	Winter (NH) / Summer (SH)	*FS Polarstern* (DE)
BLAST-II [a,b]	Bremerhaven, Germany (October 18, 1994) - Punta Arenas, Chile (November 21, 1994)	Winter (NH) / Summer (SH)	*FS Polarstern* (DE)
GasEx98[b,c]			
Leg 1	Miami, FL (May 7, 1998) - Lisbon, Portugal (May 25, 1998)	Early summer (NH)	*R/V Ron Brown* (US)
Legs 2 to 4	Lisbon, Portugal (June, 1998) - Miami, FL (July 15, 1998)	Summer (NH)	*R/V Ron Brown* (US)
References	a. *Lobert et al.,* 1996 b. *Butler et al*., 2006 c. *King et al*., 2000		

4.2 Method

4.2.1 Gas Analyses

Trace gases were separated and analyzed using a cryo-trapping and focusing system with gas chromatography-mass spectrometry (GC-MS) detection. Detailed analytical system configurations were described in *Yvon-Lewis et al.* [2004]. Modifications made to improve trapping and drying performance over the course of time are summarized in *Butler et al.* [2007]. For the HalocAST-A cruise, dry mole fractions of the BrVSLS in the atmosphere and seawater were measured alternately every ~52 minutes, or ~112 minutes when calibration standard was run in sequence, which was after every forth injection. Dual calibration standards were used during the HalocAST-A cruise to ensure measurement accuracy. Equilibrium partial pressures for

surface seawater were measured in headspace samples collected from a Weiss-type equilibrator with continuous seawater flowing from the ship's underway-pumping system. Atmospheric samples were collected from a sampling line with its inlet mounted on the mast at the bow of the ship. The samples were dried with two Nafion dryers (Perma Pure, NJ) in series, cryo-trapped and focused at -80 °C, and then desorbed at 200°C into a DB-VRX column (Agilent J&W; I.D. 0.18 mm; Film 1.0 μm; 10 m pre-column and 30 m main column). For the CLIVAR A16N and A16S cruises, during which continuous underway measurements of the trace gases were not available, discrete seawater samples were collected from CTD casts daily with 100 mL glass syringes, and analyzed using an automated purge-and-trap system with a GC-MS configured similar to the HalocAST-A cruise but with a different column (Agilent J&W; I.D. 0.25 mm; Film 1.4 μm; 15 m pre-column and 45 m main column). Details of the automated purge and trap system configuration are described in *Yvon-Lewis et al.* [2004]. Purge efficiencies for $CHBr_3$ and CH_2Br_2 determined for the two cruises were > 82%. For the CLIVAR A16N and A16S cruises, air samples were collected daily with stainless-steel canisters with the air inlet extended ~5 m above deck and into the wind.

Calibration standards were whole air working-standards calibrated before and after the cruises against a whole air working-standard obtained from the NOAA Global Monitoring Division (GMD). Detection limits for $CHBr_3$, CH_2Br_2, $CHBrCl_2$ and $CHClBr_2$ during these cruises were 0.02 ppt, 0.03 ppt, 0.01 ppt, and 0.01 ppt, or lower. The largest analytical uncertainty was 7.0% for $CHBr_3$, 6.0% for CH_2Br_2, and 9.0% for $CHBrCl_2$ and $CHClBr_2$. Analytical and calibration methods for the BLAST-II

and GasEx98 cruises were described in *King et al.* [2000] and *Lobert et al.* [1996] and were similar to methods used in the later cruises.

All BrVSLS were measured in dry mole fraction. For atmospheric values, dry mole fraction (atmospheric mixing ratio in ppt) was reported; hence, the values do not vary with local humidity. For the equilibrated seawater values, the measured dry mole fraction was corrected to partial pressure (in pico atmosphere, patm) and sea surface conditions (temperature and seawater vapor pressure), and then converted to pico molar (pmol L^{-1}) using the gas constant and Henry's Law constant (H) [*Moore et al.*, 1995a]. For seawater concentrations measured from discrete water samples (*i.e*. A16N and A16S), concentrations were corrected to pmol L^{-1} with the known sample volume. Atmospheric and seawater dry mole fractions were converted to patm using appropriate water vapor corrections [*Weiss and Price*, 1980] for calculating saturation anomalies (Δ) and fluxes (F).

4.2.2 Saturation anomaly and flux calculations

Saturation anomalies (Δ, %) are defined as percent deviation from equilibrium, where positive Δ and negative Δ indicated the BrVSLS in seawater were supersaturated and undersaturated relative to the atmosphere. Saturation anomalies were calculated with the following equation:

$$\Delta = \frac{p_w - p_a}{p_a} \times 100\% \qquad \text{(Equation 4.1)}$$

where, p_w (patm) is the partial pressure for the surface seawater, corrected from partial pressure measured in the equilibrator (p_{eq}, patm), and p_a (patm) is the partial pressure in the atmosphere.

The net sea-to-air fluxes (F, nmol m^{-2} d^{-1}) for $CHBr_3$ and CH_2Br_2 were calculated with the following equation:

$$F = k_w(C_w - \frac{p_a}{H}) \quad \text{(Equation 4.2)}$$

where, k_w (m s^{-1}) is the gas exchange coefficient using the *Sweeney et al.* [2007] parameterization and corrected for the Schmidt number of the gases. Wind speeds were corrected to 10 m (u_{10}; m s^{-1}) above the sea surface from the height where they were originally measured [*Erickson*, 1993] for determining k_w (Figure 4-2). The Schmidt numbers for the BrVSLS were calculated from the kinematic viscosity of seawater based on viscosity and density of the seawater [*Millero*, 1974; *Millero and Poisson*, 1981] and diffusivities of the gases [*Hayduk and Laudie*, 1974]. H (L atm mol^{-1}) is the Henry's law constant converted from the dimensionless Henry's law constant reported by *Moore et al.* [1995a]. C_w (mol L^{-1}) is equilibrium concentrations of the gas in seawater. p_a (atm) is partial pressure of the gas in the atmosphere as defined above.

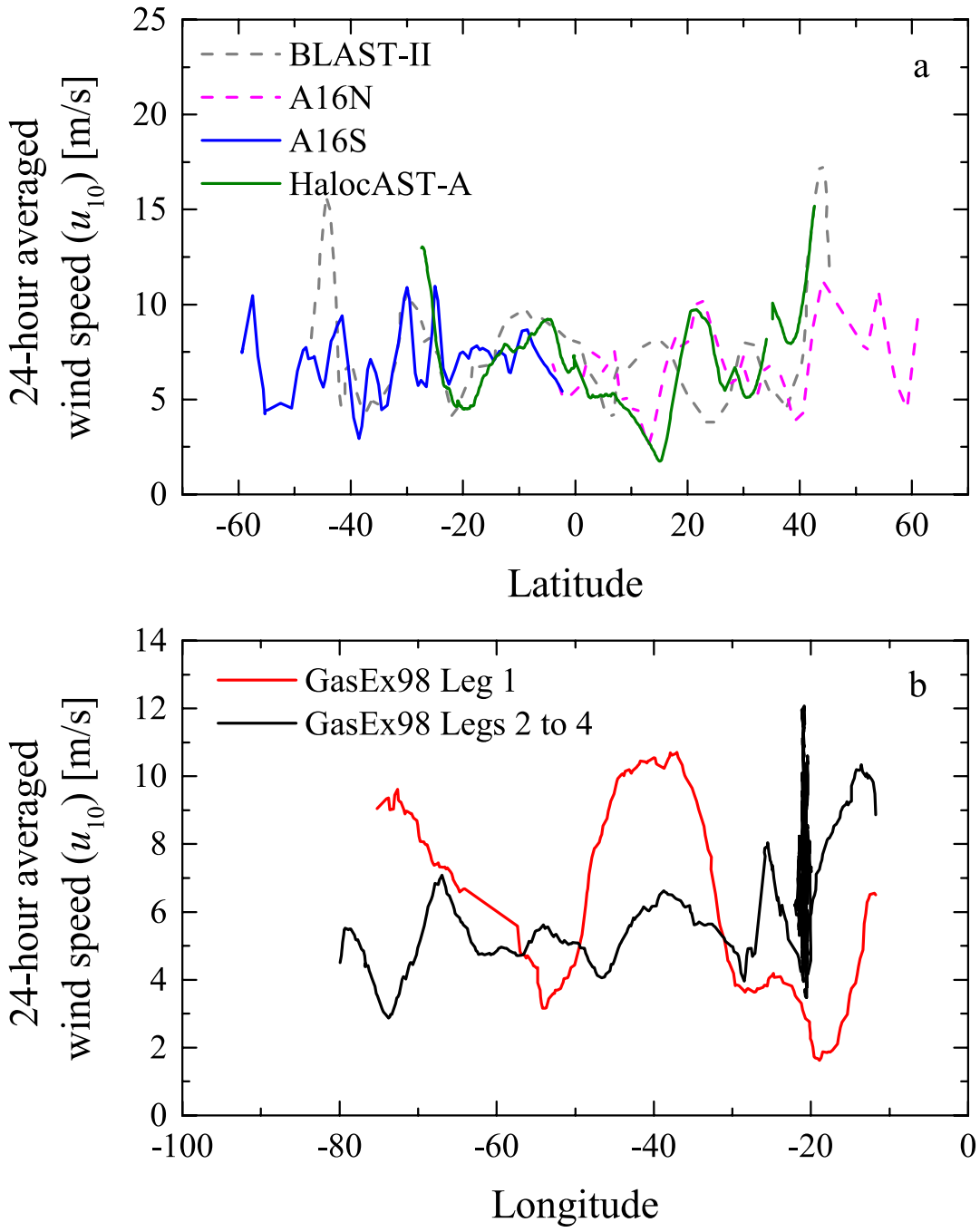

Figure 4-2. 24 hours averaged wind speed at 10 m above sea surface (u_{10}) for (a) the BLAST-II, A16N, A16S, and HalocAST-A cruises and (b) GasEx98 Legs 1, 2, 3, and 4.

4.2.3 Measurements of other biogeochemical variables

For the HalocAST-A cruise, a series of biogeochemical samples were collected to better understand source distributions of $CHBr_3$ and CH_2Br_2 and their relationships with photosynthetic biomass in seawater. Each day, samples for picoplankton abundance, dissolved nutrient concentrations, dissolved organic carbon (DOC) concentration, and pigment concentrations were collected from the ship's membrane seawater-pumping system, which was designed for collecting underway biogeochemical samples. To account for spatial change of ship's location and variability of biogeochemical and halocarbon data, all the biogeochemical measurements were paired with the nearest halocarbon measurements based on sampling location. While this is the most conservative approach to ensure less bias, it is possible that different turnover times of each variable may lead to some uncertainties in correlations between the BrVSLS and biogeochemical data.

Dissolved nutrients, urea (CH_4N_2O), nitrate (NO_3^-), nitrite (NO_2^-), ammonium (NH_4^+), phosphate (PO_4^{3-}), and silicate (SiO_4^{4-}), and DOC samples were filtered through pre-combusted 0.7 μm nominal pore size GF/F filters and stored at -20 °C until analysis. The dissolved nutrient samples were sent to the Geochemical and Environmental Research Group (GERG) at Texas A & M University for analysis. Dissolved nutrient samples were analyzed following well-established protocols on an Astoria-Pacific Analyzer [*Armstrong et al.*, 1967; *Bernhardt and Wilhelms*, 1967; *Harwood and Kühn*, 1970]. DOC analyses were performed on a Shimadzu TOC-

VCSH/CSN analyzer using high-temperature catalytic oxidation (HTC), as described by *Guo et al.* [1994].

For each pigment sample, 5 to 10 L of seawater were filtered through a pre-combusted 0.7 μm nominal pore size GF/F filters until color were visible on the filters. The filters were frozen immediately at -80 °C and kept frozen until analysis back in the laboratory with high performance liquid chromatography (HPLC). The phytoplankton pigment extraction procedure was followed as described in *Wright et al.* [1991]. Details of the analytical method are described in [*Liu et al.*, 2013], following the analytical configuration described in *Chen et al.* [2003].

For flow cytometry sample collection, 1 mL of water collected from the flow-through membrane pump was filtered into a round-bottom tube with a 35 μm mesh cell strainer (BD Falcon) and fixed with 20 μL 10% paraformaldehyde for 10 minutes (final concentration 0.2%). The fixed samples were then quickly frozen at -80 °C in cryotubes and kept frozen until analysis. Picoplankton and heterotrophic bacteria were counted with a Becton Dickinson FACSCalibur flow cytometer following configuration and protocol described in *Campbell* [2001]. For non-pigmented, heterotrophic bacteria, cells were stained with SYBR Green (Molecular Probes) prior to introduction into the flow cytometer. Data were analyzed using CytoWIN [*Vaulot*, 1989].

4.2.4 Data handling and statistical methods

Exceptionally high or low values were re-verified for potential instrumental error and removed if necessary. Abnormal values of BrVSLS concentrations due to instrumental error were determined from CFC-11 within the same run as an inert tracer. All data were tested for normality to determine the most appropriate statistical method used for data interpretation. Spearman's rank correlation was chosen to assess the association between parameters, due to the non-normal distribution of the data. Spearman's rank correlation analyses were evaluated at the 95% confidence level. Significance of correlation was determined using the two-tailed test. Significant differences of means from different environmental regimes (see section 3) were determined using the one-way analysis of variance (ANOVA). All statistical analyses were done with the OriginPro© version 9.0 (OriginLab©) statistic module.

4.3 Results and discussion

To assess BrVSLS variability in different geographical regimes, the ocean was divided into three regimes: open ocean, mid-ocean islands, and coastal ocean. The mid-ocean island regime was defined as locations within 200 kilometers radius of any mid-ocean islands. The coastal ocean regime was defined as locations with water depth $\leq$ 200 m. To better assess the relationship between $CHBr_3$ and CH_2Br_2 with the presence of photosynthetic biomass, the open ocean regime was further divided into three sub-regimes based on satellite observed chlorophyll *a* concentration: low

([chlorophyll *a*] < 0.1 mg m^{-3}), medium (0.1 mg m^{-3} ≤ [chlorophyll *a*] < 0.2 mg m^{-3}), and high ([chlorophyll *a*] ≥ 0.2 mg m^{-3}).

Upwelling regions, where nutrients are brought to the surface from deeper waters, are unique ecosystems compared to the rest of the open ocean. Therefore, during the HalocAST-A cruise, $CHBr_3$ and CH_2Br_2 production in the upwelling systems was examined using the biogeochemical data collected during this cruise. The African upwelling zones were defined following *Hurrell et al.* [2006]. During the HalocAST-A cruise, the ship encountered waters influenced by the Northwestern African upwelling (7 - 25°N), equatorial upwelling (3°N - 5°S), and the Southwestern African upwelling (10 – 27°S) systems. These definitions were supported by monthly-time averaged primary production data, which were derived from chlorophyll *a* data at a 9-km resolution retrieved from the Sea-viewing Wide Field-of-view Sensor (SeaWiFS) during the time of the cruise [*Acker and Leptoukh*, 2007].

4.3.1 Temporal and spatial variations in $CHBr_3$ and CH_2Br_2 concentrations

Data from the BLAST-II, GasEx98, A16N, A16S, and HalocAST-A cruises show overall temporal variations of $CHBr_3$ in its atmospheric mixing ratios and seawater concentrations in the Atlantic basin (Figure 4-3). The A16N and the northern hemispheric segment of BLAST-II cruises were conducted in similar regions but in different seasons (Table 4-1). $CHBr_3$ seawater concentrations and atmospheric mixing ratios in this region were almost three times higher in the boreal summer (A16N) compared to winter (BLAST-II), if we assume that inter-annual variations in $CHBr_3$

production is less significant than seasonal variations (Figure 4-3, Table 4-2). Although the differences for CH_2Br_2 were not as substantial, seawater concentrations and atmospheric mixing ratios in this region were still higher during the boreal summer (A16N). The HalocAST-A cruise data were not considered for this particular comparison to avoid spatial effects, as the cruise track in the northern hemisphere is closer to the continent than the A16N and BLAST II cruises (Figure 4-1).

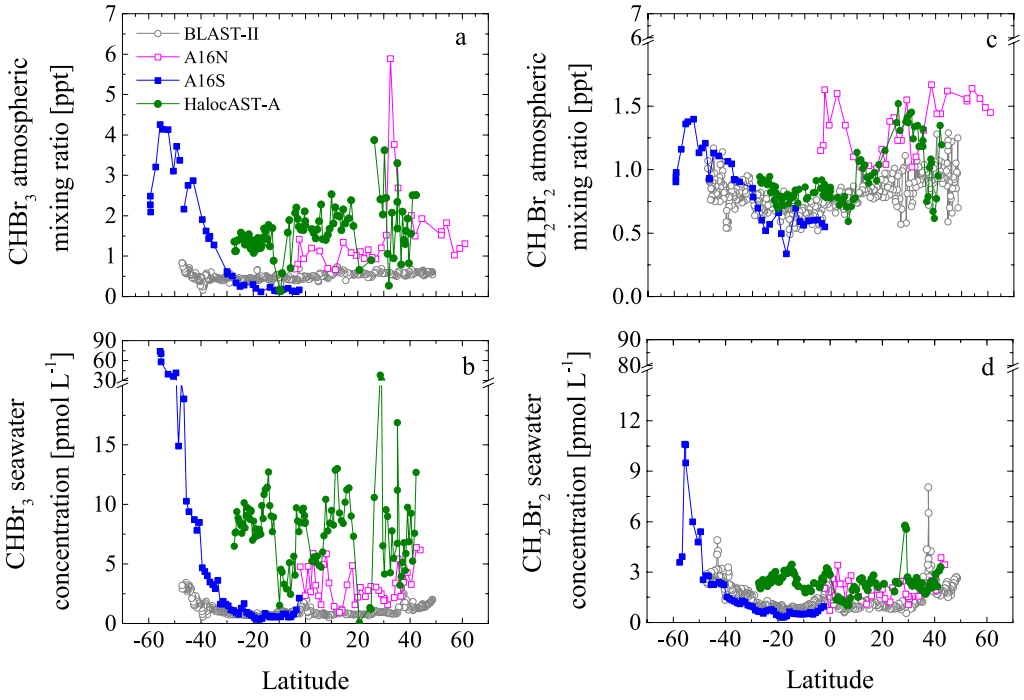

Figure 4-3. Latitudinal distributions of $CHBr_3$ and CH_2Br_2 atmospheric mixing ratios (a and c) and seawater concentrations (b and d) measured during the BLAST-II, A16N, A16S, and HalocAST-A cruises.

Table 4-2. Mean (range) of BrVSLS atmospheric mixing ratios, seawater concentrations, saturation anomalies, and fluxes during the A16N, A16S, HalocAST-A, BLAST-II and GasEx98 in different hemispheres and seasons.

	Atmospheric mixing ratio (ppt)	Seawater concentration (pmol L^{-1})	Saturation anomaly (%)	Flux (nmol m^{-2} d^{-1})
Northern Hemisphere				
HalocAST-A (winter)				
$CHBr_3$	1.9 (0.3 to 3.9)	8.5 (0.08 to 38.0)	233.2 (-91.1 to 884.6)	12.1 (-3.8 to 71.8)
CH_2Br_2	1.0 (0.6 to 1.5)	2.3 (1.0 to 5.8)	133.2 (31.8 to 296.4)	3.0 (0.4 to 13.7)
$CHClBr_2$	0.7 (0.5 to 1.2)	1.7 (0.9 to 2.4)	215.2 (64.2 to 501.2)	2.5 (0.3 to 7.6)
$CHBrCl_2$	0.5 (0.3 to 0.8)	0.5 (0.3 to 2.6)	140.0 (-9.5 to 335.9)	0.4 (-1.2 to 2.0)
GasEx98 Leg 1 (early summer)				
$CHBr_3$	0.5 (0.2 to 1.4)	1.5 (0.3 to 3.8)	57.9 (-51.6 to 213.2)	1.2 (-1.2 to 4.6)
CH_2Br_2	1.0 (0.3 to 2.0)	1.7 (0.5 to 3.3)	46.1 (-55.4 to 171.0)	1.2 (-1.8 to 6.5)
GasEx98 Legs 2 to 4 (summer)				
$CHBr_3$	0.4 (0.1 to 4.6)	1.5 (0.1 to 5.5)	97.2 (-39.2 to 761.0)	1.7 (-2.9 to 13.6)
CH_2Br_2	1.3 (0.2 to 2.6)	2.8 (0.2 to 5.8)	83.5 (-21.1 to 490.2)	3.7 (-1.0 to 16.3)
A16N (summer)				
$CHBr_3$	1.5 (0.7 to 5.9)	3.2 (0.9 to 6.4)	71.1 (-61.7 to 231.7)	3.5 (-8.4 to 12.1)
CH_2Br_2	1.3 (1.0 to 1.7)	2.0 (0.7 to 3.9)	48.0 (-40.8 to 116.4)	2.0 (-0.9 to 6.5)
Blast II (winter)				
$CHBr_3$	0.6 (0.4 to 0.7)	1.1 (0.5 to 4.8)	30.2 (-10.6 to 369.4)	0.5 (-1.0 to 5.0)
CH_2Br_2	0.9 (0.6 to 1.3)	1.5 (0.6 to 8.0)	66.9 (-12.6 to 673.5)	1.7 (-1.3 to 9.7)
Southern Hemisphere				
HalocAST-A (summer)				
$CHBr_3$	1.4 (0.1 to 2.2)	8.0 (1.5 to 12.7)	299.2 (57.9 to 2190.2)	14.1 (3.7 to 35.0)
CH_2Br_2	0.8 (0.7 to 0.9)	2.6 (1.8 to 3.4)	197.4 (72.6 to 382.2)	4.3 (1.6 to 7.8)
$CHClBr_2$	0.6 (0.4 to 0.8)	2.0 (1.3 to 4.6)	308.2 (158.2 to 690.4)	3.6 (1.3 to 9.8)
$CHBrCl_2$	0.3 (0.2 to 0.4)	0.6 (0.2 to 1.9)	383.3 (45.4 to 1272.1)	1.1 (0.3 to 4.3)
A16S (Fall)				
$CHBr_3$	1.5 (0.1 to 4.3)	9.7 (0.3 to 73.8)	235.4 (13.8 to 1027.1)	8.4 (0.5 to 41.9)
CH_2Br_2	0.9 (0.3 to 1.4)	1.9 (0.3 to 10.6)	39.8 (-9.9 to 143.9)	0.9 (-1.1 to 5.6)
Blast II (summer)				
$CHBr_3$	0.5 (0.2 to 0.8)	1.2 (0.5 to 3.4)	34.2 (-39.1 to 312.6)	0.9 (-1.5 to 7.6)
CH_2Br_2	0.8 (0.5 to 1.2)	1.6 (0.7 to 4.9)	66.2 (-15.9 to 307.5)	1.9 (-1.0 to 23.8)

In the southern hemisphere, the highest seawater concentrations and atmospheric mixing ratios of $CHBr_3$ were observed during the austral fall (A16S) (Figure 4-3, Table 4-2). These differences may be influenced by seasonal variation in $CHBr_3$ production, and the fact that the A16S, HalocAST-A and BLAST-II cruises were conducted in different regions of the southern Atlantic Ocean. Atmospheric mixing ratios of CH_2Br_2 in the southern hemisphere were comparable among the A16N, BLAST-II, and HalocAST-A cruises. Seawater concentrations of CH_2Br_2 were comparable among the A16N and BLAST-II cruises between 0° to 40 °S (Figures 4-3c and 4-3d). However, during the HalocAST-A cruises, seawater concentrations of CH_2Br_2 were higher than those observed in the A16S and BLAST-II cruise in the southern hemisphere (Figures 4-3c and 4-3d).

Data from all the cruises discussed in this study indicate that $CHBr_3$ seawater concentrations vary significantly across the Atlantic basin (Figures 4-3 and 4-4). To eliminate seasonal effects, only HalocAST-A and BLAST-II data were compared, since they were conducted in the same season. Seawater concentrations of $CHBr_3$ were substantially higher during the HalocAST-A cruise (Table 4-2), which was somewhat east of BLAST-II. If we assume that inter-annual variations in $CHBr_3$ production is less significant than spatial variations, then the differences in seawater concentrations between HalocAST-A and BLAST- II may have been due to the fact that the HalocAST-A cruise was in closer proximity to the African continent and African upwelling zones, but the BLAST-II cruise was further away from these systems. This would also be true for the atmospheric mixing ratios for $CHBr_3$. CH_2Br_2 seawater concentrations measured during the HalocAST-A cruise were also higher than those

measured in the BLAST-II cruise, but the differences were not as substantial as $CHBr_3$ (Table 4-2). CH_2Br_2 atmospheric mixing ratios were comparable during both cruises, which is consistent with longer-lived gases being more homogeneously mixed in the atmosphere than short-lived ones, like $CHBr_3$.

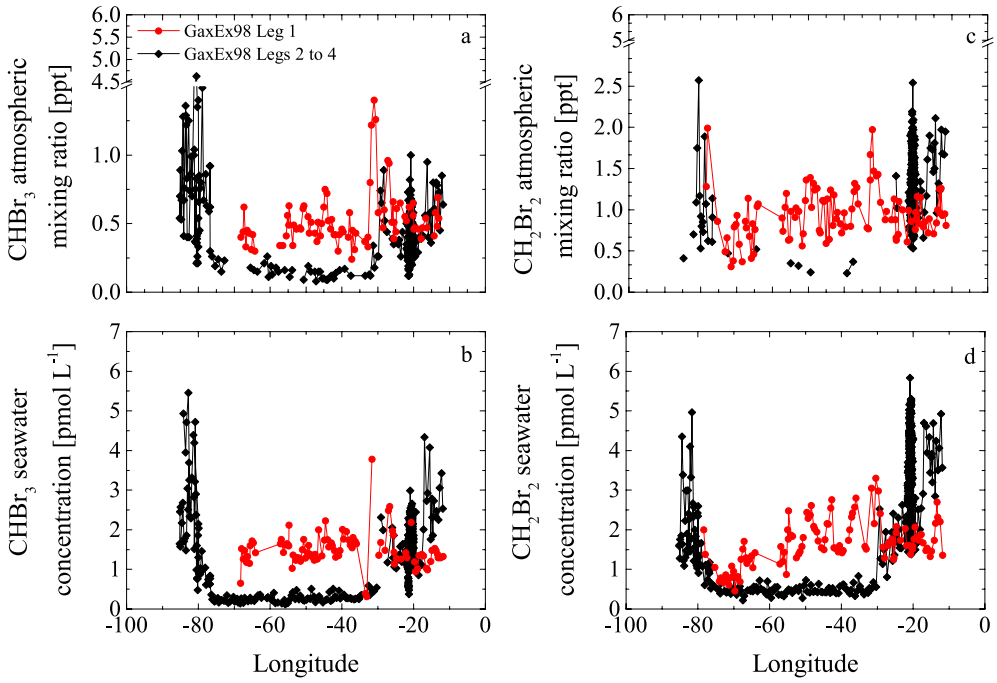

Figure 4-4. Longitudinal distributions of $CHBr_3$ and CH_2Br_2 atmospheric mixing ratios (a and c) and seawater concentrations (b and d) measured during the GasEx98 cruise Leg 1 and GasEx98 Legs 2 to 4.

The GasEx98 cruise data provide us with the opportunity to look into longitudinal variations of $CHBr_3$ and CH_2Br_2. This particular cruise had four segments in the Atlantic Ocean, two of which were conducted over an almost identical cruise track a month apart (*i.e.* Legs 1 and 3). This cruise provided us with a unique

opportunity to examine temporal variability of $CHBr_3$ and CH_2Br_2 over a shorter time scale in the same region. Significant spatial variability of $CHBr_3$ and CH_2Br_2 was observed during the GasEx98 cruise (Figure 4-4). $CHBr_3$ and CH_2Br_2 seawater concentrations and atmospheric mixing ratios were much higher during Leg 2, which was conducted in an eddy system at higher latitude, and the segment of Leg 4 in the Gulf of Mexico, than in the North Atlantic Gyre (*i.e.* Legs 1 and 3) (Figure 4-4 and 4-5). Clear temporal variations for these two BrVSLS were observed. In the North Atlantic gyre, $CHBr_3$ and CH_2Br_2 seawater concentrations and atmospheric mixing ratios were substantially higher during Leg 1, which took place in May (Figure 4-4), than Leg 3, which took place in June and July.

$CHBr_3$ and CH_2Br_2 seawater concentrations and atmospheric mixing ratios presented in this study not only indicate strong temporal and spatial variations of these BrVSLS in the Atlantic basin, they also provided a better picture of these BrVSLS on a global scale. *Butler et al.* [2007] presented a comprehensive set of BrVSLS seawater concentration and atmospheric mixing ratio data in the global ocean. The authors mentioned the Pacific Ocean tends to have higher $CHBr_3$ atmospheric mixing ratios and seawater concentrations. Such conclusions, however, were based on datasets heavily biased toward the Pacific Ocean, with the Atlantic Ocean data represented only by the BLAST-II and GasEx98 cruises. In this study, the A16N, A16S, and HalocAST-A cruises provided three additional datasets, which were measured in different regions and seasons to provide a more complete picture in the Atlantic Ocean. The results indicate that the Atlantic Ocean could have comparable or even higher $CHBr_3$ atmospheric mixing ratios and seawater concentrations than the Pacific

Ocean, which suggests source strengths are not significantly different between the two ocean basins. These findings confirmed the observed, overall temporal and spatial variations in BrVSLS in the Atlantic basin. Consequently, conclusions based on limited amounts of data to determine the global BrVSLS distributions and budgets should be treated with caution, as data from a single or only a few expedition(s) may not be globally representative. Therefore, better data coverage both temporally and spatially would be needed to better constrain the distributions and budgets of short-lived compounds. Results observed from the GasEx98 cruise suggest that data with higher temporal resolution are essential for better understanding of the dynamics of $CHBr_3$ and CH_2Br_2.

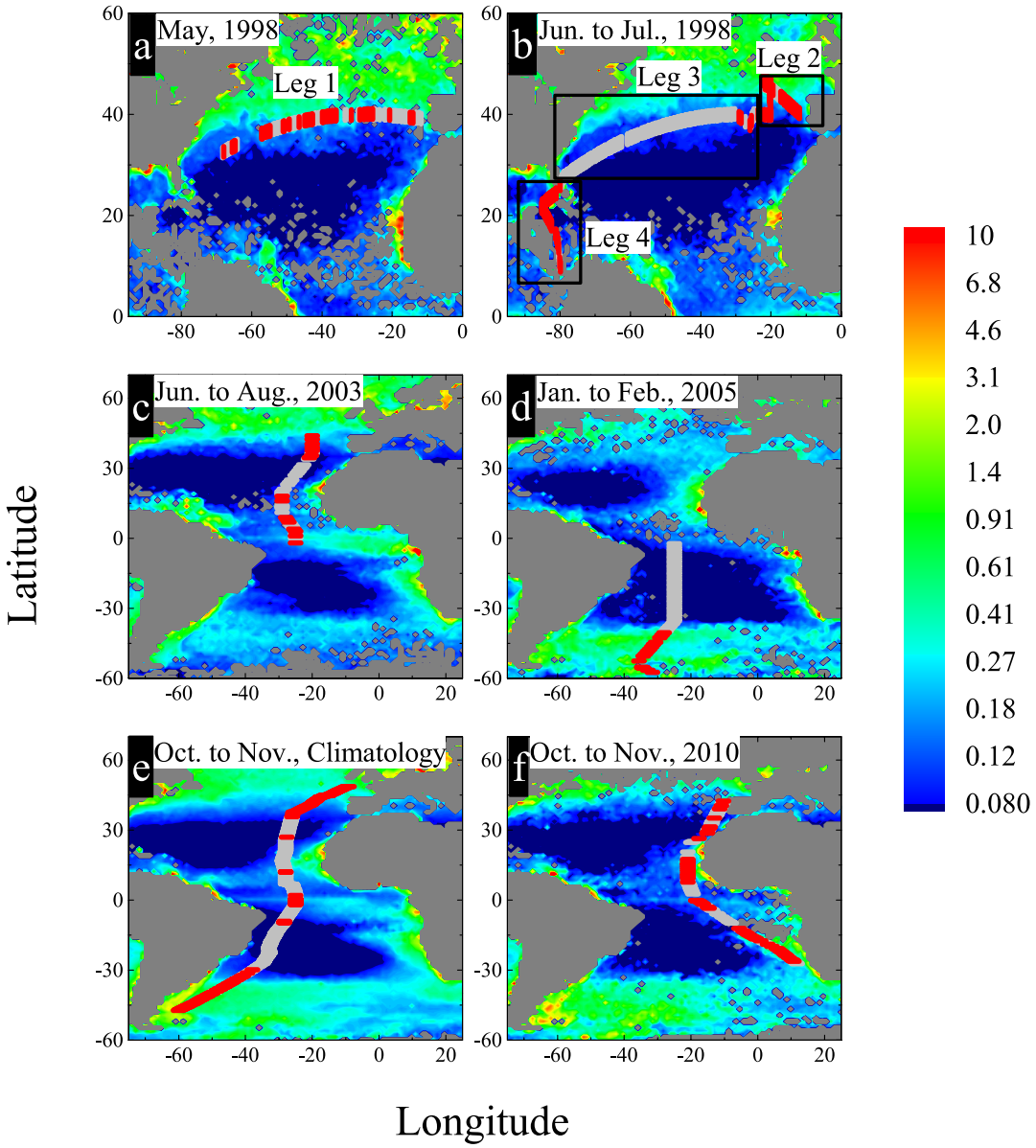

Figure 4-5. Data deviation from individual cruise mean of $CHBr_3$ during the GasEx98 leg 1 (a), legs 2 to 4 (b), A16N (c), A16S (d), BLAST-II (e), and HalocAST-A (f) cruises, superimpose on 9-km resolution monthly averaged chlorophyll *a* concentration observed during the time of the cruise from SeaWiFS, except for the BLAST-II cruise, for which monthly climatology was used (NASA Giovanni [*Acker and Leptoukh*, 2007]). Time frame over which the data were acquired is labeled on each plot. Red data points indicate positive deviation and grey data points indicate negative deviation. Color bar indicates chlorophyll *a* concentration.

4.3.2 Saturation anomalies and fluxes

Results from these cruises show that $CHBr_3$ and CH_2Br_2 were supersaturated in most parts of the Atlantic basin, with only a few locations where $CHBr_3$ and CH_2Br_2 were undersaturated in seawater (Figures 4-6 and 4-7). This observation is consistent with findings reported elsewhere (*e.g. Butler et al.* [2007], *Liu et al.* [2011], and *Quack and Wallace* [2003]). As there is no evidence supporting significant biogeochemical removal of $CHBr_3$, the observed undersaturations may be due to physical effects, such as radiative cooling, mixing of water masses, temporal changes in vertical circulation, or elevated atmospheric mixing ratios being occasionally transported from elsewhere. Bacterial-mediated degradation of CH_2Br_2 has only been studied in coastal water incubations and phytoplankton isolates [*Goodwin et al.*, 1998; *Hughes et al.*, 2013]. Although conditions in these studies may not represent global open ocean conditions, biological removal of CH_2Br_2 may still, in part, contribute to the open ocean undersaturations observed in this study.

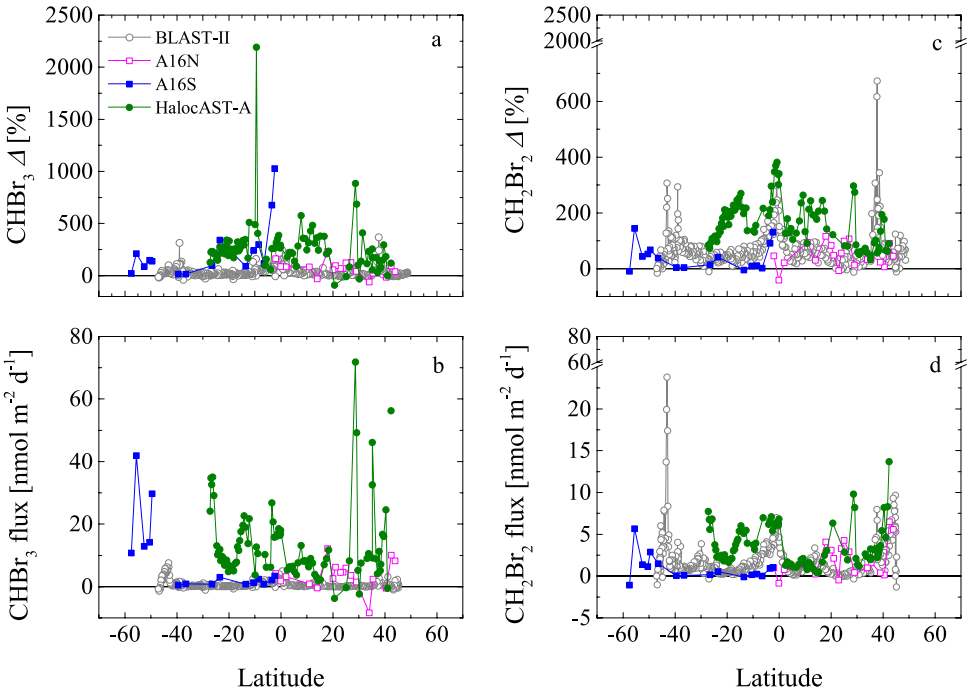

Figure 4-6. Latitudinal distributions of $CHBr_3$ and CH_2Br_2 saturation anomalies (Δ) (a and c) and fluxes (b and d) calculated for the BLAST-II, A16N, A16S, and HalocAST-A cruises.

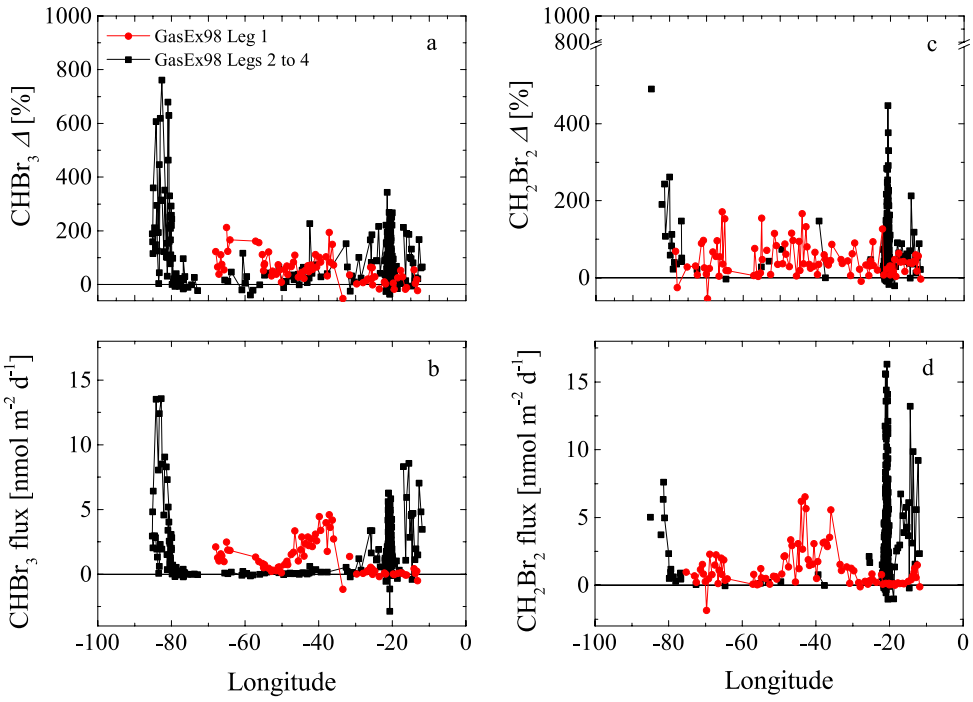

Figure 4-7. Longitudinal distributions of $CHBr_3$ and CH_2Br_2 saturation anomalies (Δ) (a and c) and fluxes (b and d) calculated for the GasEx98 cruise Leg 1 and Legs 2 to 4.

Maximum fluxes (Figures 4-6 and 4-7) for $CHBr_3$ and CH_2Br_2 were generally noted in regions with high photosynthetic biomass, such as in high productivity open-ocean waters and near shore (*i.e.* near mid-ocean islands and near the coasts) (Table 4-3), presumably due to significant biological sources in these regions. These findings are in agreement with other studies [*Butler et al.*, 2007; *Carpenter et al.*, 2009; *Quack and Wallace*, 2003]. Most of the negative fluxes of $CHBr_3$ and CH_2Br_2 were observed in the temperate Atlantic Ocean, which is consistent with findings by *Chuck et al.* [2005]. Fluxes measured over the open ocean were extrapolated to a global scale to assess bromine contributions to the atmosphere. Assuming the $CHBr_3$ and CH_2Br_2

open ocean fluxes measured in the Atlantic basin are globally representative, the mean extrapolated global open ocean annual sea-to-air fluxes calculated from the five cruises are 0.24 to 3.80 Gmol Br yr^{-1} and 0.11 to 0.77 Gmol Br yr^{-1} for $CHBr_3$ and CH_2Br_2, respectively (Table 4-4). To facilitate comparisons, the area of global open ocean was defined following *Quack and Wallace* [2003], who extrapolated the Atlantic open ocean flux to provide a global open ocean annual flux of 3 (-0.4 to 10) Gmol Br yr^{-1}. The mean extrapolated fluxes from the five cruises were within the range estimated by *Quack and Wallace* [2003]. However, it should be noted that global open ocean annual flux estimated by *Quack and Wallace* [2003] was calculated using the *Wanninkhof* [1992] gas exchange coefficient (k_w) parameterization. Using the same parameterization to calculate fluxes for the five cruises resulted in an average value that is about 46 % higher than using the *Sweeney et al.* [2007] parameterization for $CHBr_3$ and CH_2Br_2. While fully acknowledging the importance of coastal contributions, extrapolation of global net fluxes including coastal fluxes was not considered due to the scarceness of coastal data in this study (n = 6), which may not be a legitimate representation of $CHBr_3$ and CH_2Br_2 in coastal waters. Since coastal environments differ significantly worldwide, extrapolating coastal data collected from only a few coastal areas may not be appropriate for the BrVSLS [*Liu et al.*, 2011].

Table 4-3. Mean (ranges) of BrVSLS atmospheric mixing ratios, seawater concentrations, saturation anomalies, and fluxes during the A16N, A16S, HalocAST-A, BLAST-II and GasEx98 cruises in different environmental regimes. Open ocean is defined as water depth > 200 m, mid-ocean island is defined as 200 km radius of mid-ocean islands, and coastal ocean is defined as water depth ≤ 200 m.

	Atmospheric Mixing Ratio (ppt)	Seawater Concentration (pmol L^{-1})	Saturation Anomaly (%)	Flux (nmol m^{-2} d^{-1})
Open Ocean - Low Chlorophyll a ([chl a] < 0.1 mg m^{-3})				
$CHBr_3$	0.6 (0.09 to 5.9)	1.3 (0.1 to 16.9)	75.1 (-61.7 to 2190.2)	1.7 (-8.4 to 46.1)
CH_2Br_2	0.8 (0.2 to 2.0)	1.0 (0.2 to 4.4)	48.9 (-26.3 to 490.2)	1.0 (-0.5 to 5.5)
$CHClBr_2$ [H]	0.7 (0.5 to 1.1)	1.7 (1.3 to 2.4)	202.3 (68.2 to 331.4)	3.0 (1.2 to 5.4)
$CHBrCl_2$ [H]	0.4 (0.2 to 0.8)	0.5 (0.3 to 2.6)	142.0 (-9.5 to 415.1)	0.6 (-0.2 to 1.7)
Open Ocean - Medium Chlorophyll a (0.1 mg m^{-3} ≤ [chl a] < 0.2 mg m^{-3})				
$CHBr_3$	0.7 (0.1 to 2.5)	2.0 (0.1 to 11.4)	88.5 (-91.1 to 1027.1)	2.1 (-3.8 to 26.8)
CH_2Br_2	0.9 (0.2 to 2.0)	1.4 (0.3 to 5.0)	87.4 (-55.4 to 369.0)	1.8 (-1.8 to 9.9)
$CHClBr_2$ [H]	0.7 (0.5 to 1.2)	1.7 (0.9 to 2.6)	250.5 (82.6 to 408.0)	2.8 (0.3 to 7.0)
$CHBrCl_2$ [H]	0.4 (0.2 to 0.7)	0.4 (0.3 to 0.9)	197.9 (-8.9 to 500.5)	0.6 (-0.1 to 2.0)
Open Ocean - High Chlorophyll a ([chl a] ≥ 0.2 mg m^{-3})				
$CHBr_3$	0.6 (0.1 to 3.7)	2.9 (0.3 to 41.7)	84.5 (-51.6 to 578.4)	2.7 (-2.9 to 56.2)
CH_2Br_2	1.2 (0.5 to 2.5)	3.1 (1.2 to 5.8)	84.3 (-40.8 to 447.8)	3.5 (-1.3 to 23.8)
$CHClBr_2$ [H]	0.6 (0.4 to 0.9)	2.0 (1.3 to 4.6)	290.2 (64.2 to 690.4)	3.4 (0.7 to 9.8)
$CHBrCl_2$ [H]	0.3 (0.2 to 0.7)	0.7 (0.2 to 1.9)	380.3 (35.3 to 1272.1)	1.0 (-1.2 to 4.3)
Mid-ocean Islands				
$CHBr_3$	1.0 (0.1 to 4.3)	12.3 (0.4 to 73.8)	153.7 (-24.2 to 884.6)	8.3 (-0.2 to 71.8)
CH_2Br_2	1.2 (0.7 to 2.0)	3.4 (0.4 to 10.6)	171.4 (-9.5 to 673.5)	3.2 (-0.1 to 9.8)
$CHClBr_2$ [H]	0.6 (0.5 to 0.7)	2.36 (2.32 to 2.40)	415.2 (329.2 to 501.2)	3.78 (3.76 to 3.80)
$CHBrCl_2$ [H]	0.44 (0.42 to 0.45)	0.48 (0.45 to 0.51)	143.3 (134.0 to 152.5)	0.6 (0.5 to 0.7)
Coastal ocean				
$CHBr_3$	1.7 (0.5 to 4.6)	2.5 (1.5 to 4.2)	52.8 (22.2 to 107.6)	3.1 (0.4 to 7.3)
CH_2Br_2	1.5 (0.7 to 2.6)	2.3 (1.2 to 2.7)	15.3 (-0.2 to 68.8)	5.0

H: Data from the HalocAST-A cruise only.

Table 4-4. Extrapolated global open ocean net sea-to-air fluxes of $CHBr_3$ and CH_2Br_2 (Gmol Br yr^{-1}), based on data from the A16N, A16S, HalocAST-A, BLAST-II and GasEx98 cruises.

	$CHBr_3$	CH_2Br_2
HalocAST-A	3.80	0.75
GasEx98 Leg 1	0.40	0.25
GasEx98 Legs 2 to 4	0.54	0.77
A16N	1.09	0.41
A16S	1.71	0.11
BLAST-II	0.24	0.38

4.3.3 $CHBr_3$ and CH_2Br_2 concentrations in different environments and their relationship with ocean photosynthetic biomass

$CHBr_3$ and CH_2Br_2 are predominantly produced by natural sources in the marine environment, and their production may be partly attributable to enzyme-mediated halogenation of organic matter (OM) by hypobromous acid (HOBr). HOBr is formed via haloperxoidase-mediated oxidation of bromine in seawater, in the presence of hydrogen peroxide (H_2O_2) [*Theiler et al.*, 1978; *Wever et al.*, 1993]. Subsequently, HOBr can react with a wide range of OM in the surrounding waters and formed halogenated organic molecules, including the volatile gases such as $CHBr_3$ [*Theiler et al.*, 1978; *Wever et al.*, 1993]. Two haloperoxidases, bromoperoxidase and iodoperoxidase, are found in some phytoplankton (such as diatoms and cyanobacteria) and in various macroalgae [*Hill and Manley*, 2009; *Johnson et al.*, 2011; *Moore et al.*, 1996; *Wever et al.*, 1993]. Laboratory studies have identified BrVSLS production from certain specific taxa of diatoms and coccolithophores [*Colomb et al.*, 2008; *Moore et al.*, 1996].

Numerous efforts have been made to understand the relationship between $CHBr_3$ production and photosynthetic biomass [*Abrahamsson et al.*, 2004; *Karlsson et al.*, 2008; *Liu et al.*, 2013; *Mattson et al.*, 2012; *Quack et al.*, 2007a; *Raimund et al.*, 2011; *Roy*, 2010]. *Schall et al.* [1997] and *Carpenter et al.* [2009] found that $CHBr_3$ seawater concentrations are usually elevated in regions with high chlorophyll *a* concentrations. However, correlations between $CHBr_3$ seawater concentrations and chlorophyll *a* concentrations are often not straightforward. Several studies have showed that correlations between $CHBr_3$ seawater concentrations and chlorophyll *a* concentrations are statistically insignificant [*Abrahamsson et al.*, 2004; *Carpenter et al.*, 2009; *Hughes et al.*, 2009; *Liu et al.*, 2011; *Mattson et al.*, 2012]; yet, another study observed significant positive correlations between the two in certain water masses in the Mauritanian upwelling system [*Quack et al.*, 2007a]. These studies suggested that sea-to-air fluxes of $CHBr_3$, mixing in seawater, different production rates among the phytoplankton species, and degradation in seawater may have altered correlations between $CHBr_3$ concentrations and chlorophyll *a* concentrations. In the urbanized coastal ocean, it is also possible that the correlation between $CHBr_3$ and chlorophyll *a* is masked in part by anthropogenic sources of $CHBr_3$, such as the water disinfection processes [*Liu et al.*, 2011]. The authors also suggest that photodegradation of $CHBr_3$ could be significant in shallow coastal waters, which may have also altered the correlation between $CHBr_3$ and chlorophyll *a*.

Ocean color observed from satellites facilitates looking for trends on a large spatial scale. As discussed above, various factors can alter the correlation between $CHBr_3$ seawater concentrations and chlorophyll *a* concentrations. Therefore, we used

an alternate approach to assess the relationship between $CHBr_3$ production and chlorophyll *a* concentrations. Deviation from individual cruise mean (10^{th} to 90^{th} percentile) was used to relate elevated $CHBr_3$ seawater concentrations with satellite-observed chlorophyll *a* concentrations. A positive deviation indicates elevated $CHBr_3$ seawater concentrations and a negative deviation indicates $CHBr_3$ seawater concentrations below the cruise means. Time-averaged 9-km resolution SeaWiFS ocean color data were downloaded from NASA Giovanni [*Acker and Leptoukh*, 2007]. For the GasEx 98, A16N, A16S, and HalocAST-A cruises, monthly time-averaged data during the time of the cruises were used. For the BLAST-II cruise, when satellite data during the expedition was not available, climatology derived from data from1997 to 2011, October to November, monthly-averaged data was used as our best estimate. On a basin-wide scale, most of the positive deviations were located in or near regions with higher chlorophyll *a* concentrations (Figure 4-5), which were consistent with observations by *Carpenter et al.* [2009] in the tropical and North Atlantic Ocean.

To better assess $CHBr_3$ and CH_2Br_2 distributions in different environments with different ecosystems and their concentration gradients as a function of photosynthetic biomass abundance, data from all five cruises were combined and binned into environmental regimes as described at the beginning of section 4.3. Low, medium, and high chlorophyll *a* regimes represent different ecosystems in the open ocean. The mid-ocean island regime represents ecosystems where biogeochemical constituents in the surrounding seawater may have been influenced by the islands and coastal upwelling systems. Based on satellite retrieved chlorophyll *a* concentrations and pigment analysis for the HalocAST-A cruise, waters near the mid-ocean islands

tend to have relatively low photosynthetic biomass compared to mainland coastal waters and upwelling regions.

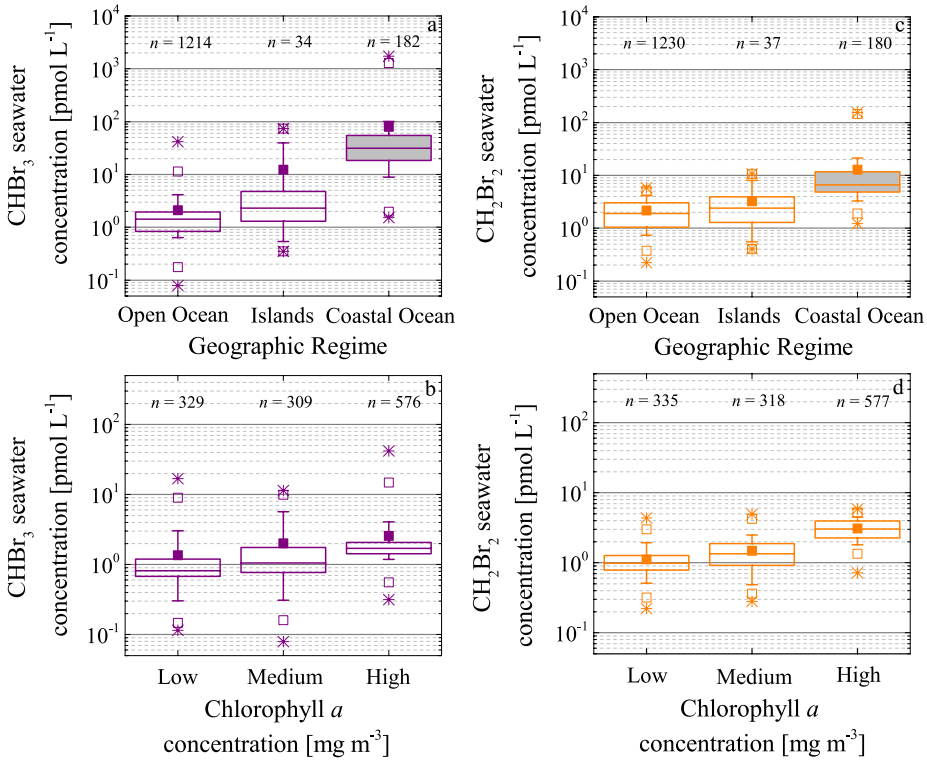

Figure 4-8. Boxplots of data from the A16N, A16S, HalocAST-A, BLAST-II and GasEx98 cruises in different geographical regimes (a and c). Due to the scarcity of coastal data from these cruises (n = 6), coastal data collected from the Gulf of Mexico and East Coast Carbon (GOMECC) cruise [*Liu et al.*, 2011] were added to the coastal data when creating the boxplot and serve as a reference for representative comparison (grey shaded box). The open ocean regime is further divided into regimes with low ([chl *a*] < 0.1), medium (0.1 ≤ [chl *a*] < 0.2), and high ([chl *a*] ≥ 0.2) chlorophyll *a* concentrations (b and d). Line in the box indicates median of data, filled square indicates mean of data, box range indicates 25th to 75th percentile of data, whisker indicates 10th to 90th percentile of data, open box indicates 5th to 95th percentile of data. Stars indicate minimum and maximum of data.

In the Atlantic basin, there were distinct $CHBr_3$ and CH_2Br_2 seawater concentration gradients ranging from high to low in waters near the mid-ocean islands, and open ocean, respectively (Figures 4-8a and 4-8c). In the open ocean, $CHBr_3$ and CH_2Br_2 also exhibited seawater concentration gradients ranging from high to low in high, medium, and low chlorophyll *a* concentration waters (Figures 4-8b and d), which was consistent with the distributions of their concentration deviations from the cruise means (Figure 4-5).

Results from this study suggest that $CHBr_3$ and CH_2Br_2 concentrations are qualitatively related to ocean photosynthetic biomass and/or any biogeochemical processes that are associated with photosynthetic biomass. This relationship was most evident during the GasEx98 cruise, during which Legs 1 and 3 passed through the same open ocean region at different times. During Leg 1 of the GasEx98 cruise, the ship was sailing near a "chlorophyll front" and positive values for deviations from the cruise mean were observed along the transit. However, during Leg 3, the retreating chlorophyll front in the temperate region led to the majority of the data observed in the North Atlantic gyre exhibiting negative deviations (Figure 4-5). In fact, as shown in section 4.3.1, $CHBr_3$ and CH_2Br_2 seawater concentrations and atmospheric mixing ratios were substantially higher during Leg 1, which may be explained by the different phytoplankton abundance, as reflected in differences in chlorophyll *a* concentrations between the two legs.

The temporal and spatial differences in $CHBr_3$ concentrations discussed in section 4.3.1 may also be explained by variations in chlorophyll *a* concentrations. In addition to seasonal differences, $CHBr_3$ seawater concentrations measured during the

HalocAST-A cruise were generally higher than the other cruises (Figures 4-3 and 4-4). This may be attributed to influences of African upwelling waters encountered during the HalocAST-A cruise, where primary production is, in general, higher than the rest of the open ocean (Figure 4-5). In the northern hemisphere, $CHBr_3$ seawater concentrations were higher in the boreal summer (A16N) than early winter (BLAST-II). This was likely a function of the relative intensities of the phytoplankton bloom occurred in the equatorial upwelling zone during each cruise (Figure 4-5). It has been shown that the equatorial phytoplankton bloom is usually more intense during the boreal summer than during early winter [*Grodsky et al.*, 2008]. In the southern hemisphere, substantially elevated $CHBr_3$ and CH_2Br_2 were also observed in the high chlorophyll *a* regions during the austral fall (A16S). $CHBr_3$ and CH_2Br_2 concentrations were lower and less variable in oligotrophic waters during austral fall (Figures 4-3 and 4-5).

While our results suggest using satellite observed chlorophyll *a* concentrations to relate BrVSLS concentrations and emissions in model simulations seem to be a legitimate approach, using such an approach is still a rather crude and qualitative approach. Spearman's rank correlation (ρ) between satellite observed chlorophyll *a* and shipboard measured $CHBr_3$ concentrations varied from cruise to cruise, which ranged from 0.07 to 0.79 (Figure 4-9a, Table 4-5), which confirmed that the relationship between $CHBr_3$ and chlorophyll *a* is not always straightforward. Furthermore, $CHBr_3$ water concentrations varied significantly within each chlorophyll *a* concentration gradient, which suggested $CHBr_3$ production strength varied greatly among areas (Figures 4-8a and b). Such variations may be explained by the complex

factors that control bromoperoxidase-mediated reactions, such as species-specific production of bromoperoxidase [*Hill and Manley*, 2009], specific moieties of DOC that are susceptible to halogenation and release $CHBr_3$ [*Lin and Manley*, 2012], availability of H_2O_2 [*Abrahamsson et al.*, 2003], and organismal interactions within the ecosystem. Therefore, photosynthetic biomass abundance alone is not sufficient to resolve the complex dynamic of $CHBr_3$ in seawater. Hence, further investigation of other parameterizations to constrain $CHBr_3$ emission in model studies should be considered. In the Atlantic Ocean, chlorophyll *a* and CH_2Br_2 were generally correlated significantly, and their relationships did not vary as substantially as $CHBr_3$ (Figure 4-9b). Spearman's rank correlations (ρ) between chlorophyll *a* and CH_2Br_2 calculated for the five cruises ranged from 0.32 to 0.81 (Table 4-5). CH_2Br_2 seawater concentration variability in each open ocean regime was not as substantial as $CHBr_3$ (Figure 4-8d). Based on the results in this study, it is reasonable to assume that CH_2Br_2 may have a more direct relationship with chlorophyll *a* concentrations than $CHBr_3$, in the open ocean (Table 4-5).

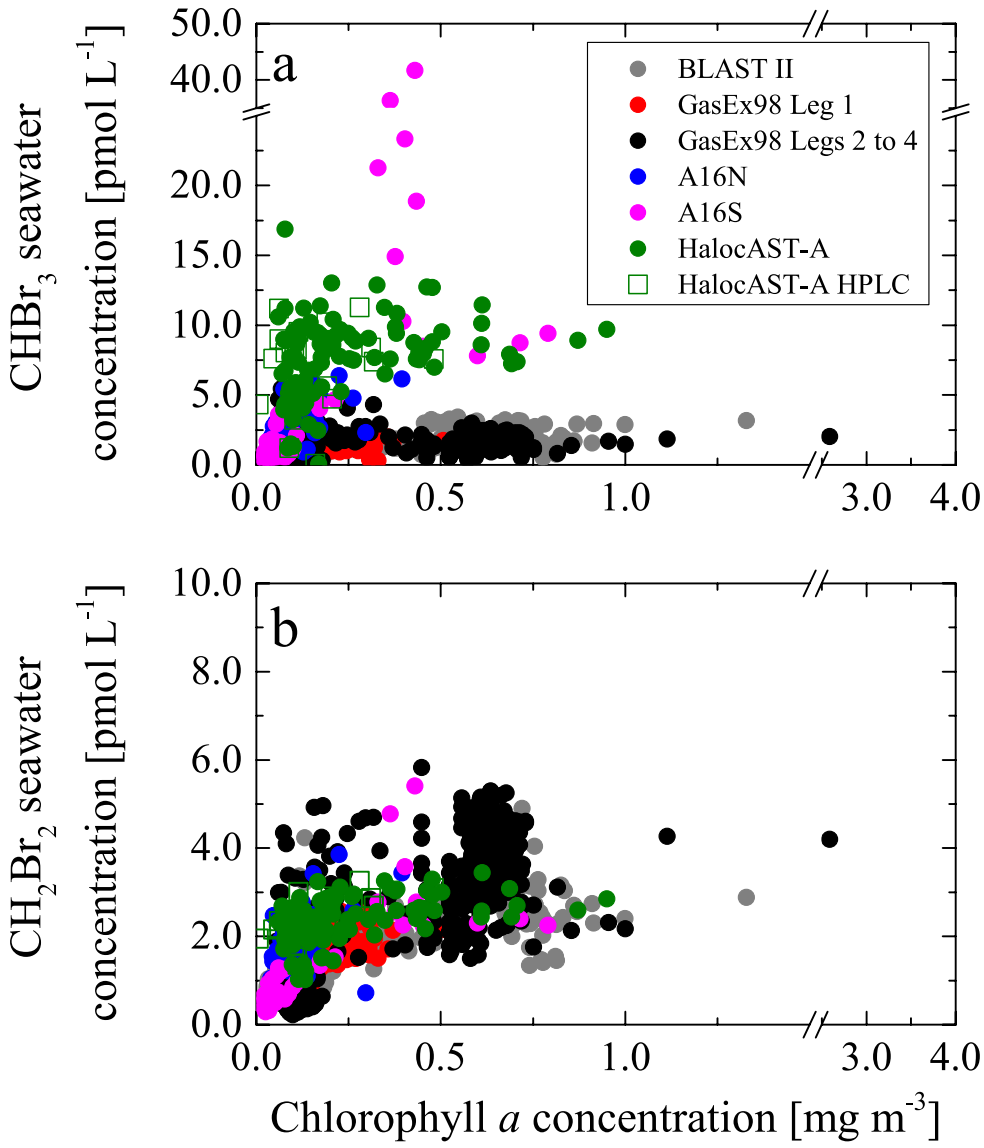

Figure 4-9. Scatter plots of $CHBr_3$ (a) and CH_2Br_2 (b) concentrations *vs*. chlorophyll *a* concentration, for the BLAST-II, GasEx98, A16N, A16S, and HalocAST-A cruises.

Table 4-5. Spearman's rank correlation coefficient (ρ) between chlorophyll *a* concentrations with $CHBr_3$ and CH_2Br_2 open ocean seawater concentrations, based on data from the A16N, A16S, HalocAST-A, BLAST-II, and GasEx98 cruises, and all data combined. *p*-value and number of samples (*n*) are in parentheses. "ns" indicates the correlation is not significant. Note that unless it is indicated in the table, correlation coefficient is based on satellite observed chlorophyll *a* data.

	$CHBr_3$	CH_2Br_2
HalocAST-A	0.37 (<< 0.001; 102)	0.53 (<< 0.001; 101)
HalocAST-A (HPLC)	0.27[nc] (0.29; 51)	0.63 (0.008; 49)
GasEx98 Leg 1	0.07[nc] (0.49; 83)	0.59 (<< 0.001; 101)
GasEx98 Legs 2 to 4	0.33 (<< 0.001; 501)	0.65 (<< 0.001; 512)
A16N	0.46 (0.004; 38)	0.32 (0.05; 37)
A16S	0.79 (<< 0.001; 49)	0.81 (<< 0.001; 49)
BLAST-II	0.76 (<< 0.001; 430)	0.79 (<< 0.001; 433)
All data	0.47 (<< 0.001; 1214)	0.77 (<< 0.001; 1230)

4.3.4 A closer look into $CHBr_3$ and CH_2Br_2 sources during the HalocAST-A cruise

While the ocean color observed from satellite provided valuable insights to the relationship between BrVSLS concentration and photosynthetic biomass abundance, it ignores a considerable amount of detail needed to better understand BrVSLS sources in the ocean. During the HalocAST-A cruise, samples for pigments, nutrients, and DOC concentrations, as well as picoplankton and heterotrophic bacteria abundances were collected, to examine the relationship between marine biogeochemical processes and BrVSLS production in seawater. Several recent studies have utilized pigment biomarker information to identify possible phytoplankton groups that may contribute to $CHBr_3$ production in seawater [*Abrahamsson et al.*, 2004; *Karlsson et al.*, 2008; *Liu*

et al., 2013; *Mattson et al.*, 2012; *Quack et al.*, 2007a; *Raimund et al.*, 2011; *Roy*, 2010]. Some of these studies identified phytoplankton groups such as cyanobacteria, diatoms, and prymnesiophytes as potential $CHBr_3$ and CH_2Br_2 producers.

It is essential to gain more detailed information on phytoplankton *in situ* composition to better understand BrVSLS sources given the fact that their production appears to be species specific (*e.g*. *Colomb et al.* [2008], *Hill and Manley* [2009], *Hughes et al.* [2011], *Moore et al.* [1996], and *Tokarczyk and Moore* [1994]). Phytoplankton community composition based on pigments is not sufficient to attribute BrVSLS production to specific species or genera. For example, zeaxanthin is commonly used as a pigment biomarker for cyanobacteria [*Bianchi and Canuel*, 2011]; but the two most important cyanobacterial genera in the ocean (*Synechococcus* and *Prochlorococcus*) cannot be distinguished by zeaxanthin alone. These two genera can easily be distinguished and enumerated using flow cytometry, based on their sizes and fluorescence properties [*Campbell*, 2001]. Moreover, flow cytometry provided valuable information on picoeukaryote (< 3 μm algae including chlorophytes, pelagophytes, and haptophytes) counts and heterotrophic bacteria counts.

During the HalocAST-A cruise, seawater $CHBr_3$ concentrations were significantly correlated with *Synechococcus* and picoeukaryote abundances (Table 4-6). However, $CHBr_3$ seawater concentrations were not significantly correlated with any of the phytoplankton pigment biomarkers, which is consistent with *Abrahamsson et al.* [2004] and *Mattson et al.* [2012]. Although our results agree with the two prior studies in acknowledging pigment biomarkers are probably not reliable for identifying $CHBr_3$ producers, we suggest a more detailed analysis of phytoplankton composition

may provide better insights into $CHBr_3$ sources. Our results are consistent with *Karlsson et al.* [2008] and *Quack et al.* [2007a], who identified cyanobacteria as potential sources for $CHBr_3$. The insignificant correlation with cyanobacteria biomarker zeaxanthin is likely due to the presence of *Prochlorococcus*, which significantly contribute to zeaxanthin concentrations but were probably not responsible for $CHBr_3$ production in our study region, as the correlations between *Prochlorococcus* abundances and BrVSLS concentrations were not significant (Table 4-6).

During the HalocAST-A cruise, CH_2Br_2 seawater concentrations were significantly correlated with *Synechoccocus*, picoeukaryotes, total chlorophyll *a*, and a series of phytoplankton pigments that could indicate contributions from diatoms and prymnesiophytes (Table 4-6). CH_2Br_2 seawater concentrations were also significantly correlated with heterotrophic bacteria, which is consistent with findings from the Halocarbon Air-Sea Transect – Pacific (HalocAST-P) cruise [*Liu et al.*, 2013]. However, there are no studies that have demonstrated the bacterial production of CH_2Br_2 in a way that can unequivocally be used to determine their significance in regulating surface water concentrations in the ocean. Heterotrophic bacteria abundance is generally positively correlated with chlorophyll *a* concentrations, making it difficult to separate the role of heterotrophic bacteria and phytoplankton in CH_2Br_2 dynamics.

Table 4-6. Spearman's rank correlation coefficient (ρ) between biological variables with $CHBr_3$ and CH_2Br_2 open ocean seawater concentrations during the HalocAST-A cruise, *p*-value and number of samples (*n*) are in parentheses. "ns" indicates the correlation is not significant. Only parameters exhibit significant correlation ($p < 0.05$) are shown.

	Proc	*Syn*	picoeuk	Hbac	Tchl *a*	Chl *c2*	Chl *c3*	Fuco	19'-but	19'-hex	Diad
Open ocean - Entire cruise											
$CHBr_3$	ns	0.33 (0.03; 51)	0.33 (0.03; 51)	ns	ns	ns	ns	ns	ns	ns	ns
CH_2Br_2	ns	0.38 (0.01; 51)	0.63 (<< 0.001; 51)	0.46 (<< 0.001; 58)	0.57 (0.01; 23)	0.78 (<< 0.001; 23)	0.75 (<< 0.001; 23)	0.80 (<< 0.001; 23)	0.78 (<< 0.001; 23)	0.76 (<<0.001; 23)	0.77 (<<0.001; 23)
Open ocean - Northwestern African upwelling influenced											
$CHBr_3$	ns	0.70 (0.03; 9)	ns	ns	ns	ns	ns	ns	ns	ns	ns
CH_2Br_2	ns	ns	ns	ns	ns	ns	ns	ns	ns	ns	ns
Open ocean - Equatorial upwelling											
$CHBr_3$	ns	ns	ns	ns	ns	ns	ns	ns	ns	ns	ns
CH_2Br_2	ns	ns	0.90 (0.04; 6)	ns	ns	ns	ns	ns	ns	ns	ns
Open ocean - Southwestern African upwelling influenced											
$CHBr_3$	ns	ns	ns	ns	ns	ns	ns	ns	ns	ns	ns
CH_2Br_2	-0.54 (0.01; 20)	0.54 (0.04; 15)	0.55 (0.03; 15)	0.69 (0.002; 18)	ns	ns	ns	0.89 (0.007; 7)	ns	ns	0.79 (0.04; 7)

Abbreviations: *Proc* (*Prochlorococcus*), *Syn* (*Synechococcus*), Picoeuk (Picoeukaryotes), Hbac (Heterotrophic bacteria), Tchl *a* (total chlorophyll *a*), Chl c2 (chlorophyll *c2*), Chl c3 (chlorophyll *c3*), Fuco (fucoxanthin), 19'-but (19'-butanoyloxyfucoxanthin), 19'-hex (19'-hexanoyloxyfucoxanthin), Diad (diadinoxanthin).

$CHBr_3$ and CH_2Br_2 seawater concentrations correlate with different biogeochemical variables in different upwelling systems (Table 4-6). While $CHBr_3$ and CH_2Br_2 are thought to be derived from common sources, results from this study and the HalocAST-P cruise in the Pacific Ocean [*Liu et al.*, 2013] suggests that there are also processes which affect the production of each gas separately. Similar relationships were also observed in the Mauritanian upwelling system by *Quack et al.* [2007a], who observed $CHBr_3$ and CH_2Br_2 correlated with different pigment biomarkers.

In waters off the Canary Islands (~28 °N), significant increases in $CHBr_3$ and CH_2Br_2 seawater concentrations were observed (Figure 4-3). The maxima of $CHBr_3$ and CH_2Br_2 during the HalocAST-A cruise were also observed in this region, and corresponded to low chlorophyll *a* concentrations. These findings were consistent with *Carpenter et al.* [2009] observations in the same area. While such a feature contradicts with the general trend between the BrVSLS and chlorophyll *a* concentrations observed in this and other studies, it also highlights the importance of mid-ocean island environments as unique ecosystems that may contribute considerable amounts of BrVSLS to the adjacent atmosphere. Urea concentrations and heterotrophic bacteria abundances were also elevated in this area. Urea has been used as an indicator of bacterial degradation of amino acids [*Remsen*, 1971; *Zehr and Ward*, 2002]. While there was no direct evidence that bacterial cycling of amino acids related to $CHBr_3$ and CH_2Br_2 production, it may suggest unique DOC sources around the mid-ocean islands, which may be more reactive for the enzyme-medicated formation of these BrVSLS. Although it is difficult to assess potential anthropogenic influences on the

BrVSLS concentrations in this region, such a sources cannot be excluded, as water treatments in coastal waters may be significant sources for $CHBr_3$ as well [*Liu et al.*, 2011; *Quack and Wallace*, 2003].

DOC concentrations were measured during the HalocAST-A cruise in order to estimate the impact of DOC concentrations on $CHBr_3$ and CH_2Br_2 concentrations. However, DOC concentrations were not significantly correlated with $CHBr_3$ and CH_2Br_2 seawater concentrations, which may suggest that specific moieties within the bulk DOC pool are required as organic substrates for enzyme-mediated halogenation. For example, *Theiler et al.* [1978] found that ketones are better organic substrates than phenols for a bromoperoxidase extracted from red algae. *Lin and Manley* [2012] also found that $CHBr_3$ and CH_2Br_2 production rates were functions of DOC quality and varied significantly depending on the DOC origins, which suggest that bulk DOC concentration was not an effective indicator of BrVSLS production.

During the HalocAST-A cruise, seawater concentrations of $CHBr_3$ and CH_2Br_2 were significantly correlated ($\rho = 0.53$, $p << 0.001$, $n = 101$), but the correlations were lower than those observed in other studies [*Carpenter and Liss*, 2000; *Carpenter et al.*, 2009; *Liu et al.*, 2011; *Quack et al.*, 2007a]. This observation reflects the fact that these gases likely have different sources and were influenced by different biogeochemical processes in different regions. While $CHClBr_2$ and $CHBrCl_2$ were not specifically discussed in this study, it is worth mentioning that they only weakly correlated with $CHBr_3$ ($\rho < 0.40$, $p < 0.01$, $n > 100$).

It should also be noted that although CH_2Br_2 and $CHBr_3$ seawater concentrations correlated significantly in most of the cruises, their relationships varied

from cruise to cruise (Figure 4-10). Significant correlations between $CHBr_3$ and CH_2Br_2 seawater concentrations were observed during the BLAST-II ($\rho = 0.86$, $p << 0.001$, $n = 450$), A16N ($\rho = 0.79$, $p << 0.001$, $n = 37$), A16S ($\rho = 0.98$, $p << 0.001$, $n = 54$), and GasEx98 Legs 2 to 4 ($\rho = 0.60$, $p << 0.001$, $n = 516$) cruises. However, $CHBr_3$ and CH_2Br_2 were not significantly correlated with each other during GasEx98 cruise Leg 1 ($\rho = 0.17$, $p = 0.12$, $n = 89$). These results confirmed findings deduced from the HalocAST-A cruise and suggested that $CHBr_3$ and CH_2Br_2 formation may have, in part, been due to different biogeochemical processes. Different DOC chemical properties in different waters may also affect the ratio between $CHBr_3$ and CH_2Br_2 concentrations, which ultimately will influence the correlation between the two. *Lin and Manley* [2012] found that CH_2Br_2 was not always formed when treating different DOC size fraction with vanadium bromoperoxidase. Results presented by *Lin and Manley* [2012] indirectly confirmed by findings of *Hughes et al.* [2013], whose experimental results suggest CH_2B_2 is biologically transformed from $CHBr_3$, rather than from the same enzyme-mediated reaction that yields $CHBr_3$.

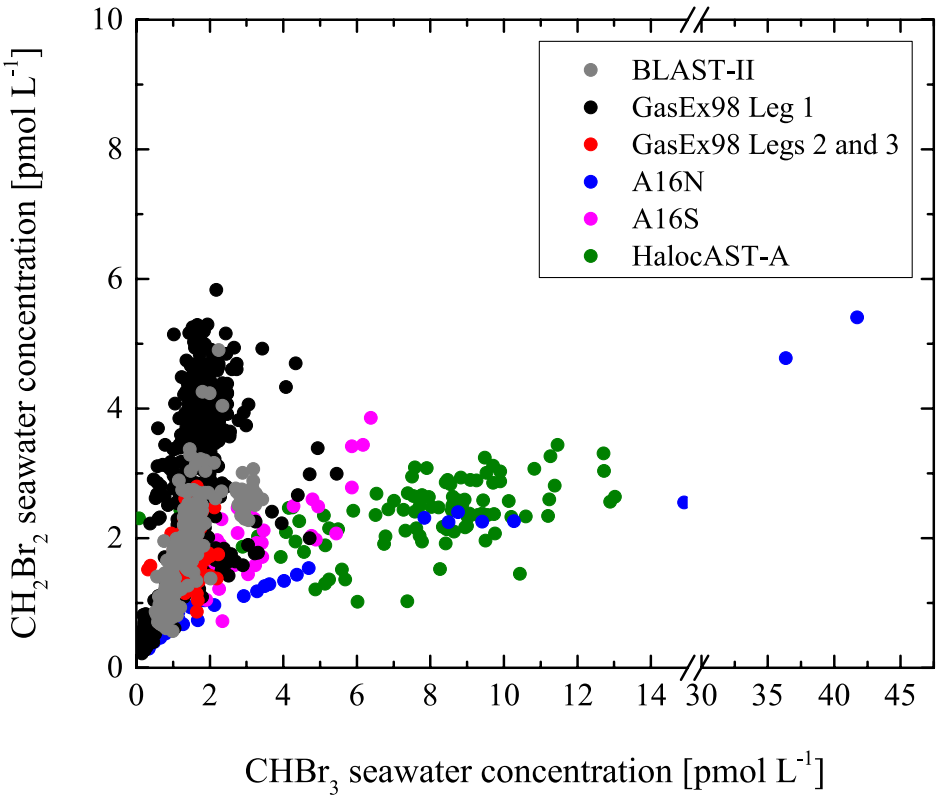

Figure 4-10. Scatter plots of $CHBr_3$ seawater concentration *vs.* CH_2Br_2 seawater concentration for the BLAST-II, GasEx98, A16N, A16S, and HalocAST-A cruises.

4.4 Conclusion

Given the heterogeneity of $CHBr_3$ in the ocean, estimated global $CHBr_3$ budgets may be biased if the data used is not diverse enough in space and time. Although the A16N, A16S, and HalocAST-A cruises add substantial amount of data to the record, more data are needed to better estimate the global budget of these and other trace gases with short lifetimes. Our results further suggest that $CHBr_3$ and CH_2Br_2 production may be attributable to biogeochemical processes related to photosynthetic biomass, such as interactions with heterotrophic bacteria, grazing, and DOC cycling.

However, chlorophyll *a* and pigment biomarkers alone are not sufficient to explain $CHBr_3$ and CH_2Br_2 concentrations and production in seawater. $CHBr_3$ and CH_2Br_2 seawater concentrations and production are influenced by different biogeochemical processes, and these trace gases may potentially be derived from disparate sources in certain regions. The complexity within the ecosystem and its impact on the BrVSLS concentrations and production suggests that additional information on the biogeochemical drivers of these gases are needed to better understand the sensitivity of their distributions and fluxes in relation to climate change. This is especially important, as many of the anthropogenic, ozone depleting substances (ODS) controlled by the Montreal Protocol continue to decrease in abundance, ultimately leaving naturally produced ODS as the source of ozone-depleting substances in the atmosphere.

CHAPTER V

MARINE DISSOLVED ORGANIC MATTER (DOM) COMPOSITION DRIVES THE PRODUCTION AND CHEMICAL SPECIATION OF BROMINATED VERY SHORT-LIVED SUBSTANCES

5.1 Introduction

Bromoform ($CHBr_3$), dibromomethane (CH_2Br_2), chlorodibromomethane ($CHClBr_2$), and bromodichloromethane ($CHBrCl_2$) constitute a significant fraction of atmospheric brominated very short-lived substances (BrVSLS), which defined as brominated trace gases with atmospheric lifetimes < 0.5 year. The major very short-lived substances (VSLS), $CHBr_3$ and CH_2Br_2, account for ~ 80% of the very short-lived organic bromine in the marine boundary layer [*Law and Sturges*, 2007]. Though only present at trace concentrations, BrVSLS play an important role in catalytic ozone destruction cycles, as bromine is more efficient in destroying ozone than chlorine, on an atom-by-atom basis [*Garcia and Solomon*, 1994; *Solomon et al.*, 1995]. $CHBr_3$, CH_2Br_2, $CHClBr_2$, and $CHClBr_2$ can contribute a significant amount of inorganic bromine (Br_y) to the atmosphere via photolysis and reaction with the hydroxyl radicals (OH). The resulting Br_y can then participate in catalytic ozone destruction in the troposphere and stratosphere. $CHBr_3$, CH_2Br_2, $CHClBr_2$, $CHBrCl_2$, and other VSLS constituents combined are capable of supplying 1 to 8 parts per trillion (ppt) of Br_y to the stratosphere (Br_y^{VSLS}), which is equivalent to ~ 4 to 36% of the total stratospheric

bromine [*Montzka and Reimann*, 2011]; with naturally emitted $CHBr_3$ and CH_2Br_2 account for a large fraction of the Br_y^{VSLS} [*Hossaini et al.*, 2012a].

$CHBr_3$, CH_2Br_2, $CHClBr_2$, and $CHBrCl_2$ are mainly derived from natural sources in seawater. As most of the anthropogenic ozone depleting substances (ODSs), such as methyl bromide (CH_3Br) and halons, have phased out under the Montreal Protocol, the naturally derived ODSs are becoming more important in controlling ozone chemistry. These natural BrVSLS are sensitive to climate change in multiple aspects. First, it was predicted that stronger tropical conventions in response to future climate change could transport more $CHBr_3$ to the stratosphere [*Hossaini et al.*, 2012b]; while alteration in OH demands in the atmosphere in a future climate also favor source gas injections (SGI) of CH_2Br_2, $CHClBr_2$, and $CHBrCl_2$ [*Hossaini et al.*, 2012b]. Second, these naturally produced BrVSLS are thought to be associated with macro- and micro-algal production by an enzyme-mediated pathway. It has been suggested that haloperoxidases, such as the vanadium bromoperoxidases (V-BrPO), catalyze oxidation of halogens in the presence of hydrogen peroxide (H_2O_2) and form reactive halogen intermediates, such as hypobromous acid ($HOBr_{enz}$). The resulting $HOBr_{enz}$ can halogenate a wide range of organic matter (OM), and subsequently release halogenated trace gases, such as $CHBr_3$ [*Butler and Carter-Franklin*, 2004; *Lin and Manley*, 2012; *Manley and Barbero*, 2001; *Moore et al.*, 1996; *Theiler et al.*, 1978; *Wever and Van der Horst*, 2013; *Wever et al.*, 1993]. The components required for $CHBr_3$ formation under the enzyme-mediated pathway will likely influence by climate change. Therefore, it is important to understand the production and controlling

factors of BrVSLS, which are the key for assessing their global emissions, distributions, and responses to future climate change.

For more than a decade, scientists devoted to understand $CHBr_3$, CH_2Br_2, $CHClBr_2$, and $CHBrCl_2$ natural sources have used various analytical tools to understand their source types and the environmental forcing affecting the production of these compounds. Most researchers have hypothesized that there is a direct relationship between BrVSLS production and the composition and biomass of the phytoplankton community. This approach assumes that our lack of understanding of BrVSLS production *in situ* stems from a failure to identify the phytoplankton taxa responsible. Chlorophyll *a* and other accessory pigments have been widely used to understand contributions from specific taxa of photosynthetic biomass to the production of $CHBr_3$, CH_2Br_2, $CHClBr_2$, and $CHBrCl_2$ [*Abrahamsson et al.*, 2004; *Ekdahl et al.*, 1998; *Karlsson et al.*, 2008; *Liu et al.*, 2013; *Liu et al.*, Submitted; *Mattson et al.*, 2012; *Quack et al.*, 2007a; *Roy et al.*, 2011]. However, it had been shown that the relationships between the phytoplankton biomass proxies and BrVSLS are not straightforward [*Abrahamsson et al.*, 2004; *Liu et al.*, 2013; *Liu et al.*, Submitted; *Mattson et al.*, 2012]. Hence, pigment biomarkers may not be a useful indicator for BrVSLS production and there may not be a direct relationship between phytoplankton community composition or biomass and BrVSLS production.

Manley and Barbero [2001] demonstrated that the removal of DOM from natural seawater reduced $CHBr_3$ production, which highlighted the essential role of DOM in controlling production of $CHBr_3$ and other trace gases produced under the same pathway. More recently, *Lin and Manley* [2012] confirmed the important role of

dissolved organic matter (DOM) in controlling $CHBr_3$ production in natural seawater, which had been hypothesized for decades [*Theiler et al.*, 1978; *Wever and Van der Horst*, 2013; *Wever et al.*, 1993]. The authors found a significant correlation between DOM molecular size and $CHBr_3$ production in V-BrPO treated natural seawater collected from the California coast. Evidence presented by *Lin and Manley* [2012] suggested the importance of DOM type and reactivity to halogenation and BrVSLS production, which has important implications for the global BrVSLS biogeochemical cycle. In this study, I examine the role of DOM in BrVSLS production in greater detail.

5.2 Methods

5.2.1 Preparation of DOM model compound stocks

A total of 28 model DOM compounds were examined for their ability to form BrVSLS upon halogenation by V-BrPO induced $HOBr_{enz}$ (Table 5-1). All DOM model compounds were purchased from Sigma-Aldrich® at their highest purity grade. To minimize DOM contamination during sample preparation, all the glassware used was combusted at 500°C for 6 hours. To avoid significant change in seawater properties, all compounds were dissolved in 0.2 μm filtered ultra-pure water (UHPW). Sub-boiling UHPW was used to dissolve tyrosine, ferulic acid, syringaldehyde, starch, and humic acid. Due to difficulty in completely dissolving humic acid, which normally dissolves in basic solutions, the bulk solution was filtered through a 0.45 μm

filter to obtain the operationally defined dissolved organic carbon (DOC) [*Bianchi*, 2011]. All stock solutions were prepare to yield a final concentration of approximately 1000 μM-C added DOC, after 1 mL of the stock solutions were added to 30 mL of artificial seawater (ASW), which was buffered to a pH of 8.11 [*Berges et al.*, 2001], for the halogenation experiment.

Though using high purity salts for making the ASW, it has an average DOC concentration of 285 μM-C, probably due to organic contaminants sorbing to the hydrated salts used in the seawater recipe. Therefore, a relatively high DOC concentration was needed to suppress the influence of background DOC present in the ASW. Moreover, a high concentration of model DOM compound was used to ensure that the DOM did not become a limiting factor for BrVSLS production. Actual DOC concentrations for each model compound in ASW were determined with a Shimadzu TOC-VCSH/CSN analyzer using high-temperature catalytic oxidation (HTC), as described by *Guo et al.* [1994].

Table 5-1. List of model DOM compounds used in this study with their chemical formula, with final DOC concentrations (μM) after added to artificial seawater (ASW), and summary of BrVSLS production properties. "N/A" indicates bulk macromolecule without a defined chemical formula. "Interfered" notes DOM that yielded significantly less BrVSLS than V-BrPO treated ASW. "No observable effect" notes addition of DOM did not enhance or interfere with BrVSLS production, relative to V-BrPO treated ASW. "Enhanced" notes DOM that is capable of producing significantly more BrVSLS than V-BrPO treated ASW. It should be note that DOM that interfered with BrVSLS production is not due to inhibition of V-BrPO.

	Chemical formula	Measured DOC concentration (μM)	BrVSLS production properties
Blank seawaters			
Artificial seawater (ASW)	N/A	285.13	BrVSLS produced
Aged Gulf of Mexico seawater (GoMSW)	N/A	171.00	Enhanced
Seawater with model DOM added			
Tryptophan	$C_{11}H_{12}N_2O_2$	1702.50	Interfered
Tyrosine	$C_9H_{11}NO_3$	1650.83	Interfered
Ferulic Acid	$C_{10}H_{10}O_4$	1488.33	Interfered
Phenol Red	$C_{19}H_{14}O_5S$	1691.67	Interfered
Thiamine	$C_{12}H_{17}N_4OS$	831.17	Interfered
Vanillin	$C_8H_8O_3$	1640.83	Interfered
Lignin	N/A	734.75	Interfered
Syringaldehyde	$C_9H_{10}O_4$	1950.83	Interfered
Glutamic Acid	$C_5H_9NO_4$	1663.33	Interfered
Ascorbic Acid	$C_6H_8O_6$	1455	Interfered
Aspartic Acid	$C_4H_7NO_4$	1570.83	Interfered
D-Glucose	$C_6H_{12}O_6$	1759.58	No observable effect
Glucuronic Acid	$C_6H_{10}O_7$	819.58	No observable effect
Galactose	$C_6H_{12}O_6$	1575.00	No observable effect
Xylose	$C_5H_{10}O_5$	1606.67	No observable effect
Maltoheptaose	$C_{42}H_{72}O_{36}$	979.17	No observable effect
Starch	$(C_6H_{10}O_5)_n$	1347.50	No observable effect
Pyruvic Acid	$C_3H_4O_3$	1205.83	No observable effect
Maltose	$C_{12}H_{22}O_{11}$	1240.83	No observable effect
Methanol	CH_4O	1367.50	No observable effect
Acetone	C_3H_6O	903.33	No observable effect
Vitamin B_{12}	$C_{63}H_{88}CoN_{14}O_{14}P$	1480.00	No observable effect
Mannose	$C_6H_{12}O_6$	1247.50	No observable effect
Glycolic Acid	$C_2H_4O_3$	1485.83	Enhanced
Alginic Acid	$(C_6H_8O_6)_n$	771.25	Enhanced
Citric Acid	$C_6H_8O_7$	1264.17	Enhanced
Humic Acid	N/A	324.42*	Enhanced*
Urea	CH_4N_2O	1771.11	Enhanced

* Flags low DOC concentration due to difficulty in completely dissolving the compounds into ultra-pure water.

5.2.2 Preparation of V-BrPO stocks

V-BrPO extracted from a red calcifying macroalga, *Corallina officinalis*, was purchased from Sigma-Aldrich®. The enzyme powder was dissolved in 50 mM MES buffer at pH 6.4 and subsequently diluted to an appropriate concentration, such that delivering 10 μL of V-BrPO stock to 30 mL of ASW yielded a final enzyme concentration of ~ 0.07 units mL^{-1} for the experiment. One unit V-BrPO is defined as the catalytic conversion of 1.0 μM of monochlorodimedon (MCD) to monobromochlorodimedon per min at pH 6.4 at 25°C [*Rush et al.*, 1995]. The conversion of MCD to its brominated product was monitored with a Shimadzu UV mini 1240 model UV-vis spectrophotometer, at 290 nm in disposable UV cuvettes (applicable range λ = 220 to 900 nm, 1 mL sample volume, 1 cm path width). The assay instruction was provided by Sigma-Aldrich®, which is based on *Rush et al.* [1995]. Four different batches of enzyme were used during the experiments.

5.2.3 Halogenation reaction – single DOM model compound

Halogenation reaction mediated by V-BrPO was conducted in a 100 mL ground glass gas tight syringe, with 30 mL of ASW, 1 mL of model DOM compound stock (final concentration ~1000 μM-C), 10 μL V-BrPO (final concentration 0.07 units mL^{-1}), and 10 μL H_2O_2 (final concentration 5.0 μM). All components were added to the syringe without headspace and without bubbles. The addition of H_2O_2 activated the reaction. The reaction fluid was mixed by gently inversing the syringe with two

small pre-combusted glass beads inside to facilitate mixing. The reaction was conducted in dark at 24.1 °C in a temperature controlled incubator for 4 hours. All experiments were conducted in triplicate.

Six control sets were run to determine influences of different reaction components on BrVSLS production: (1) blank ASW was run for each of the three batches made during the experiment (ASW blank); (2) only H_2O_2 added to ASW with model DOM compounds, which was run at the beginning of the experiment (H_2O_2 control); (3) only V-BrPO added to ASW with model DOM compounds, which also was run at the beginning of the experiment (V-BrPO control); (4) only model DOM compounds added to ASW, which was run for each model compounds (DOM control); (5) V-BrPO mediated halogenation of ASW without model DOM compound added, which was run whenever a new batch of ASW and/or V-BrPO was used (HASW). Therefore, final BrVSLS concentrations yielded from halogenation of each model DOM compound were compared to BrVSLS yielded from halogenation of the same batch of ASW and enzyme.

5.2.4 Halogenation reaction – dual DOM model compounds

To better understand how DOM dynamics and interactions in the natural environment may influence BrVSLS production, an over simplified DOM pool was created by mixing two model DOM compounds. A model DOM compound that interfered with BrVSLS production was mixed with a model DOM compound that enhanced BrVSLS production in the following proportions: 50%, 10%, 0.5%, and 0%

of DOM that interfered with BrVSLS production in a total added DOM concentration of 1000 μM-C. A model DOM compound that did not affect BrVSLS production was also mixed with a model DOM compound that enhanced BrVSLS production in the same proportion as aforementioned, to compare BrVSLS production with the aforementioned experiment. The DOM model compounds selected for this experiment were based on results obtained from the single model DOM compound experiments.

5.2.5 BrVSLS analytical method

Samples for BrVSLS analysis were immediately transferred to a purge-and-trap sample storage module after 4 hours of halogenation reaction. Sample replicates run at different times in 8 hours after the reaction yield consistent BrVSLS concentrations, which indicated BrVSLS production was completed and stable at the time for analysis. $HOBr_{enz}$ reaction with DOM is a rapid process, which occurred on the order of seconds to a maximum of 1 hour. Therefore, the long analytical time (~40 min per sample) did not affect BrVSLS quantification.

The purge-and-trap sample storage module is a compact thermoelectric refrigerator held at ~ 24 ºC for this particular experiment. Inside, seven ~10 mL calibrated volume glass bulbs were connected to a loop selection valve (Valco Instrument Co.), which was connected to the purge-and-trap system. This configuration allowed the samples to be stored in a constant temperature, in dark, and gas tight environment until injection to the analytical system [*Yvon-Lewis et al.*, 2004]. Each sample was gently injected into the appropriate bulb through a 0.45μm

cellulose acetate syringe filter. BrVSLS samples with and without passing through the filters were compared and showed consistent results, which indicated the cellulose acetate syringe filter did not affect BrVSLS quantification. All samples were analyzed within 8 hours from the end of reaction.

For BrVSLS analysis, each sample in the glass bulb was sequentially transferred into a glass sparger with an ultra-pure nitrogen gas stream, and purged at 144 mL min^{-1} at room temperature. The whole sample line was then flushed with the same ultra pure nitrogen gas stream until it was time for the next sample to ensure no residue from the previous sample was left in the line. The sample purge stream was dried with two in-line Nafion driers (Perma Pure, NJ), and the analytes were pre-concentrated on one cryotrap and then focused on a second cryotrap that were both held at -75°C, and then desorbed at 210ºC. The analytes were desorbed from the focusing trap and transferred by the same stream of ultra-pure nitrogen transfer gas into the gas chromatograph – mass spectrometer (GC-MS) for quantification (Agilent GC 6890N and MS 5973N; DB-VRX 0.240 ID column with 15m pre-column and 45m main column). Detailed analytical methods were described in *Yvon-Lewis et al.* [2004] and references therein.

Moist whole air gas calibration standards used in the experiment were calibrated against gas standards obtained from the National Oceanic and Atmospheric Administration Global Monitoring Division (NOAA GMD). The experiment calibration standard was run after every fourth injection. The ultra-pure nitrogen gas stream was run as a blank after every three samples to monitor flushing efficiency. The detection limits for $CHBr_3$ and CH_2Br_2 were 1.0×10^{-3} pmol L^{-1}, and 5.0×10^{-3}

pmol L^{-1} for $CHClBr_2$ and $CHBrCl_2$. Analytical uncertainty was determined by multiple injections of the calibration standard. The averaged analytical uncertainty was 4.4% for $CHBr_3$, 6.0% for CH_2Br_2 , 1.5% for $CHClBr_2$, and 2.6% for $CHBrCl_2$. Purge efficiency was determined by re-stripping seawater samples three times, and the percentage in total concentration for the first stripping was 85.2% for $CHBr_3$, 89.0% for CH_2Br_2, 96.1% for $CHClBr_2$, and 98.7% for $CHBrCl_2$. BrVSLS concentrations reported here were corrected for purge efficiencies.

5.2.6 Data quality control and statistics

Dixon's *Q*-test was used to determine significant outliers from a small number of samples ($n = 3$) at a 90% confidence level. Data points rejected by the Dixon's *Q*-test were removed when interpreting the data. All data were combined and examined the overall correlations between the BrVSLS. The combined data were checked for normality. Since the combined data showed a non-normal distribution, Spearman Rank correlation was used to determine association between the BrVSLS, at a 95% confidence level. The significance of the correlation was determined using a two-tailed test. Significant differences of means between data groups were determined using the One-Way ANOVA test at a 95% confidence level. All statistical analyses were done with the OriginLab© version 9.0 statistic module.

5.3 Results

5.3.1 BrVSLS production by single DOM model compounds

Results from the control groups indicate that the DOM control, H_2O_2 control, and V-BrPO control do not produce BrVSLS in ASW on their own. BrVSLS concentrations observed from these control experiments were not significantly different from the ASW blanks. These control groups and ASW blanks consistently yield a mean concentration of 9.1 ± 5.4 pmol L^{-1}, 7.6 ± 3.0 pmol L^{-1}, and 3.8 ± 1.7 pmol L^{-1}, for $CHBr_3$, $CHClBr_3$, and $CHBrCl_2$, respectively. CH_2Br_2 was not detectable in the controls. Variability in BrVSLS concentrations were mainly due to different background trihalomethane (THM) concentrations in the ultra-pure water used to make up the ASW. ASW itself is capable of producing significant amounts of BrVSLS upon halogenation (*i.e.* HASW), with an average $CHBr_3$ concentration ranging from 845.7 ± 290.5 pmol L^{-1} to 2140.9 ± 273.6 pmol L^{-1} between treatments by different batches of V-BrPO (Table 4-2).

Table 5-2. BrVSLS concentrations measured after 4-hours reaction of V-BrPO treated artificial seawater (ASW), aged Gulf of Mexico seawater, and samples with model DOM compounds added to ASW.

	Chemical formula	BrVSLS Concentrations (pmol L^{-1})		
		$CHBr_3$	$CHClBr_2$	$CHClBr_2$
Seawaters				
Artificial seawater 1	N/A	2140.9 ± 273.6	160.6 ± 61.1	44.7 ± 11.7
Artificial seawater 2	N/A	845.7 ± 290.5	59.1 ± 24.0	22.4 ± 10.7
Artificial seawater 3	N/A	954.5 ± 370.4	83.3 ± 26.6	23.4 ± 5.7
Artificial seawater 4	N/A	1861.6 ± 557.2	109.6 ± 29.7	39.2 ± 9.8
Aged Gulf of Mexico seawater	N/A	3609.6 ± 267.2	241.0 ± 18.2	70.3 ± 1.8
Seawater with model DOM added				
Tryptophan	$C_{11}H_{12}N_2O_2$	8.9 ± 0.6	12.5 ± 9.8	4.7 ± 3.3
Tyrosine	$C_9H_{11}NO_3$	23.7 ± 10.8	11.0 ± 1.8	4.0 ± 0.4
Ferulic Acid	$C_{10}H_{10}O_4$	18.4 ± 9.6	8.8 ± 1.7	3.5 ± 0.6
Phenol Red	$C_{19}H_{14}O_5S$	41.3 ± 21.4	10.1 ± 2.8	9.2 ± 5.9
Thiamine	$C_{12}H_{17}N_4OS$	25.1 ± 20.9	11.6 ± 0.3	6.9 ± 3.0
Vanillin	$C_8H_8O_3$	54.4 ± 11.8	20.8 ± 7.3	7.4 ± 2.4
Lignin	N/A	139.8 ± 60.0	14.7 ± 0.2	5.0 ± 0.004
Syringaldehyde	$C_9H_{10}O_4$	66.8 ± 22.5	15.5 ± 4.3	5.4 ± 1.3
Glutamic Acid	$C_5H_9NO_4$	177.1 ± 94.2	24.6 ± 19.9	6.0 ± 0.4
Ascorbic Acid	$C_6H_8O_6$	109.3 ± 83.7	26.3 ± 8.5	16.4 ± 3.3
Aspartic Acid	$C_4H_7NO_4$	1359.0 ± 518.7	38.2 ± 27.4	10.7 ± 4.1
D-Glucose	$C_6H_{12}O_6$	373.0 ± 13.1	53.1 ± 8.5	26.0 ± 3.8
Glucuronic Acid	$C_6H_{10}O_7$	657.3 ± 28.7	46.1 ± 1.9	15.8 ± 4.5
Galactose	$C_6H_{12}O_6$	717.1 ± 495.3	40.9 ± 22.6	12.8 ± 7.3
Xylose	$C_5H_{10}O_5$	759.2 ± 312.9	216.2 ± 141.9	24.6 ± 7.2
Maltoheptaose	$C_{42}H_{72}O_{36}$	1926.9 ± 8.9	183.3 ± 13.4	42.9 ± 5.1
Starch	$(C_6H_{10}O_5)_n$	848.7 ± 325.4	60.1 ± 8.1	22.0 ± 5.0
Pyruvic Acid	$C_3H_4O_3$	921.3 ± 238.3	62.1 ± 18.7	13.6 ± 4.8
Maltose	$C_{12}H_{22}O_{11}$	1215.6 ± 456.7	89.4 ± 31.2	24.3 ± 7.3
Methanol	CH_4O	1214.7 ± 137.5	72.3 ± 10.2	23.1 ± 3.9
Acetone	C_3H_6O	1633.9 ± 670.7	83.1 ± 25.1	31.1 ± 11.5
Vitamin B_{12}	$C_{63}H_{88}CoN_{14}O_{14}P$	1151.9 ± 145.4	70.9 ± 4.4	23.1 ± 1.4
Mannose	$C_6H_{12}O_6$	1215.6 ± 456.7	89.4 ± 31.2	24.3 ± 7.3
Glycolic Acid	$C_2H_4O_3$	1646.8 ± 499.9	199.4 ± 100.0	33.3 ± 6.8
Alginic Acid	$(C_6H_8O_6)_n$	1689.7 ± 185.3	140.5 ± 20.9	59.2 ± 4.1
Citric Acid	$C_6H_8O_7$	5511.2 ± 590.7	562.7 ± 3.0	104.4 ± 22.6
Humic Acid	N/A	2633.8 ± 171.6	202.9 ± 12.1	83.9 ± 12.0
Urea	CH_4N_2O	6980.1 ± 1748.2	203.3 ± 50.0	56.2 ± 6.9

Based on final BrVSLS concentrations observed at the end of the 4-hours reaction with model DOM compounds added, the model DOM compounds were categorized into three groups based on their BrVSLS production properties: (1) enhanced BrVSLS production ($DOM_{enhanced}$), (2) no observable effect on BrVSLS production (DOM_{no_effect}), and (3) interfered with BrVSLS production ($DOM_{interfered}$) (Table 5-1, Figure 5-1). Enhanced BrVSLS production indicates the observed concentrations were significantly higher than their corresponding batch of ASW

treated with the corresponding batch of V-BrPO. No observable effect on BrVSLS production indicates the observed concentrations were not significantly different from their corresponding batch of ASW treated with the corresponding batch of V-BrPO. Interfered with BrVSLS production indicates the observed concentrations were significantly lower than their corresponding batch of ASW treated with the corresponding batch of V-BrPO.

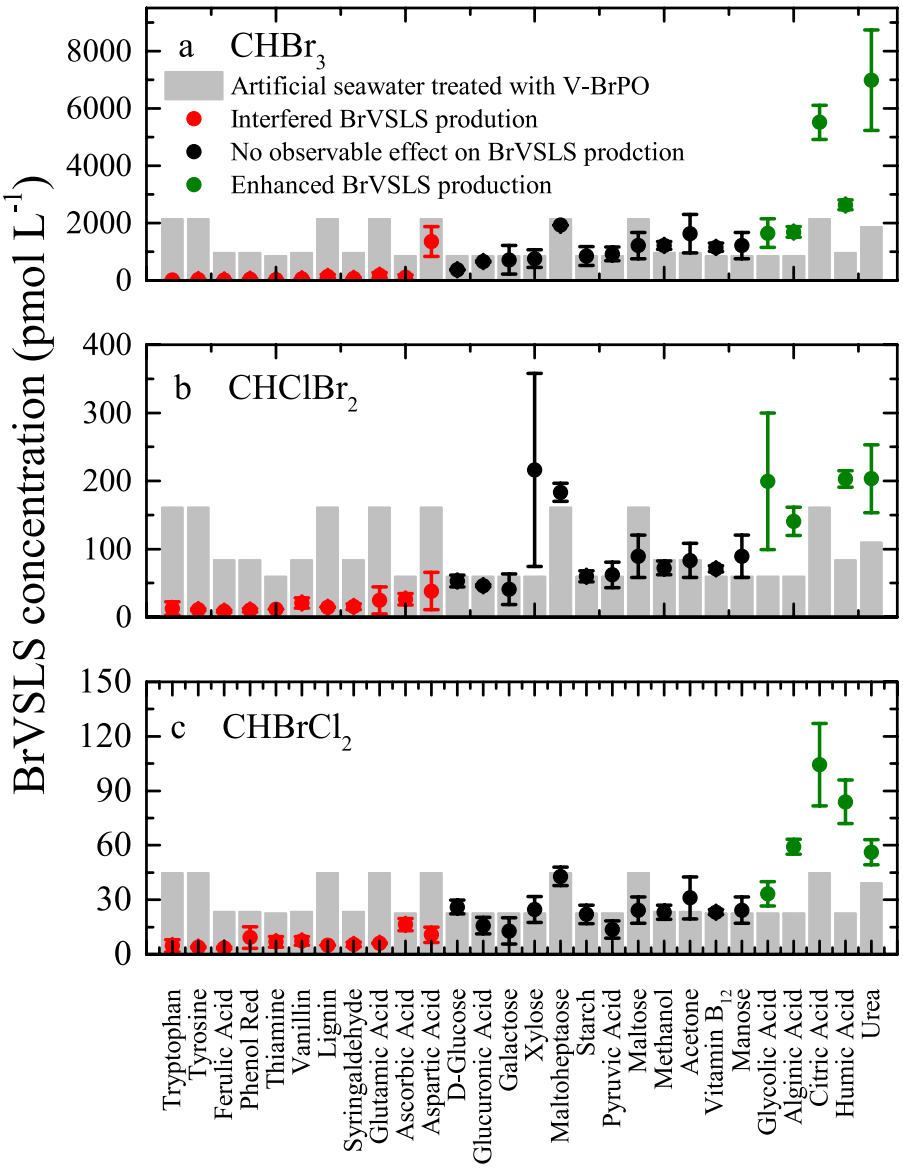

Figure 5-1. BrVSLS concentrations of (a) $CHBr_3$, (b) $CHClBr_2$, and (c) $CHBrCl_2$, measured from $HOBr_{enz}$ halogenation of a series of model DOM compounds. Grey bar chart shows BrVSLS concentration resulted from different batches of ASW treated with different batches of V-BrPO. Filled circles are mean concentrations of BrVSLS produced by each individual model DOM compound, with error bar of ± 1 standard deviation, plotting on top of their corresponding batch of ASW halogenated by their corresponding batch of V-BrPO. DOM group labeled red indicates BrVSLS production was significantly less than V-BrPO treated ASW without model DOM added (interfered). DOM group labeled black indicates BrVSLS production was not significantly different from V-BrPO treated ASW without model DOM added (no observable effect). DOM group labeled green indicated BrVSLS production was significantly higher than V-BrPO treated ASW without model DOM added (enhanced).

A total of 11 out of 28 DOM model compounds significantly interfered with BrVSLS production in ASW. Tryptophan, tyrosine, and ferulic acid effectively interfered with BrVSLS production, such that the observed BrVSLS concentrations were not significantly different from the ASW blanks. Only 5 out of 8 model DOM compounds were capable of enhancing BrVSLS production, which included glycolic acid, alginic acid, citric acid, humic acid, and urea. It should be noted that humic acid was presented at a much lower concentration in the ASW than the rest of model DOM compounds, since only a small fraction of it can be dissolved in ultra-pure water (Table 5-1). The rest of the model DOM compounds showed no observable effects on BrVSLS production in seawater. With all the data in this experiment combined, these BrVSLS showed a significant overall correlation with each other (Table 5-3, Figure 5-2). CH_2Br_2 production was not observed across all DOM model compounds tested.

Table 5-3. Spearman rank correlation coefficient (ρ) between the BrVSLS (p-value; number of samples n).

	$CHClBr_2$	$CHBrCl_2$
V-BrPO halogenation		
Single substrate experiment		
$CHBr_3$	0.94 (<< 0.001; 80)	0.85 (<< 0.001; 78)
$CHClBr_2$	-	0.92 (<< 0.001; 78)
Mix substrate experiment		
$CHBr_3$	0.94 (<< 0.001; 48)	0.83 (<< 0.001; 48)
$CHClBr_2$	-	0.89 (<< 0.001; 48)

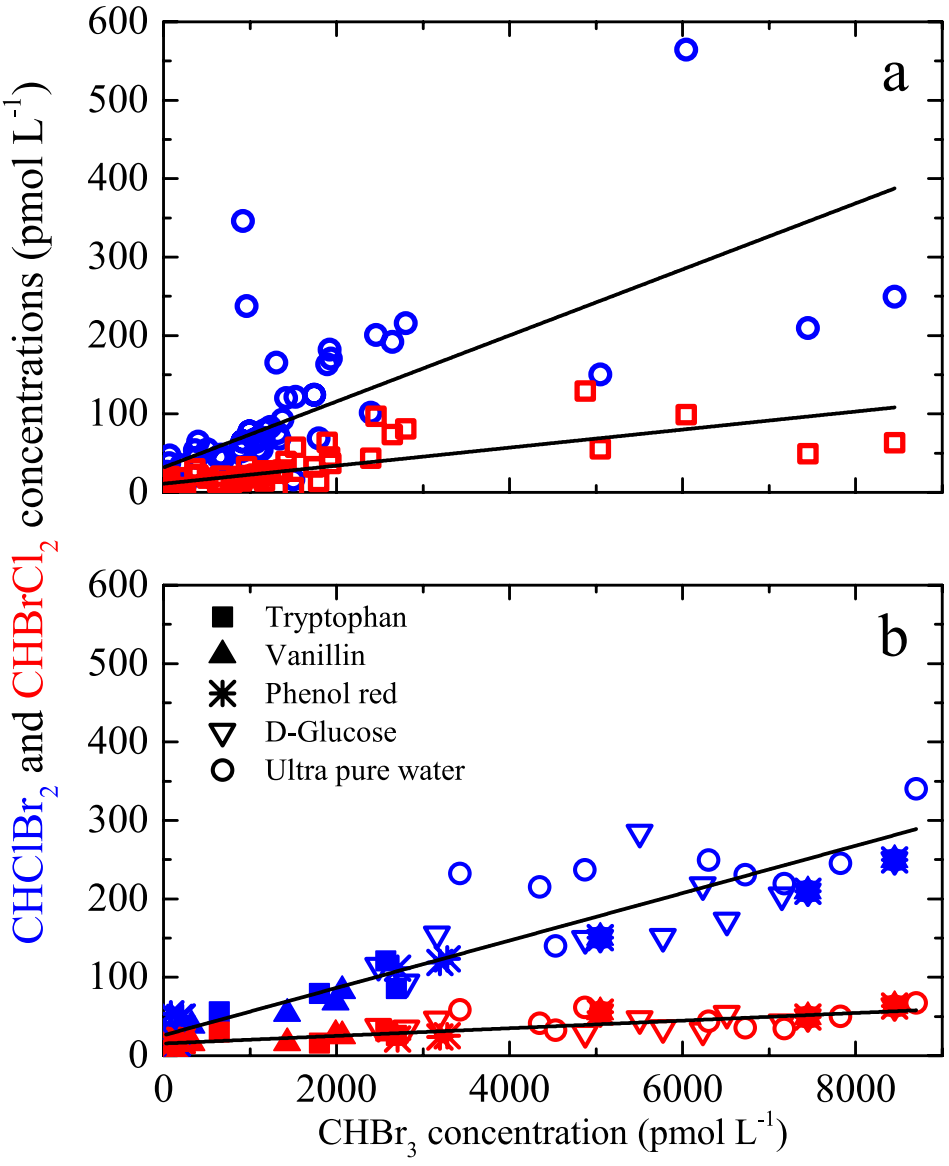

Figure 5-2. Scatter plot of $CHBr_3$ concentration *vs*. $CHClBr_2$ and $CHBrCl_2$ concentrations for (a) single DOM model compound experiment and (b) dual DOM model compounds experiment. Blue data points presented $CHBr_3$ concentration *vs*. $CHClBr_2$ concentration. Red data points presented $CHBr_3$ concentration *vs*. $CHBrCl_2$ concentration. In panel (b), Filled squares are data observed from tryptophan mixed with urea. Filled triangles are data observed from vanillin mixed with urea. Stars are data observed from phenol red mixed with urea. Open up-side-down triangles are data observed from D-glucose mixed with urea. Open circles are data observed from ultra-pure water mixed with urea.

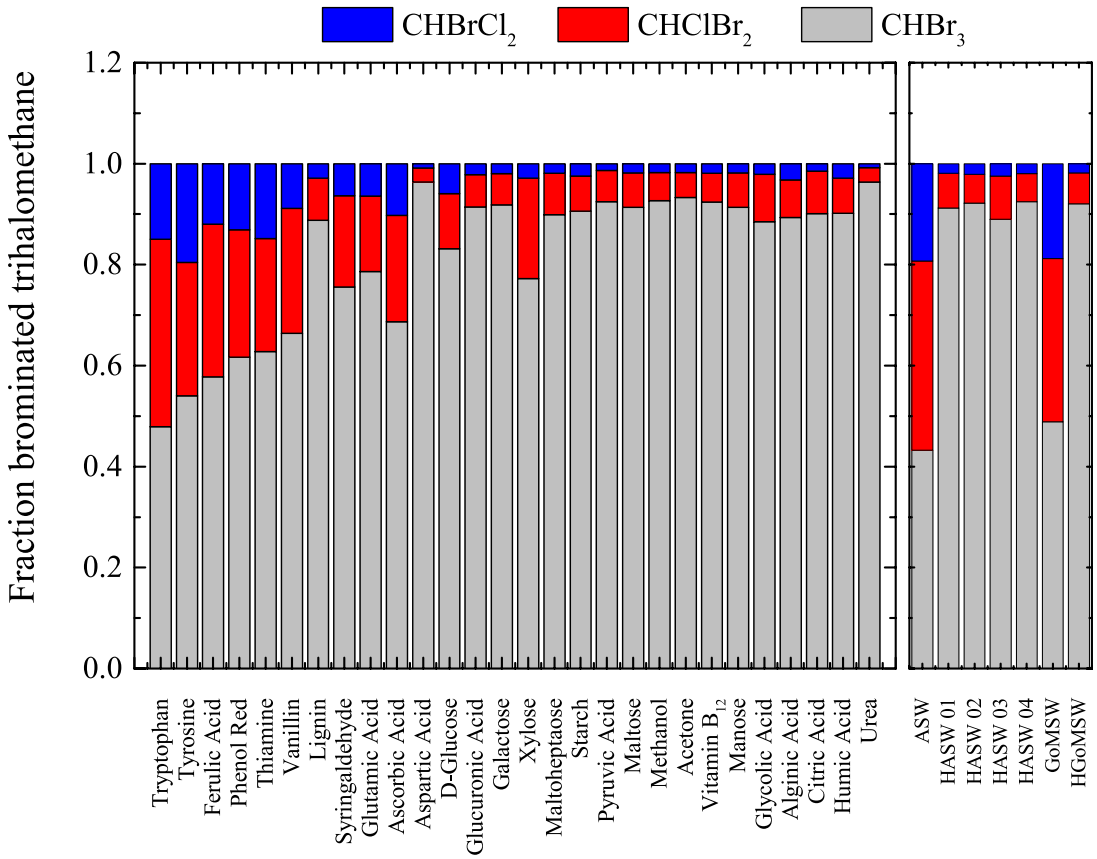

Figure 5-3. Brominated trihalomethane speciation across the model DOM compounds examined, and in comparison with pre- and post- V-BrPO treated artificial seawater (ASW and HASW, respectively) and aged Gulf of Mexico seawater (GoMSW and HGoMSW, respectively).

$CHBr_3$, $CHBrCl_2$, and $CHClBr_2$, are also known as brominated trihalomethanes (BTHM). Although significantly correlated with each other, the relative abundances of these compounds varied significantly as a function of DOM type (Figure 5-3). Relative abundances of $CHClBr_2$ and $CHBrCl_2$ tend to be higher in samples with $DOM_{interfered}$ added. $CHClBr_2$ and $CHBrCl_2$ relative abundances were also higher in non-V-BrPO treated artificial seawater and aged Gulf of Mexico seawater (GoMSW). Upon V-BrPO induced halogenation, $CHBr_3$ relative abundances significantly increased in ASW and GoMSW.

5.3.2 BrVSLS production by dual DOM model compounds

Three model $DOM_{interfered}$ compounds, tryptophan, vanillin, and phenol red, were chosen for the dual DOM experiment. Each compound was mixed at ratios defined in section 5.2.4 with urea, a $DOM_{enhanced}$. In addition, D-glucose, which belongs to the DOM_{no_effect} group, and ultra-pure water were individually mixed with urea.

As shown in Figure 5-4, mixtures containing tryptophan, vanillin, and phenol red at the relative proportions of 50%, 10%, and 0.5% of the added DOM concentration resulted in significant reductions in BrVSLS concentrations, relative to 0% addition of these compounds (*i.e.* 100% added urea). $CHBr_3$ concentration trends between these treatments were consistent, as determined by one-way ANOVA test. D-glucose mixed with urea in various proportions exhibited a similar trend as ultra-pure water mixed with urea, as determined with a one-way ANOVA test. Such a

consistency between D-glucose and ultra-pure water mix experiments confirmed that the $CHBr_3$ production trends observed from these experiments were resulted from dilution of urea, and D-glucose does not affect $CHBr_3$ production.

$CHClBr_2$ and $CHBrCl_2$ concentration trends observed from all dual model DOM compounds experiments were similar to $CHBr_3$. With all the data in the mixing experiments combined, these BrVSLS exhibited a significant overall correlation with each other, which suggested $CHClBr_2$ and $CHBrCl_2$ production responded to DOM dynamics in a similar fashion as $CHBr_3$ (Table 5-3 and Figure 5-2). BTHM relative abundances also changed across different mixing proportion of $DOM_{interfered}$ (Figure 5-5). 50% and 10% relative proportion of $DOM_{interfered}$ yield significantly less relative abundances of $CHBr_3$ than those observed from 0.5% and 0% relative proportion of $DOM_{interfered}$.

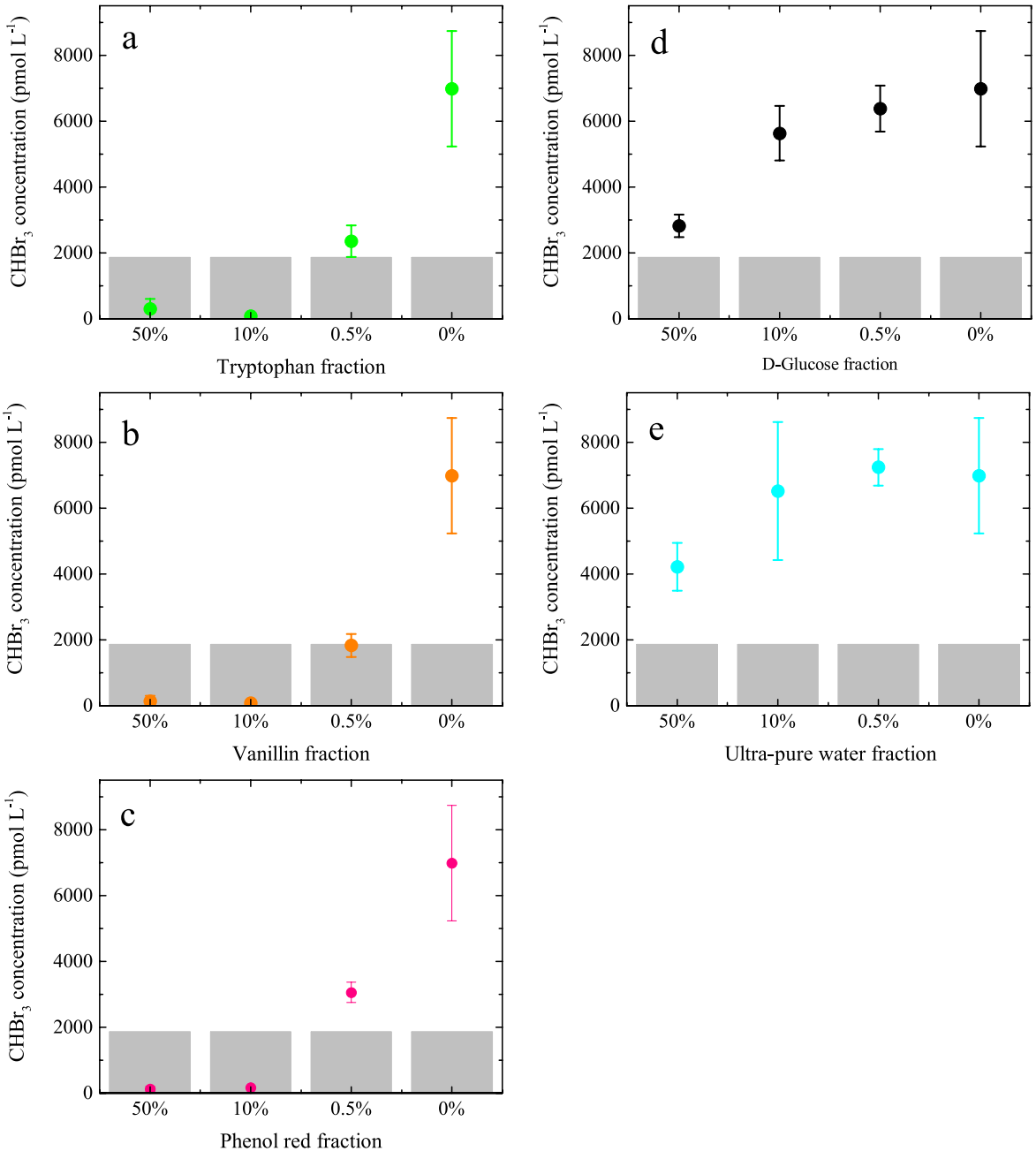

Figure 5-4. $CHBr_3$ concentrations observed from dual model DOM compound experiment. (a) Tryptophan, (b) vanillin, (c) phenol red, (d) D-glucose, and (e) ultra-pure water were mixed with urea at relative proportions of 50%, 10%, 0.5%, and 0% (*i.e.* 100% urea), to make up a total DOM concentration of ~1000 µM. Grey bar chart plots $CHBr_3$ concentration observed from V-BrPO treated ASW.

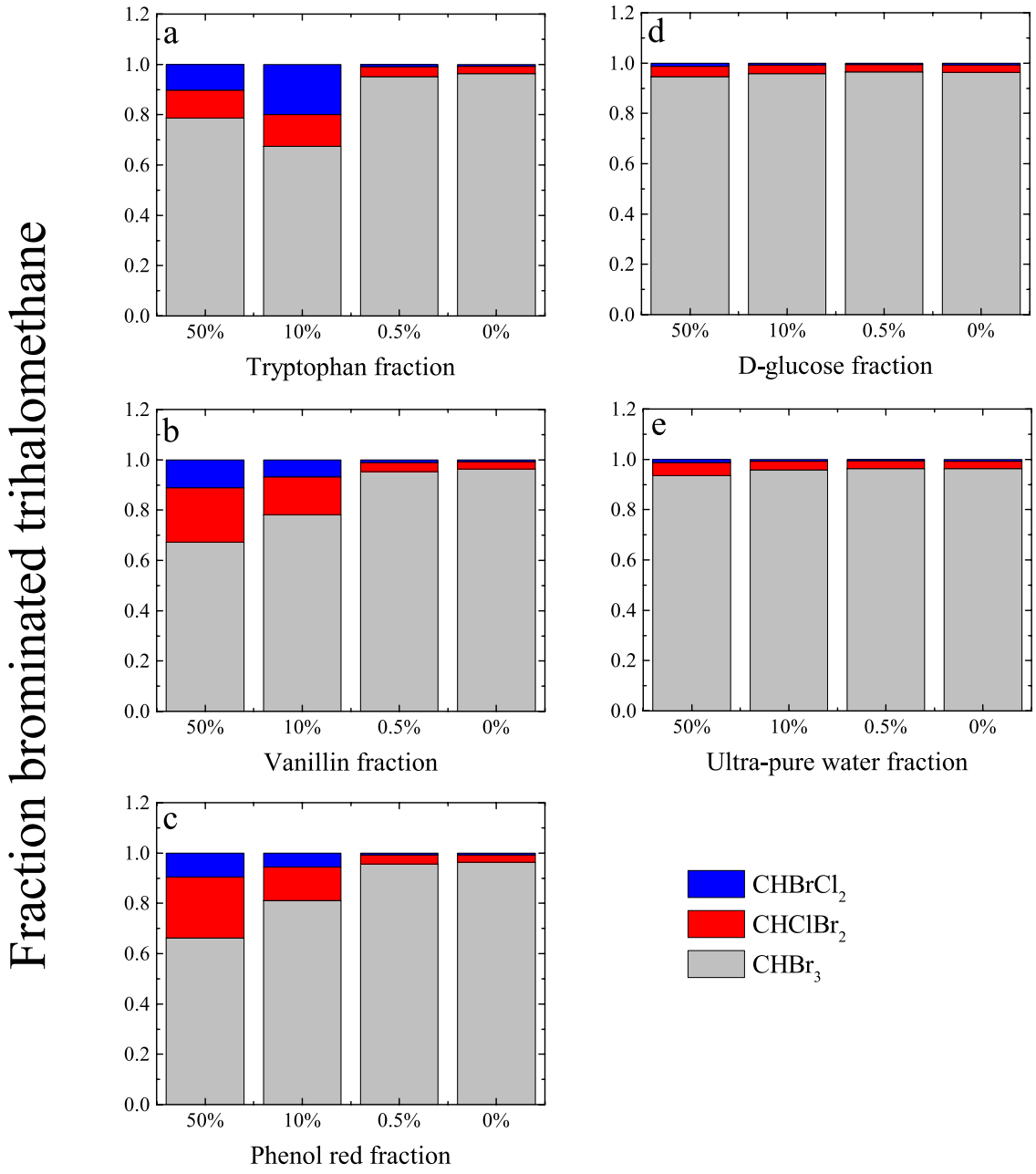

Figure 5-5. Brominated trihalomethane speciation at mixing proportion of 50%, 10%, 0.5%, and 0% of $DOM_{interfered}$ and DOM_{no_effect} with urea: (a) Tryptophan, (b) vanillin, (c) phenol red, (d) D-glucose, and (e) ultra-pure water.

5.4 Discussion

5.4.1 BrVSLS production sensitivity to DOM type

Our results from V-BrPO induced $HOBr_{enz}$ halogenation of single DOM model compounds show a significant effect of DOM type on BrVSLS production and speciation (Figures 5-1 and 5-3), when V-BrPO and H_2O_2 were present. The majority of the model DOM compounds examined did not express observable effect on BrVSLS production, relative to V-BrPO treated ASW. All carbohydrates examined in this study expressed such a BrVSLS production pattern. Carbohydrate is one of the dominant extracellular DOM produced by phytoplankton and encompasses a significant fraction of the DOM in the ocean [*Aluwihare and Repeta*, 1999; *Aluwihare et al.*, 1997; *Hansell et al.*, 2002]. In the surface ocean, carbohydrate can account for as much as 50% of the bulk DOM [*Aluwihare et al.*, 1997; *Benner et al.*, 1992; *McCarthy et al.*, 1996]. It is not surprising that such a ubiquitous pool of DOM does not have a significant effect on BrVSLS production, as BrVSLS only presented at trace level on a global scale in a patchy distribution pattern.

The rest of the model DOM compounds either interfered with or enhanced BrVSLS production, with more of them interfering with BrVSLS production. Interestingly, amino acids and DOM compounds with phenolic ring structures, which have been shown to produce considerable amounts of BrVSLS during drinking water chlorination processes at alkaline pH (*e.g.* pH 8) [*Hong et al.*, 2009; *Reckhow et al.*, 1990], interfered with BrVSLS production relative to HASW. Drinking water

chlorination is analogous to V-BrPO induced halogenation [*Quack and Wallace*, 2003; *Ram et al.*, 1990; *Wever and Van der Horst*, 2013]. Therefore, we substituted V-BrPO and H_2O_2 with NaOCl, an active ingredient in commercial bleach, to confirm whether these compounds competitively inhibited the enzyme. These compounds also interfered with BrVSLS production via NaOCl induced halogenation relative to NaOCl treated ASW, which confirmed that the reduction in BrVSLS production was not caused by competitive inhibition of the enzyme. However, unlike drinking water treatment, amino acids in ASW interfered with BrVSLS production, which may suggest different halogenation kinetics for these compounds in the seawater matrix, with relatively low concentration of NaOCl. Amino acids and lignin phenols are important DOM fraction present in the coastal seawater [*Bianchi*, 2011; *Duan and Bianchi*, 2007], where significant amounts of BrVSLS being produced and served as an important source of these ODSs to the atmosphere [*Carpenter et al.*, 2009; *Liu et al.*, 2011; *Liu et al.*, 2013; *Quack and Wallace*, 2003]. Therefore, their interference with BrVSLS production in seawater can potentially influence coastal BrVSLS dynamics.

Although only a few of the DOM compounds examined in this study enhanced BrVSLS production relative to HASW, most of these compounds are important metabolites produced by phytoplankton. Glycolic acid was one of the DOM compounds that slightly enhanced BrVSLS production upon V-BrPO induced halogenation. This particular metabolite is produced during photorespiration by phytoplankton [*Leboulanger et al.*, 1997; *Leboulanger et al.*, 1998a; *Leboulanger et al.*, 1998b]. H_2O_2, which is required for V-BrPO to generate $HOBr_{enz}$, is also produced

in light via photolysis of DOM and phytoplankton photosynthesis [*Cooper et al.*, 1988; *Manley*, 2002]. A strong correlation between H_2O_2 and $CHBr_3$ concentrations were observed from several species of phytoplankton isolated from the Baltic Sea under photo-oxidative stress [*Abrahamsson et al.*, 2003]. Such a condition is favorable for $CHBr_3$ formation, and now we show that it is not only because more H_2O_2 is available for $HOBr_{enz}$ formation, but it is also owing to the fact that some metabolites, such as glycolic acid, can enhance $CHBr_3$ production during photorespiration.

Urea, an important metabolite produced by organisms, showed significant enhancement of BrVSLS production. A substantially elevated $CHBr_3$ concentration was observed near the Canary Islands with low chlorophyll *a* concentration [*Carpenter et al.*, 2009; *Liu et al.*, Submitted]. Elevated heterotrophic bacteria abundance and urea concentration were also observed in this area [*Liu et al.*, Submitted]. *Liu et al.* [Submitted] speculated that the presence of reactive DOM led to elevated BrVSLS concentrations in this area, and the results presented in this study support this hypothesis. Urea is an indicator for amino acid cycling by bacteria [*Remsen*, 1971; *Zehr and Ward*, 2002], and it is also one of the DOM types that is effective for BrVSLS production. In addition, bacteria can excrete and utilize urea [*Zehr and Ward*, 2002] and many other DOM molecules. Since bacteria play an important role in regulating DOM composition in seawater, they may play an important, though maybe indirect, role in BrVSLS production.

Alginic Acid, a polysaccharide that is widely distributed in macroalgae [*McLachlan*, 1985], also enhanced BrVSLS production. It is well known that brown algae are prolific producers of BrVSLS [*Carpenter and Liss*, 2000]. V-BrPO activity

was observed in a diverse group of macroalgae [*Manley*, 2002; *Manley and Barbero*, 2001; *Theiler et al.*, 1978; *Wever and Van der Horst*, 2013; *Wever et al.*, 1991; *Wever et al.*, 1993]. The prolific BrVSLS production from macroalgae has long been explained by the presence of abundant V-BrPO. However, it was shown that $CHBr_3$ production was reduced when the macroalgae (*Ulva lactuca*) was exposed to common macroalgal metabolites [*Manley and Barbero*, 2001]. Therefore, the presence of V-BrPO does not necessarily lead to enhanced BrVSLS production, unless a suitable DOM is present, such as alginic acid.

Contrary to the phenolic DOM that interfered with BrVSLS production, humic acid was able to substantially enhance BrVSLS production at low concentration, which is consistent with results reported by drinking water treatment studies [*Oliver and Thurman*, 1983; *Reckhow et al.*, 1990]. Humic acid has been shown as a reactive substrate for BrVSLS formation upon halogenation with HOBr, which formed either via an enzyme-mediated pathway or NaOCl [*Lin*, 2011; *Oliver and Thurman*, 1983; *Reckhow et al.*, 1990]. This finding suggests only a small amount of reactive DOM is required to have a significant impact on BrVSLS production, which is consistent with observation by *Lin and Manley* [2012]. The authors observed a higher BrVSLS production by halogenating high molecular weight (HMW) DOM. Although the relative DOC concentration was lower in the HMW fraction, it was capable of producing comparable amounts of BrVSLS as the low molecular weight (LMW) DOM, which comprised a larger fraction of the bulk DOC. However, I speculate that the presence of reactive functional groups is more important than DOM molecular size alone. Besides the phenolic components, humic acids are also enriched in carboxylic

components, which are known to be reactive THM precursors [*Boyce and Hornig*, 1983].

It should be noted that CH_2Br_2 production was not observed in any of the treatments. This result is also consistent with *Lin and Manley* [2012], who found that only trace amount of CH_2Br_2 was produced upon V-BrPO induced halogenation of seawater collected from certain locations in a certain season at the California coast. Based on results from field observations, *Liu et al.* [2013] suggested CH_2Br_2 and $CHBr_3$ may not be derived from common sources (*i.e*. the same enzymatic mediated path). The co-production of these two BrVSLS may be controlled by different biogeochemical factors within the same ecosystem [*Liu et al*., 2013]. The same conclusion was drawn from large BrVSLS datasets presented in the Atlantic Ocean [*Liu et al.*, Submitted]. A recent laboratory study by *Hughes et al.* [2013] suggested that CH_2Br_2 was formed via biological mediated transformation of $CHBr_3$. Our results add further evidence for such a hypothesis, as CH_2Br_2 was not produced upon completion of V-BrPO induced halogenation reaction, and phytoplankton or bacteria cells were not present to facilitate the biological mediated transformation as proposed by *Hughes et al.* [2013]. However, the possibility of CH_2Br_2 production being more selective in DOM types cannot be excluded. Nonetheless, these would still suggest that CH_2Br_2 is not always co-produce with $CHBr_3$ via the same enzyme-mediated BrVSLS production pathway.

5.4.2 BrVSLS production in a dynamic DOM environment

The dual model DOM compounds experiment conducted in this study only presented a highly simplified scenario compared with *in situ*. Nonetheless, it is clear that BrVSLS production is govern by complex processes, such as the interaction between different DOM molecules. The presences of $DOM_{interfered}$, even at trace relative concentrations (0.5%), can substantially reduce BrVSLS production. Ultimately, BrVSLS production is driven by the relative concentrations of different compounds within the complex DOM pool in seawater and their reactivity.

DOM that is susceptible to V-BrPO induced halogenation does not necessarily lead to BrVSLS production. The interference of BrVSLS production observed in this study may be due to the fact that those molecules are more susceptible to halogenation, but they formed halogenated non-volatile compounds instead of producing BrVSLS. For example, aspartic acid and amino acids with similar properties may form haloacetic acid (HAA) upon halogenation [*Hong et al.*, 2009]. Phenol red is known to be a reactive DOM for halogenation, and it was used in a $HOBr_{enz}$ assay [*Hill and Manley*, 2009; *Sandy et al.*, 2011; *Wever et al.*, 1991]. Phenol red is yellow in acidic condition ($pH \leq 6$) and red in alkaline condition ($pH \geq 8$). Upon bromination by HOBr, it turns into bromophenol blue, which is blue. Such a color change upon bromination can be observed with a spectrophotometer. I followed the transformation of phenol red to its brominated product. I found that while phenol red significantly reduced BrVSLS production when the it was mixed with urea, it also transformed into bromophenol blue (Figure 5-6). At trace relative concentration

(0.5%), phenol red also substantially reduced BrVSLS production, which suggests phenol red is probably more susceptible to halogenation than urea.

These findings are consistent with *Manley and Barbero* [2001] who also found that addition of phenol red reduced $CHBr_3$ production. The halogenation of phenol red occurs at its phenol rings; it is therefore reasonable to assume that lignin phenols behave similarly. In fact, phenols are known antioxidants [*Vinson et al.*, 2001], which means they can react readily with oxidants like HOBr. Therefore, although not producing volatile compounds, it is not surprising that these molecules are reactive in forming other products, such as the non-volatiles, upon reaction with HOBr. Along this line, although not containing phenolic structure, ascorbic acid (vitamin C) is also a $DOM_{interfered}$ and an antioxidant. Therefore, chemical properties of DOM and relative abundances of different DOM types govern the halogenated products, such as the relative abundance of halogenated volatile and non-volatile compounds. This will ultimately govern the amounts of BrVSLS being produced in seawater.

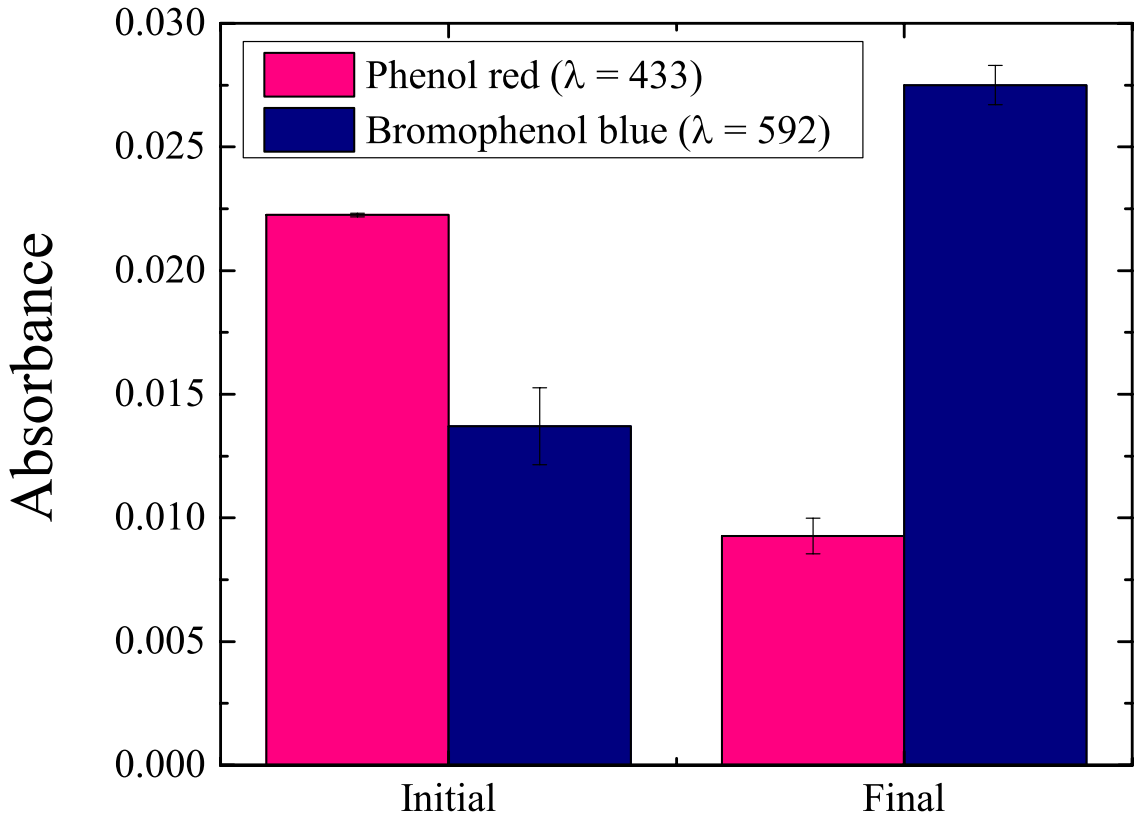

Figure 5-6. Absorbance of phenol red (λ = 433) and bromophenol blue (λ = 592) before (initial) and after (final) V-BrPO treatment of 10% phenol red + 90% urea samples.

5.4.3 Influence of DOM on brominated trihalomethane speciation

Our results showed that the relative abundance of $CHBr_3$, $CHClBr_2$, and $CHBrCl_2$ in the total BTHM pool is also sensitive to DOM type (Figure 5-5). Interestingly, the relative abundance of the BTHM in non-V-BrPO treated ASW and GoMSW was similar to those observed from the V-BrPO treated $DOM_{interfered}$. I postulate that the $DOM_{interfered}$ are kinetically more favorable in forming halogenated

non-volatile compounds rather than forming volatile compounds like BrVSLS. The BTHM pools in the V-BrPO treated $DOM_{interfered}$ are, therefore, remained unaltered as the untreated seawaters samples.

The dual model DOM compounds mixing experiments also showed different BTHM relative abundances. As considerable amounts of $DOM_{interfered}$ (*i.e.* 50% and 10%) mixed with urea, they yielded a different BTHM relative abundance pattern (Figure 5-5). This finding supports the above hypothesis. As the $DOM_{interfered}$ are kinetically more favorable for halogenation than urea, but formed halogenated non-volatile molecules instead. Therefore, the BTHM pools in the 50% and 10% mixed experiments were relatively less altered than those observed in the 0.5% and 0% relative proportion of $DOM_{interfered}$. Hence, $CHBr_3$ relative abundances in the 50% and 10% mixed experiments were lower, and more similar to the untreated ASW. The effect of $DOM_{interfered}$ in BTHM speciation was smaller at relative proportion of 0.5%. Therefore, BTHM relative abundances in the 0.5% mixed experiments expressed similar patterns as in the D-glucose and ultra-pure water mix experiments and the 100% urea (*i.e*. 0% $DOM_{interfered}$) experiment.

In a dynamic environment, such as the ocean, the relative abundances of $DOM_{interfered}$ in the bulk DOM pool may lead to different patterns of BTHM relative abundance, as observed in the Atlantic Ocean (Figure 5-7).

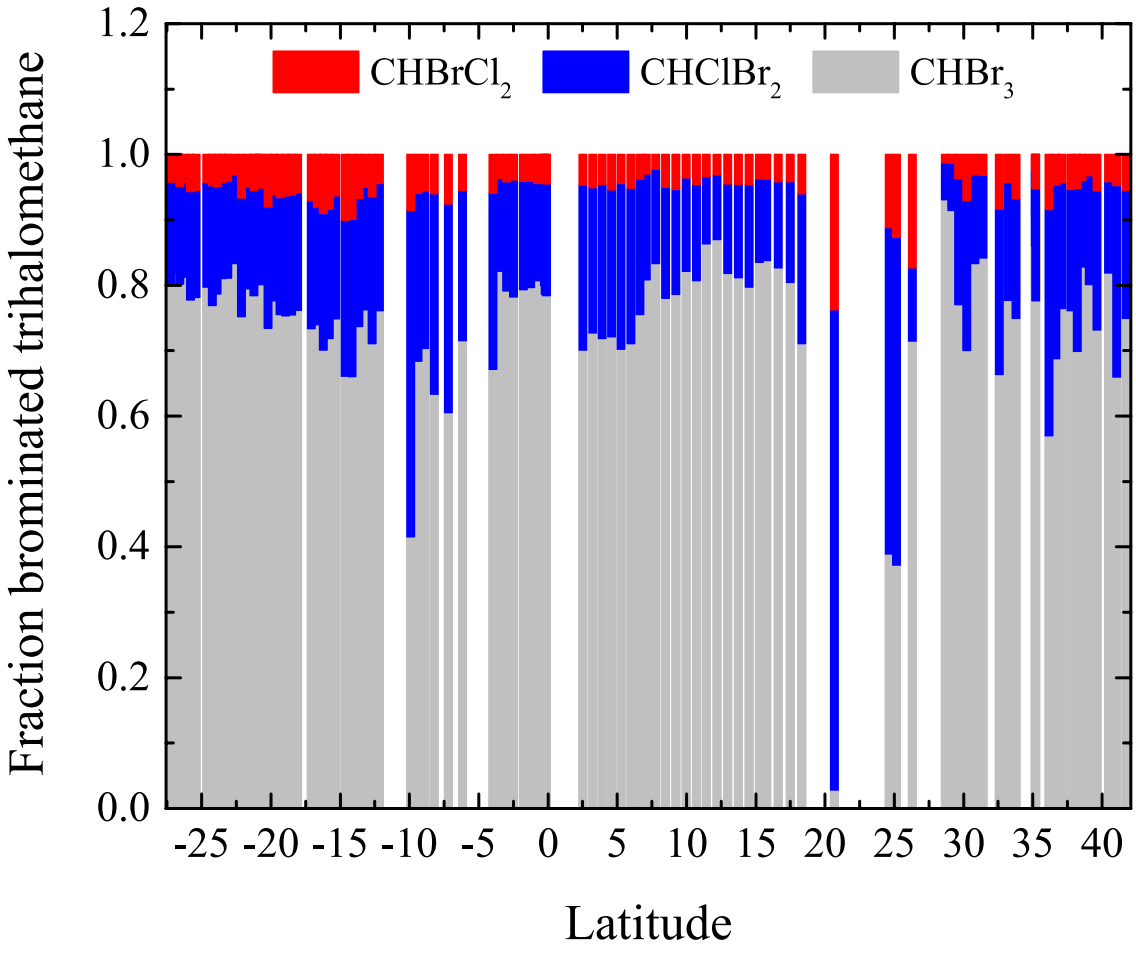

Figure 5-7. Brominated trihalomethane speciation observed during the Halocarbon Air-sea Transect – Atlantic (HalocAST-A) cruise.

5.4.4 Implications for BrVSLS biogeochemistry in the ocean

$CHBr_3$ concentration in seawater follows a broad trend with chlorophyll *a* concentration [*Carpenter et al.*, 2009; *Liu et al.*, Submitted; *Schall et al.*, 1997]. A clear concentration gradient of $CHBr_3$ across waters with different ranges of productivity was observed in the Atlantic Ocean [*Liu et al.*, Submitted]. In the water

column, the BrVSLS tend to be elevated near the subsurface chlorophyll maximum depth [*Liu et al.*, 2013; *Quack et al.*, 2004]. These observations show that the involvement of phytoplankton, and presumably V-BrPO activity, is essential for BrVSLS production. However, BrVSLS concentration usually does not significantly correlate with chlorophyll *a* concentration. Even though BrVSLS tend to be elevated with chlorophyll *a*, significant BrVSLS variability in productive waters was observed. Several explanations have been suggested, including effects of sea-to-air fluxes of BrVSLS, different turnover rates between BrVSLS and chlorophyll *a*, phytoplankton species specificity for BrVSLS production, physical mixing, influence of anthropogenic input, and DOM specificity for BrVSLS production [*Abrahamsson et al.*, 2004; *Hughes et al.*, 2009; *Liu et al.*, 2011; *Liu et al.*, Submitted; *Mattson et al.*, 2012].

While these processes can, to some extent, alter the relationship between BrVSLS and chlorophyll *a*, a factor that is more directly linked to the enzyme-mediated path was suggested, namely the variability in V-BrPO activity in seawater [*Wever and Van der Horst*, 2013]. However, only a small fraction of $HOBr_{enz}$ ultimately turns into $CHBr_3$, as observed by *Hill and Manley* [2009], which suggests V-BrPO induced $HOBr_{enz}$ may not be a limiting factor for BrVSLS production in seawater. Results from this study offer another plausible explanation on the significant variability of BrVSLS concentration in seawater. I hypothesize that the variability in BrVSLS production is affected by DOM type in seawater. As aforementioned, the relative abundance and reactivity of $DOM_{interfered}$ and $DOM_{enhance}$ will lead to different BrVSLS production rates in seawater.

The coastal ocean is a significant source of BrVSLS [*Carpenter et al.*, 2009; *Liu et al.*, 2011; *Quack and Wallace*, 2003; *Quack et al.*, 2007a], owing to its high productivity and presence of macroalgal habitats. Moreover, reactive DOM is also present at high concentrations in the coastal ocean. However, $DOM_{interfered}$, such as tryptophan, tyrosine, and lignin phenols can also occur in the coastal ocean. These compounds also cycle quickly in along the freshwater-to-saline water gradient [*Coble*, 2007; *Hernes and Benner*, 2003]. Therefore, the fate of different types of DOM will ultimately govern what is available for $HOBr_{enz}$ halogenation and the subsequent release BrVSLS.

Hence, to better understand BrVSLS biogeochemistry, it is important to better understand DOM characterization. CDOM comprise an important fraction of the DOM [*Coble*, 2007]. Characterization of CDOM with excitation-emission matrix couple with parallel factor analysis (PARAFC) is becoming an emerging tool to understand components in the CDOM pool. Such a method is relatively economical and can be easily deployed in the field. Therefore, it is possible to utilize information in DOM characteristic in BrVSLS modeling study; once we have more information on the relationship between DOM characteristic and BrVSLS production.

5.5 Conclusion

Our results suggest the type of DOM in seawater can significantly influence BrVSLS production, which has important implications for BrVSLS concentrations, distributions, and emissions from the ocean. These factors will ultimately affect the

global BrVSLS budget and supply to the stratosphere via SGI. Moreover, in a future climate, DOM supply to the coastal ocean and DOM fate may experience drastic changes. For example, as the artic permafrost starts thawing and more labile DOM is discharged to the coastal ocean. Such changes will likely shift relative abundances of DOM type that can influence BrVSLS, hence, significantly alter the production of BrVSLS in coastal waters. Since coastal oceans are known as "hot-spots" for the BrVSLS, such changes may have significant impacts on global BrVSLS budgets.

CHAPTER VI

PRODUCTION OF BROMINATED VERY SHORT-LIVED SUBSTANCES (BRVSLS) BY PHYTOPLANKTON

6.1 Introduction

Brominated very short-lived substances (BrVSLS) are important inorganic bromine (Br_y) suppliers to the atmosphere. Bromoform ($CHBr_3$) and dibromomethane (CH_2Br_2) account for ~80% of the very short-lived organic bromine in the marine boundary layer [*Law and Sturges*, 2007], and these two major BrVSLS account for ~76% of very short-lived substances (VSLS) derived Br_y (Br_y^{VSLS}) in the stratosphere [*Hossaini et al.*, 2012a]. Chlorodibromomethane ($CHClBr_2$) and bromodichloromethane ($CHBrCl_2$) comprise a relatively minor fraction of the BrVSLS, and they are capable of supplying moderate amount of Br_y^{VSLS} to the stratosphere [*Hossaini et al.*, 2012a]. These BrVSLS degraded into Br_y via photolysis and reaction with hydroxyl radicals (OH). The resulting Br_y can then participate in catalytic ozone destruction cycles. On an atom-by-atom basis, bromine is ~50 to 100 times more effective in destroying ozone than chlorine [*Garcia and Solomon*, 1994; *Solomon et al.*, 1995]. Therefore, numerous efforts have been made to better understand BrVSLS global budgets, distributions, and sources [*Butler et al.*, 2007; *Carpenter and Liss*, 2000; *Carpenter et al.*, 2009; *Carpenter et al.*, 2007b; *Liu et al.*, 2011; *Liu et al.*, 2013; *Liu et al.*, Submitted; *Moore and Tokarczyk*, 1993; *Moore et*

al., 1996; *Quack and Wallace*, 2003; *Quack et al.*, 2007a; *Quack et al.*, 2007b; *Quack et al.*, 2004].

$CHBr_3$, CH_2Br_2, $CHClBr_2$, and $CHBrCl_2$ are mainly derived from natural sources in seawater. Macroalgae are prolific producers of natural BrVSLS, and a wide range of macroalgal species produce substantial amounts of BrVSLS [*Carpenter and Liss*, 2000; *Gschwend and MacFarlane*, 1986]. However, despite the large BrVSLS production strengths, macroalgal habitats are constrained to certain types of coastal environments [*Lüning*, 1990]. Therefore, phytoplankton is hypothesized to be a globally significant source, owing to their ubiquitous distribution in the surface ocean [*Moore et al.*, 1995b]. Several groups of phytoplankton are known to produce BrVSLS in laboratory cultures, including diatoms and coccolithophores [*Colomb et al.*, 2008; *Hughes et al.*, 2013; *Moore et al.*, 1996]. However, owing to substantially elevated BrVSLS concentrations were observed in the Arctic and Antarctic oceans, most studies had focused on cold-water phytoplankton species.

Here, I report results observed from screening of 9 phytoplankton species for BrVSLS production.

6.2 Methods

6.2.1 Phytoplankton culture

I selected 9 phytoplankton species from diverse classes, including a few tropical and subtropical species (Table 6-1; Figure 6-1). 8 of the phytoplankton species chosen for this screening study are cosmopolitan. Selection of phytoplankton was based on (1) correlation between BrVSLS and biogeochemical markers observed from field studies, which cosmopolitan species of the taxonomic groups found to be correlated with BrVSLS were selected; (2) cosmopolitan diatoms that collected from temperate and warm waters; (3) phytoplankton species that were known to express V-BrPO activity.

Phytoplankton stock cultures were purchased from the National Center for Marine Algae and Microbiota (NCMA; formerly known as Culture Collection of Marine Phytoplankton, CCMP). All phytoplankton cultures were grown in 2 L incubation vessels with ~ 600 mL culture medium inside (Figure 6-2). 0.2 μm filtered artificial seawater (ASW) [*Beggs et al.*, 2009] was added to each culture vessel and autoclaved for 40 min and allowed to cool prior to nutrient and culture additions. Nutrients were added to each vessel at concentrations suggested by NCMA. For most phytoplankton cultures, L1 nutrients were used [*Guillard and Hargraves*, 1993]. Cyanobacteria cultures were grown in L1 media without silicate added. The crytophyte, *Guillardia theta,* was grown in K nutrients, which is designed for oligotrophic oceanic species [*Keller et al.*, 1987]. Finally, 1 mL of culture stock was

added to each vessel. Once inoculated, the culture vessel entrance were flamed and capped. All cultures were grown in triplicate.

Two incubation vessels with only ASW and nutrients added were incubated along with the cultures as blanks. All procedures were conducted in a LABCONCO vertical clean bench to avoid bacterial contaminations. All cultures were incubated in a temperature-controlled incubator at 20 °C in a 10/14 hr-light/dark cycle. Photon flux density (pfd) near the incubation vessels surfaces were ~42 μmol-photon m^{-2} s^{-1}. Trace gases in the headspaces were analyzed for each sample on the day of inoculation with gas chromatography – mass spectrometer (GC-MS). All cultures were then closed and incubated until they reached stationary phase to accumulate sufficient amounts trace gases for production measurement. Cell growth phase was estimated by light transmission through each culture vessel as described below. It should be noted that *Achnanthes longipes* was grown in both ASW and Gulf of Mexico seawater (GoMSW) to compare whether BrVSLS production was different in natural seawater.

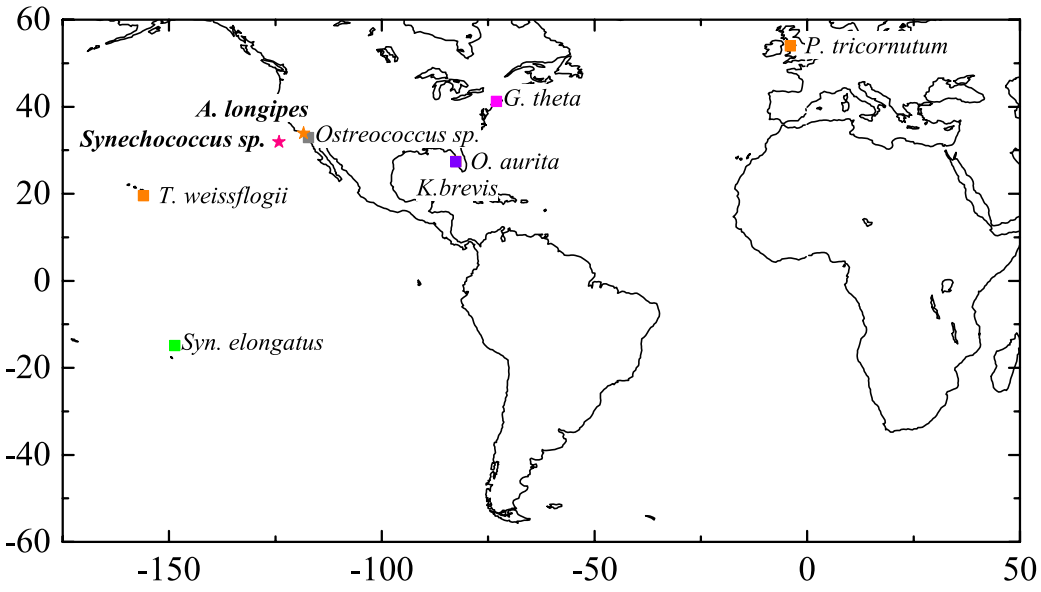

Figure 6-1. Map of locations where the stock cultures were isolated from. Information was provided by the National Center of Marine Algae and Microbiota (NCMA). Orange symbols indicate diatom species, magenta symbol indicates cryptophte species, purple symbol indicates dinoflagellate species, grey symbol indicates prasinophyte species, green symbol indicates open ocean cyanobacteria species, and pink symbol indicates coastal cyanobacteria species. Stars indicate species with BrVSLS production.

Table 6-1. Phytoplankton species screened for BrVSLS and $CHCl_3$ production. "+" indicates significant production of BrVSLS and $CHCl_3$ were observed in the culture. "-" indicates there were no observable production of BrVSLS and $CHCl_3$ in the culture. "c.d." notes production cannot be determined due to co-elution of unidentified substances with the compounds of interested.

Species	CCMP ID#	Class	Medium used	$CHBr_3$	CH_2Br_2	$CHClBr_2$	$CHBrCl_2$	$CHCl_3$
Achnanthes longipes	101	Bacillariophyceae	L1, ASW and GoMSW	+	+	+	+	+
Synechococcus sp.	2515	Cyanophyceae	L1 - Si, ASW	-	+	+	+	+
Odontella aurita	1796	Coscinodiscophyceae	L1, ASW	c.d.	c.d.	c.d.	c.d.	c.d.
Phaeodactylum tricornutum	2561	Bacillariophyceae	L1, ASW	-	-	-	-	-
Thalassiosira weissflogii	1051	Coscinodiscophyceae	L1, ASW	-	-	-	-	-
Ostreococcus sp.	2972	Prasinophyceae	L1, ASW	-	-	-	-	-
Synechococcus elongatus_cf	1379	Cyanophyceae	L1 - Si, ASW	-	-	-	-	-
Guillardia theta	327	Cryptophyceae	K, ASW	-	-	-	-	-
Karenia brevis	2228	Dinophyceae	L1 - Si, ASW	-	-	-	-	-

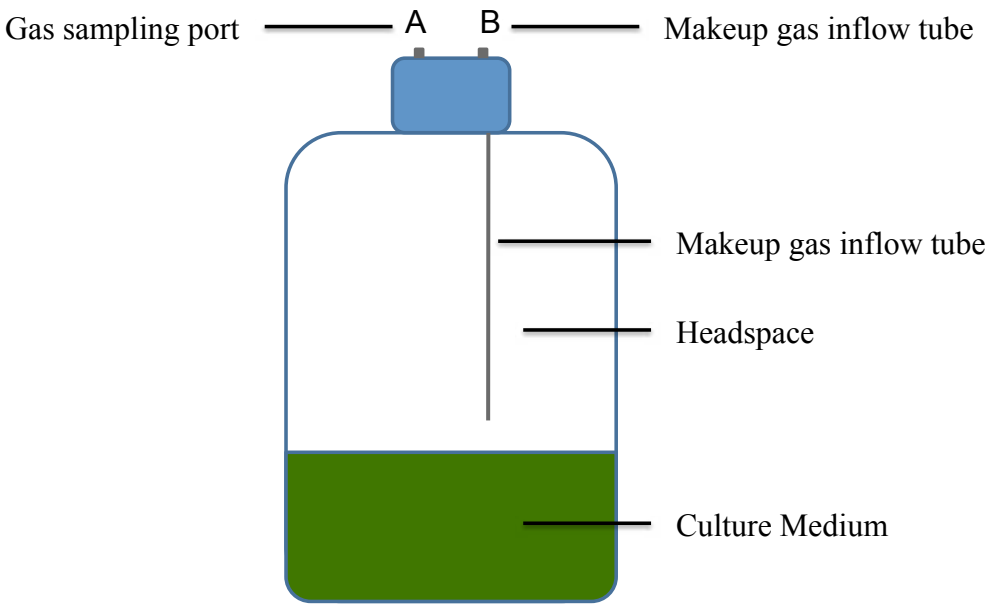

Figure 6-2. Schematic of incubation vessel used for phytoplankton culture screening. Any trace gases produced by the phytoplankton were equilibrated with the headspace. Port A was connected to the GC-MS system to analyze for halocarbon production. A 0.2µm air filter was connected to port B, which served as makeup gas inflow to compensate pressure change inside the vessel during halocarbon headspace sampling.

6.2.2 Assess cell density in culture

Due to the nature of trace gas sampling, the incubation vessels cannot be opened to draw samples for cell counts as the cultures grow. Therefore, growth in each vessel was semi-qualitatively assessed by measuring the amount of light transmitted through the culture vessel every day. Each culture vessel was rolled gently on a rolling machine and then placed in front of a constant full spectrum light source. A LiCor LI-250A light meter was placed in line with the light source on the other side of the culture vessel to measure light transmission through the culture vessel (Figures 6-3 and 6-4). The measurement of light transmission was conducted in dark to avoid ambient light interfering with the light source. Cell density is presented as a function of light transmission, which is calculated with the following equation:

$$I_{transmission} = I_{culture} - I_{blank} \quad \text{(Equation 6.1)}$$

where $I_{transmission}$ is the difference of light intensity transmitted through the culture and blank. The more negative the value, the higher the cell density in the vessel. Pfd was measured in μmol-photon m^{-2} s^{-1}.

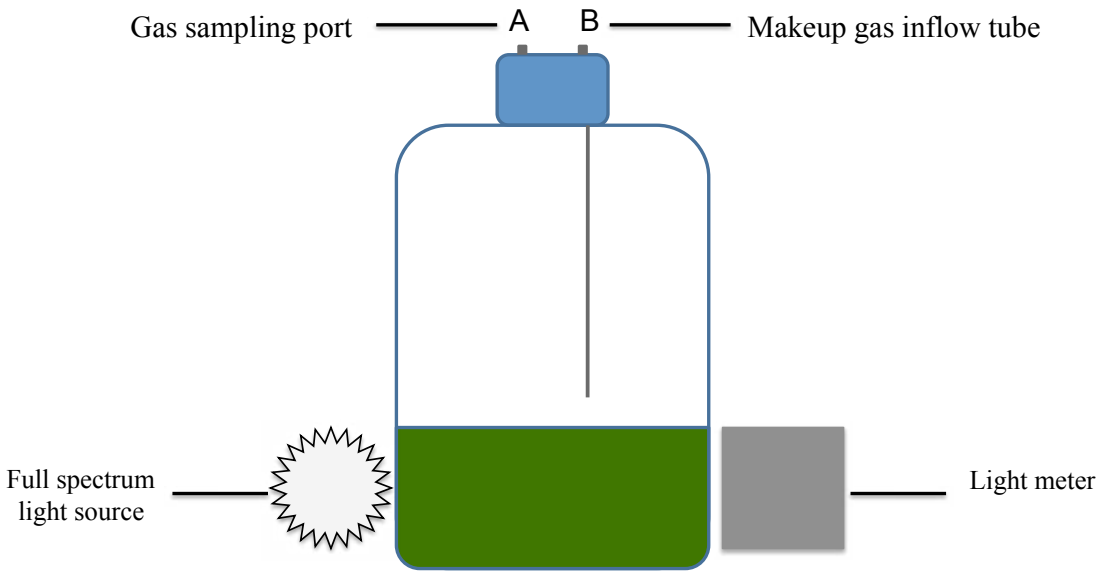

Figure 6-3. Schematic of light transmission method, used for assessing cell density. A full spectrum light source was place at one side of the incubation vessel. A LiCor LI-250A light meter was place inline on the other side of the incubation vessel to measure light transmission through the incubation vessel.

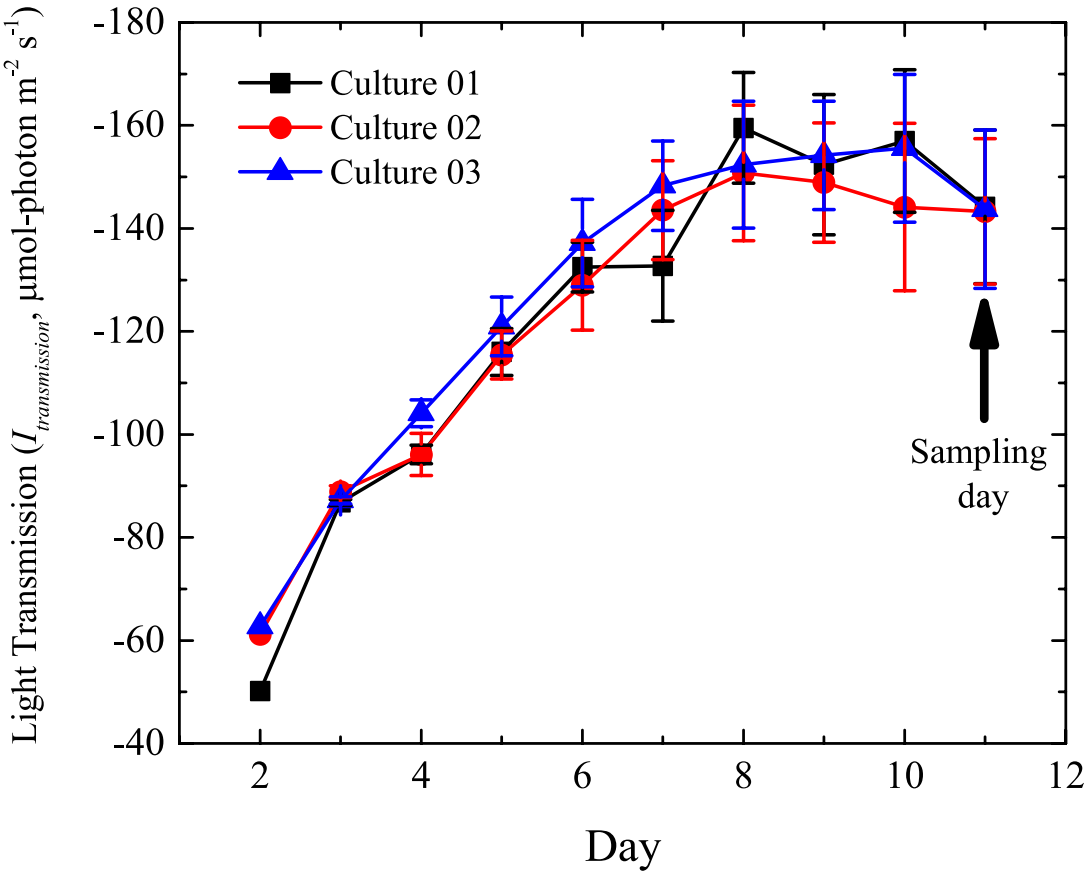

Figure 6-4. An example of cell density (*Achnanthes longipes Agardh*), presented in light transmission ($I_{transmission}$, µmol-photon m^{-2} s^{-1}), as a function of time. Trace gas samples were analyzed once the cell cultures reached stationary phase.

6.2.3 Trace gas analysis

Trace gas concentrations were measured on a cryo-trapping and focusing – GC-MS system, as described by [*Yvon-Lewis et al.*, 2004]. Each sample was gently rolled on a rolling machine for 2 hours to achieve equilibrium in the headspace, and then connected (port A, refer to Figure 6-2) to a 12-port automated stream select valve in connection with a vacuumed sampling line. A 0.2 μm membrane filter was connected to port B (refer to Figure 6-2) to ensure no bacterial contamination was introduced into the vessel when the make-up air was drawn into the vessel. Make up air was ambient room air drawn into the vessel during sample collection to compensate change in headspace pressure inside of the vessel. Approximately 1 L of headspace was drawn from the headspace of each incubation vessel. Pressure of the air collection canister was recorded for calculating the actual headspace volume drawn as trace gas sample. Subsequently, the valve was turned into the next position with an ultra-pure nitrogen stream connected. The ultra-pure nitrogen stream served as make-up gas for the trace gas analysis. Analytes were trapped and focused at -80 °C and desorbed and injected into the GC column at 210 °C.

A moist air standard, calibrated against a whole air working-standard obtained from the National Oceanic and Atmospheric Administration (NOAA) Global Monitoring Division (GMD), was used as a calibration standard. Calibration air was run at the beginning of a sequence and after every forth injection as: calibration, sample 1, sample 2, sample 3, ultra-pure nitrogen, and calibration. Ultra-pure nitrogen

stream was run after every third injection of sample to monitor the make-up gas quality, and ensure no contamination in the sampling line.

Detection limits (in pico atmosphere, patm) for $CHBr_3$, CH_2Br_2, $CHBrCl_2$, $CHClBr_2$, and $CHCl_3$ were 0.02 patm, 0.03 patm, 0.01 patm, 0.01patm, and 0.46 patm, respectively. Average analytical uncertainty was 7.0% for $CHBr_3$, 6.0% for CH_2Br_2, 9.0% for $CHBrCl_2$ and $CHClBr_2$, and 6.7% for $CHCl_3$. All trace gas concentrations reported here were converted to aqueous concentrations (C, pmol L^{-1}) using the following equation:

$$C = \frac{p}{H} \qquad \text{(Equation 6.2)}$$

where p is the equilibrated partial pressure of the gas of interested in patm, and H is the Henry's Law constant. For the BrVSLS, H was converted from the dimensionless Henry's law constant reported by *Moore et al.* [1995a], using the gas constant (0.0821 L atm K^{-1} mol^{-1}). Similarly, H for chloroform ($CHCl_3$) was calculated from the dimensionless Henry's law constant reported by *Dewulf et al.* [1995].

6.2.4 Statistics

Significant outlier was determined by Dixon's *Q-test* at a confidence level of 90%. Data points rejected by the Dixon's Q-test, if any, were removed when interpreting the data. Amounts of trace gases produced over the course of incubation were determined by the concentration differences between those observed on the day of inoculation and those observed at stationary phase. One-way ANOVA test at a

confidence level of 95% was used to determine whether the production was significant (*i.e.* significantly different from day 1).

6.3 Results

Cell growths were observed in all cultures, but only 2 out of 9 phytoplankton species screened showed observable production of BrVSLS (Table 6-1). *A. longipes* and *Synechococcus sp.* were capable of producing significant amounts of various BrVSLS over the course of incubation (Table 6-2, Figure 6-5). Significant production of $CHBr_3$, CH_2Br_2, $CHClBr_2$, $CHBrCl_2$, and $CHCl_3$ were observed in *A. longipes* cultures. Significant amounts of $CHBr_3$, $CHClBr_2$, and $CHBrCl_2$ were observed in *Synechococcus sp.* cultures. However this particular strain of *Synechococcus* did not produce observable amounts of CH_2Br_2 and $CHCl_3$.

BrVSLS concentrations and chemical speciation differ substantially between these two species. Importantly, BrVSLS concentrations and chemical speciation also differ significantly from the same species, *A. longipes*, which incubated under similar conditions but in different seawater sources and incubation lengths. Two batches of *A. longipes* were grown in ASW for 30 days and 11 days, respectively. One batch of *A. longipes* was grown in open Gulf of Mexico seawater (GoMSW) for 11 days. Although the same class of BrVSLS was produced in these batches, their relative abundances were different (Figures 6-6 and 6-7). $CHBr_3$, $CHClBr_2$, and $CHBrCl_2$ are brominated trihalomethanes (BTHM). The BTHM and $CHCl_3$ are trihalomethanes (THM). $CHBr_3$ relative abundances in the BTHM pool differ substantially in the three

batches of *A. longipes* cultures (Figure 6-6). $CHBr_3$ was consistently a minor production within the THM pool (Figure 6-7) in *A. longipes* cultures. In *Synechococcus sp.* culture, $CHBr_3$ was a major production within the BTHM pool, with a pattern similar to those observed in typical enzymatic-mediated bromination reactions [*Liu et al.*, In prep] (see Chapter V) (Figure 6-6).

Table 6-2. Concentrations (±1 standard deviation) of $CHBr_3$, CH_2Br_2, $CHClBr_2$, $CHBrCl_2$, and $CHCl_3$ produced in *A. longipes* and *Synechococcus sp.* cultures.

Species (condition)	$CHBr_3$ (pmol L^{-1})	CH_2Br_2 (pmol L^{-1})	$CHClBr_2$ (pmol L^{-1})	$CHBrCl_2$ (pmol L^{-1})	$CHCl_3$ (pmol L^{-1})
A. longipes (L1, ASW, incubated for 30 days)	179.2 ± 46.7	9.1 ± 1.0	23.3 ± 7.5	117.0 ± 25.6	1821.6 ± 529.1
A. longipes (L1, ASW, incubated for 11 days)	1507.1 ± 244.8	121.2 ± 13.8	1025.6 ± 145.7	3649.8 ± 46.6	472.6 ± 0.7
A. longipes (L1, GoMSW, incubated for 11 days)	268.9 ± 79.4	471.4 ± 58.0	601.1 ± 70.3	2190.6 ± 220.9	944.7 ± 86.6
Synechococcus sp. (L1 - Si, ASW, incubated for 14 days)	1331.8 ± 694.9	-	302.3 ± 167.6	78.5 ± 48.8	-

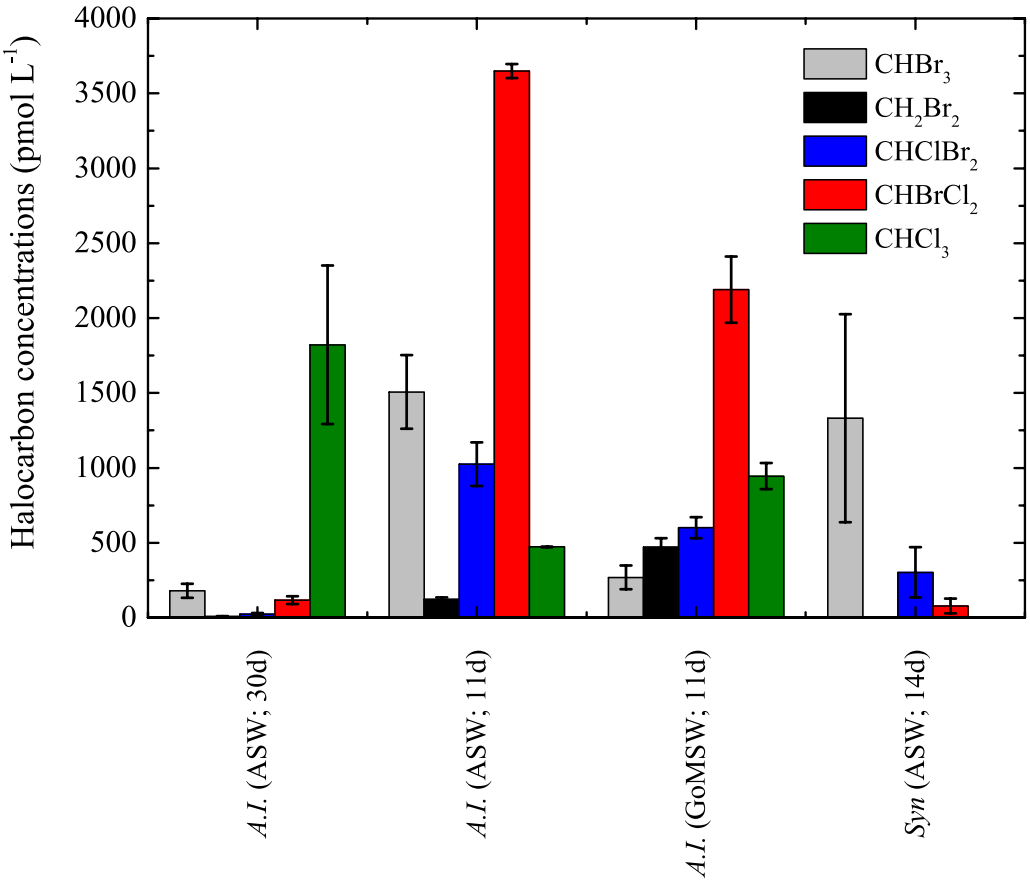

Figure 6-5. Amounts (in aqueous concentration pmol L^{-1}) of $CHBr_3$, CH_2Br_2, $CHClBr_2$, $CHBrCl_2$, and $CHCl_3$ produced by *A. longipes* and *Synechococcus sp.* in cultures of different ages. ASW indicates that the cultures were grown in artificial seawater, and GoMSW indicates that the culture was grown in Gulf of Mexico seawater.

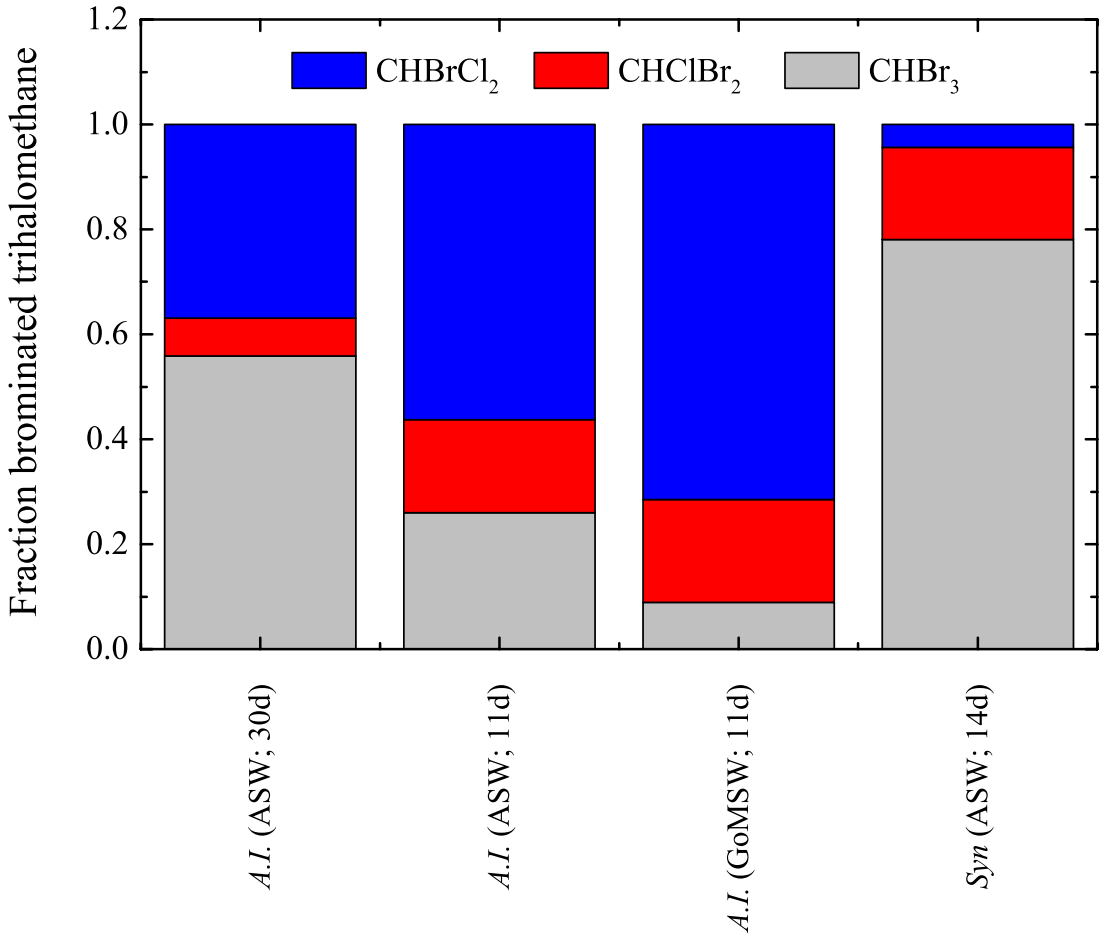

Figure 6-6. Relative abundances of $CHBr_3$, $CHClBr_2$, and $CHBrCl_2$ in the brominated trihalomethane (BTHM) pool in *A. longipes* (*A.I.*) and *Synechococcus sp.* (*Syn*) cultures. ASW indicates that the cultures were grown in artificial seawater, and GoMSW indicates that the culture was grown in Gulf of Mexico seawater.

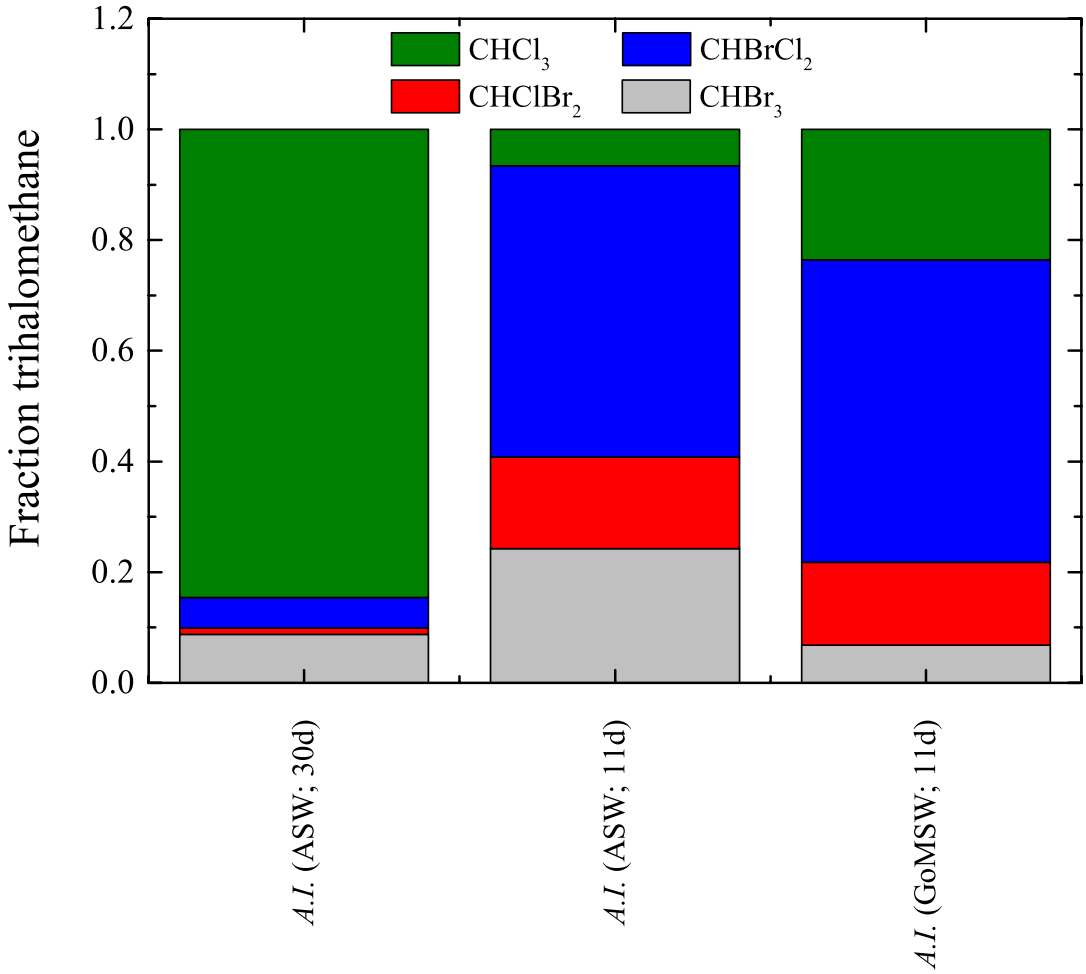

Figure 6-7. Relative abundances of $CHBr_3$, $CHClBr_2$, $CHBrCl_2$, and $CHCl_3$ in the trihalomethane (THM) pool in three different batches of *A. longipes* (*A.I.*) cultures. ASW indicates that the cultures were grown in artificial seawater, and GoMSW indicates that the culture was grown in Gulf of Mexico seawater.

6.4 Discussion

6.4.1 Is BrVSLS production species specific?

Results observed in this study indicate that the production of BrVSLS is highly species specific, which is consistent with findings from other studies [*Colomb et al.*, 2008; *Hill and Manley*, 2009; *Hughes et al.*, 2013; *Moore et al.*, 1996; *Moore et al.*, 1995b; *Tokarczyk and Moore*, 1994]. Results in this study also support numerous field observations, which found that BrVSLS concentrations do not significantly correlate with chlorophyll *a* and other pigment biomarkers; and species-specificity has long been an explanation [*Abrahamsson et al.*, 2004; *Ekdahl et al.*, 1998; *Liu et al.*, 2013; *Mattson et al.*, 2012]. However, recently, *Liu et al.* [Submitted] found that, on a basin-wide scale, elevated BrVSLS concentrations in the ocean were often located in regions with high concentrations of chlorophyll *a*. A clear gradient of $CHBr_3$ concentration was observed across waters with different production (estimated with chlorophyll *a* concentration). This observation by *Liu et al.* [Submitted] not only confirmed the importance of phytoplankton in mediating BrVSLS production, but also indicates that phytoplankton species that are capable of mediating BrVSLS production are more widespread than have long been believed.

Results presented by *Liu et al.* [In prep] (see Chapter V) provided new insights to these discrepancies. The two species that were capable of producing BrVSLS, *A. longipes* and *Synechococcus sp.*, have been shown to express bromoperoxidase activity [*Hill and Manley*, 2009; *Johnson et al.*, 2011]. Vanadium bromoperoxidase

(V-BrPO) is an enzyme involved in mediating halogenation of dissolved organic matter (DOM) and the subsequent release of BrVSLS in seawater [*Butler and Carter-Franklin*, 2004; *Lin and Manley*, 2012; *Theiler et al.*, 1978; *Wever et al.*, 1993]. Therefore, results in this study are consistent with the BrVSLS formation pathway proposed over a decade ago. However, the role of DOM has recently been suggested to play an essential role in controlling BrVSLS production [*Liu et al.*, In prep] (see Chapter V). Therefore, the apparent species specificity in BrVSLS production may have been influenced by DOM composition in the culture medium.

Liu et al. [In prep] (see Chapter V) has shown that 2 out of 3 vitamins commonly used in phytoplankton culture, namely, thiamine and ascorbic acid (vitamin C), interfered with V-BrPO mediated BrVSLS production. Common amino acids produced by phytoplankton, such as aspartic acid and glutamic acid [*Granum et al.*, 2002], also significantly interfered with V-BrPO mediated BrVSLS production. The author also suggested that these compounds formed non-volatile halogenated molecules instead of the volatile compounds. Therefore, species that only express weak V-BrPO production may not yield observable BrVSLS production, as these DOM molecules tend to be present at high concentration in a phytoplankton culture. Moreover, if the DOM molecules produced by certain phytoplankton species are more reactive in forming non-volatile molecules, then BrVSLS may not be observed.

As suggested by *Liu et al.* [In prep] (see Chapter V), BrVSLS production strength may ultimately control by the DOM pool in the environment. Some compounds enhance BrVSLS production while some interfere with BrVSLS production. Therefore, DOM present in the phytoplankton culture may significantly

alter BrVSLS production rate. The extracellular DOM produced by a phytoplankton cell is complicated and involves many factors, such as cell physiological state, any potential chemical reactions occur in the medium, environmental factors (*e.g.* temperature and light), and presence of bacteria. As discussed by *Kujawinski* [2010], DOM profile observed from monocultures can be drastically different from cultures of multiple species. This indicates interactions between different phytoplankton species and the surrounding microbial community can significantly change the DOM pool, hence, the fate of BrVSLS production.

It has been also shown that the presence and absence of bacteria can alter $CHBr_3$ production [*Hughes et al.*, 2013]. I proposed two plausible explanations. First, the composition of the DOM produced by bacteria is different from what is produced by phytoplankton. It is possible that the change in DOM characteristic with the presence of bacteria changes BrVSLS production. Second, V-BrPO has been proposed as a defense mechanism for phytoplankton [*Manley*, 2002; *Ohsawa et al.*, 2001; *Wever et al.*, 1991]. Halogenated molecules, created via V-BrPO mediated halogenation, have been shown to disrupt bacterial quorum sensing [*Sandy et al.*, 2011]. Therefore, the presence of bacteria may trigger more V-BrPO halogenation activity and alter BrVSLS production. However, controlling bacterial abundance in cultures with antibiotic may be problematic as well, as these molecules may interfere with BrVSLS production.

The ocean in reality is so much more complicated than a monoculture. Considering the complexity of DOM, results from laboratory monoculture cannot be used to understand BrVSLS biogeochemistry in the ocean. To legitimately determine

whether BrVSLS production is indeed species specific, independent of DOM influence, more information on V-BrPO activity in culture is required. Unfortunately, V-BrPO assay is usually not a routine exercise for BrVSLS production screening studies.

6.4.2 A different production path for BrVSLS in A. longipes?

As discussed by *Liu et al.* [In prep] (see Chapter V), DOM type can significantly influence the relative abundances of BTHM. Different patterns in the relative proportions of BTHM produced in different batches of *A. longipes* cultures may be an indicator of shifts in DOM composition. $CHBr_3$ was consistently a major product among the BTHM in *Synechococcus sp.* and experiments with V-BrPO treated DOM compounds, following the pattern of $CHBr_3 > CHClBr_2 > CHBrCl_2$ (Figure 6-5 and 6-6). However, $CHBr_3$ was only a minor product in *A. longipes* cultures. Chloroform ($CHCl_3$) is usually not considered in V-BrPO mediated reactions; however, $CHCl_3$ and/or $CHBrCl_2$ consistently constituted a large fraction of THM produced in *A. longipes* cultures. $CHCl_3$ was a dominant product in batch of *A. longipes* cultures incubated for 30 days. Although not as substantial, $CHCl_3$ was produced at a considerable level in the other two batches of *A. longipes* cultures incubated for 11 days (Figure 6-5 and 6-7). In these two batches, the other chlorinated THM, $CHBrCl_2$, was the dominant product. It should be noted that $CHCl_3$ was not produced in the *Synechococcus sp.* culture, in which BTHM relative production pattern followed a typical V-BrPO mediated bromination product pattern.

The first explanation of such a shift in product relative abundances in *A. longipes* cultures could be successive chlorine substitution from $CHBr_3$, following such an order: $CHBr_3 \rightarrow CHClBr_2 \rightarrow CHBrCl_2$. However, such a process is believed to be a long time scale process, occurring on the order of years to decades [*Geen*, 1992]. Such a pattern was observed in the Pacific Ocean in aged North Pacific Intermediate Water (NPIW), with an apparent CFC-11 age of a few decades [*Liu et al.*, 2013]. Therefore, while successive chlorine substitution may be one of the explanations, it would be too slow to explain the high $CHCl_3$ concentrations observed in all *A. longipes* cultures.

The second explanation could be enzyme-mediated chlorination, basically similar to V-BrPO bromination. Vanadium or iron-heme chloroperoxidases are widely distributed in terrestrial environments, where they are involved in the degradation of lignin [*Ortiz-Bermudez et al.*, 2003; *Ortiz-Bermúdez et al.*, 2007]. Unlike bromoperoxidase, which can only catalyze the oxidation of bromine and iodine, chloroperoxidase can catalyze the oxidation of chlorine, bromine, and iodine. For a long time, the marine environment is thought to only host two haloperoxidases, bromoperoxidase and iodoperoxidase. However, it has been shown that V-BrPO from a brown alga can express chloroperoxidase-like activity, *i.e.* catalyze the oxidation of chlorine [*Soedjak and Butler*, 1990; *Winter and Moore*, 2009]. Therefore, it is possible that certain phytoplankton, such as *A. longipes* can also express chloroperoxidase-like activity. Such a finding will have important implications in developing our understandings of natural chlorinated trace gas budgets. Moreover, chloroperoxidase-

like activity offers a simple explanation for the observation of elevated $CHCl_3$ concentration in the chlorophyll *a* maximum [*Liu et al.*, 2013].

6.5 Conclusion

The original objective of this study was to screen important phytoplankton species for the ability to produce BrVSLS, with the aim of elucidating which taxa are potentially important producers *in situ* and to facilitate explaining the patchy distribution of BrVSLS production in the ocean. However, screening phytoplankton for BrVSLS production may not be as useful as it has been long believed. Although it is typical that laboratory experiments tend to be different from *in situ*, the complex factors involved in BrVSLS production make it even more so. BrVSLS production seems to be maintained by interactions with a complex DOM pool, hence, traditional approaches of growing phytoplankton cultures may be problematic. Moreover, to screen for phytoplankton that can in reality produce BrVSLS, it is probably more helpful to screen for V-BrPO activity rather than the BrVSLS themselves. More attention should be paid to understand BrVSLS production pathways and environment factors that can alter their production. Finally, I demonstrated for the first time, chloroperoxidase-like behavior from a diatom.

CHAPTER VII

EFFECTS OF VANADIUM BROMOPEROXIDASE HALOGENATION ON DISSOLVED ORGANIC MATTER AND IMPLICATIONS FOR THE MARINE CARBON CYCLE

7.1 Introduction

In the marine environment, halogenated non-volatile organic compounds such as indoles, terpenes, acetogenins, phenols, and volatile organic compounds such as some of the brominated very short-lived substances (BrVSLS) are thought to be the result of halogenation reactions catalyzed by bromoperoxidase [*Butler and Carter-Franklin*, 2004]. Thus far, two major classes of bromoperoxidase are known in the marine environment: iron-heme bromoperoxidase and vanadium bromoperoxidase (V-BrPO); with the vanadium dependent type being more abundant [*Butler and Carter-Franklin*, 2004].

V-BrPO activities have been identified in many macroalgae, as well as several groups of phytoplankton, such as diatoms and cyanobacteria [*Deboer et al.*, 1986; *Gribble*, 2010; *Hill and Manley*, 2009; *Johnson et al.*, 2011; *Moore et al.*, 1996; *Wever et al.*, 1991; *Wever et al.*, 1993]. Although the exact physiological function of this class of enzymes is not clear, it has been suggested to serve two purposes: scavenging of oxidants like hydrogen peroxide (H_2O_2) and producing defensive acids like hypobromous acid ($HOBr_{enz}$) [*Manley and Barbero*, 2001; *Wever*, 2012]. HOBr is a halogenating/oxidizing agent that can act on a wide range of organic substrates.

HOBr is also a well-known mild acid that can transform aldose sugars into aldonic acids, which can potentially alter carbohydrate characteristics as well as carbohydrate bioavailability within the bulk dissolved organic matter (DOM) pool [*Varela*, 2003].

The halogenation of organic molecules, mediated by V-BrPO, starts with the catalytic oxidation of halides X (for bromoperoxidase X = Br^- and I^-) in the presence of H_2O_2, yielding oxidized halogen intermediates like $HOBr_{enz}$. The resulting $HOBr_{enz}$ can then react with suitable organic reactants to form halogenated organic molecules [*Theiler et al.*, 1978; *Wever et al.*, 1993]. Under certain conditions, volatile organic compounds such as $CHBr_3$, $CHClBr_2$, and $CHBrCl_2$ can be formed from further halogenation, with eventual cleavage from the macromolecule [*Theiler et al.*, 1978; *Wever et al.*, 1993]. Since bromine is at much higher concentration than iodine in natural seawater, the brominated products are dominant.

The idea of brominated very short-lived substances (BrVSLS) are formed via V-BrPO mediated halogenation of DOM, is a widely accepted hypothesis. However, the role of such a reaction pathway in driving global variability of BrVSLS seawater concentrations has been largely neglected. *Liu et al.* [In prep] (see Chapter V) demonstrated that BrVSLS production, hence their concentrations in seawater, varied significantly across different model DOM compounds treated with V-BrPO. This finding not only revealed a significant driver of BrVSLS global variability, but also has significant implications for the carbon cycle. Upon halogenation, DOM molecules were transformed either into unstable halogenated compounds and released BrVSLS or into stable non-volatile halogenated compounds. These non-volatile halogenated

molecules may express different chemical reactivity and bioavailability, hence, will have an impact on the carbon cycle.

Colored dissolved organic matter (CDOM) is a fraction of the bulk dissolved organic matter (DOM) pool that absorbs light in both visible and ultraviolet (UV) ranges [*Blough and Del Vecchio*, 2002]. In coastal waters, where riverine input is significant, CDOM is primarily derived from terrestrial sources [*Blough and Del Vecchio*, 2002]. This pool of DOM is important even though it is only a small fraction of the bulk DOM pool, as its optical properties can significantly influence aquatic and marine biogeochemistry. *Liu et al.* [In prep] (see Chapter V) demonstrated that certain DOM compounds interfere with BrVSLS production and transform into non-volatile products upon halogenation. Here, I used change in CDOM fluorescence to assess transformation of CDOM upon treatment with V-BrPO, a process recently termed 'bio-bleaching'. Bio-bleaching of CDOM was first hypothesized by *Lin and Manley* [2012]; it is the enzymatic-mediated degradation of CDOM as oppose to photo-bleaching. Specifically, the *Lin and Manley* [2012] referred to V-BrPO mediated oxidation of CDOM.

7.2 Method

7.2.1 Preparation of colored dissolved organic matter material

Two dissolved organic matter (DOM) pools, resembling characteristics of terrestrial- (allochthonous) and marine- (autochthonous) derived CDOM, were prepared. Lignin phenols, including vanillin, syringaldehyde, and ferulic acid, were dissolved in 0.2 μm filtered ultra pure water as stock solutions. 1 mL of stock solution was added to 30 mL of artificial seawater (ASW; buffered to a pH of 8.11 and 0.2 μm filtered) [*Berges et al.*, 2001; *Liu et al.*, In prep]. Final DOC concentrations were ~ 1000 μM-C in the DOM added ASW. Syringaldehyde and ferulic acid were dissolved in sub-boiling ultra-pure water. These lignin phenols were used as model allochthonous CDOM, as they comprise a significant fraction of the DOM pool in coastal seawaters [*Bianchi*, 2011; *Hernes and Benner*, 2003]. Moreover, the lignin phenols have defined chemical structure so we could compare their reactivity. The traditional CDOM model substances, such as humics and fulvics, were not used in this study, as they have substantial differences in chemical composition and reactivity depend on their sources.

Autochthonous CDOM was harvest from cultures of four phytoplankton species, *Achnanthes longipes* (CCMP 101), *Skeletonema costatum* (CCMP 2092), *Synechococcus sp.* (CCMP 2515), and *Synechococcus elongates* (CCMP 1379). The selection of the cultures covered two important groups of phytoplankton, diatoms and cyanobacteria. Aged cultures (*i.e.* at stationary or senescent phase) were gently filtered

through 0.2 μm filters to collect the operationally defined DOM [*Bianchi*, 2011]. It should be noted that the CDOM collected with this method is qualitative and not necessarily algal derived, as bacteria were present in the aged cultures and they may have transformed the algal CDOM and/or produced CDOM. However, this will also be true in the natural marine environment.

7.2.2 Preparation of V-BrPO and H_2O_2

V-BrPO stock was prepared as described in *Liu et al.* [In prep] (see Chapter V). Basically, the enzyme powder was dissolved in 50 mM MES buffer (MES pH = 6.4). 4 μL of V-BrPO was added to a total volume of 108 μL reaction solution (CDOM + H_2O_2 + V-BrPO). Final concentration of V-BrPO was ~13.7 units mL^{-1}. Hydrogen peroxide (H_2O_2) stock solution was made by diluting 30% v./v. H_2O_2 with ultra-pure water. 4 μL of H_2O_2 was added to a total volume of 108 μL reaction solution, with a final concentration of 0.56 mM. Concentrations of V-BrPO and H_2O_2 used in this study were two orders of magnitude higher than those used in *Liu et al.* [In prep] (see Chapter V) in order to observe measureable bleaching of CDOM with a microplate reader.

7.2.3 Fluorescence measurement

Fluorescence of CDOM was measured with a microplate reader (SpectraMAX GEMINI EM) in top-read mode. A 96-well opaque microplate was used. Inside the

plate, three controls of each CDOM were added. Controls were CDOM without V-BrPO and H_2O_2. Samples for CDOM measurements were run in duplicates, due to limited batch of V-BrPO. Basically, triplicates of CDOM were added to the microplate. H_2O_2 were added to all samples and monitored for 5 min, to ensure addition of H_2O_2 does not change CDOM fluorescence. Subsequently, V-BrPO was added to two of the CDOM samples to activate halogenation. The remainder one CDOM sample without V-BrPO was used to continue monitoring H_2O_2 induced change. Halogenation reaction with each CDOM was run for at least 1.5 hr. The microplate reader was set into kinetic mode, and made a fluorescence measurement every 30 seconds. Relative CDOM concentration was measured using an excitation of 373 nm, emission of 460 nm, and auto optical emission cutoff light below 450 nm. The microplate reader was maintained at a constant temperature of 25 °C.

7.3 Results

All CDOM samples with only H_2O_2 added showed the same trend as the controls, which indicated potential CDOM oxidation by H_2O_2 did not change fluorescence or optical properties of the CDOM types examined in this study. All the fluorescence changes were stabilized after 1.5 hrs. A percent reduction in CDOM fluorescence was calculated with the following equation:

$$\%RFU_{reduced} = \frac{RFU_{actived} - RFU_{pre\text{-}activate}}{RFU_{pre\text{-}activate}} \times 100\% \qquad \text{(Equation 7.1)}$$

where RFU is the relative fluorescence unit. Activated denoted addition of V-BrPO to activate halogenation. Pre-activate denoted addition of H_2O_2 only. % RFU offers a

qualitative measure of magnitude of bio-bleaching so that it is possible to compare reactivity of a particular CDOM to V-BrPO induced halogenation.

All three lignin phenols showed signs of bio-bleaching upon halogenation by V-BrPO induced $HOBr_{enz}$ (Figure 7-1). Vanillin, syringaldehyde, and ferulic acid showed a reduction of RFU by 38.0%, 42.5%, and 65.5%, respectively. CDOM collected from diatom cultures showed minor to no reduction in RFU (Figure 7-2). *A. longipes* showed a reduction of RFU by 22.2%, while *S. costatum* showed no clear trend in change of RFU. However, the RFU change in *A. longipes* was ambiguous as it was not much different from the controls. CDOM collected from the two cyanobacteria cultures showed a clear reduction in RFU. *S. elongatus* showed a RFU reduction of 35.5%. *Synechococcus sp*. showed a RFU reduction of 21.7%. Although such a RFU change from *Synechococcus sp*. was similar to that observed in *A. longipes*, it was clearly different from the control (Figure 7-2). Therefore, I assume alteration of *A. longipes* derived CDOM by V-BrPO induced $HOBr_{enz}$ was negligible.

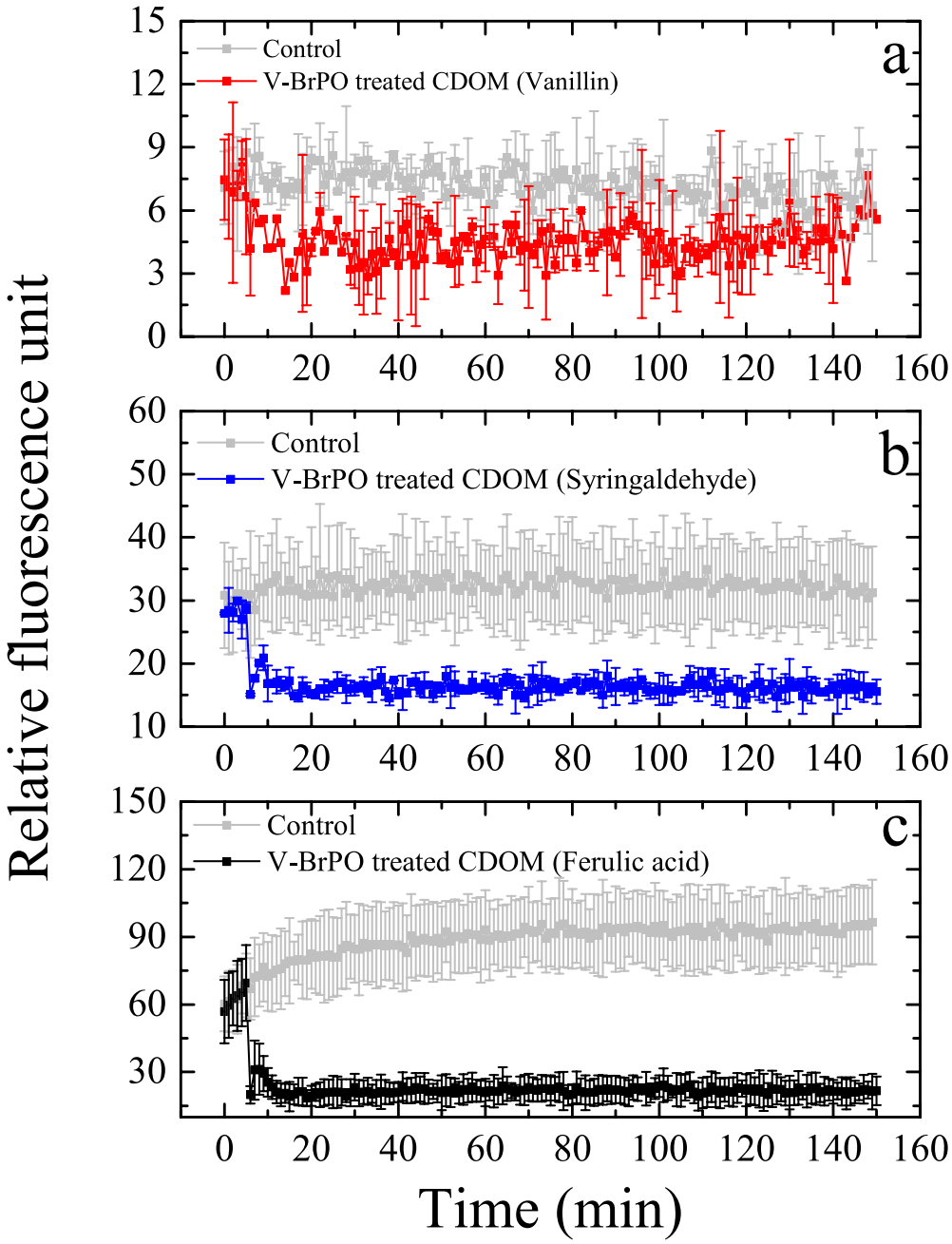

Figure 7-1. Fluorescence of V-BrPO treated (a) vanillin (red), (b) syringaldehyde (blue), and (c) ferulic acid (black) and their controls (grey) as a function of time. Error bars indicate 1 standard deviation (± 1σ) of replicates, number of samples (*n*) were 3 and 2 for control and V-BrPO treated lignin phenols, respectively.

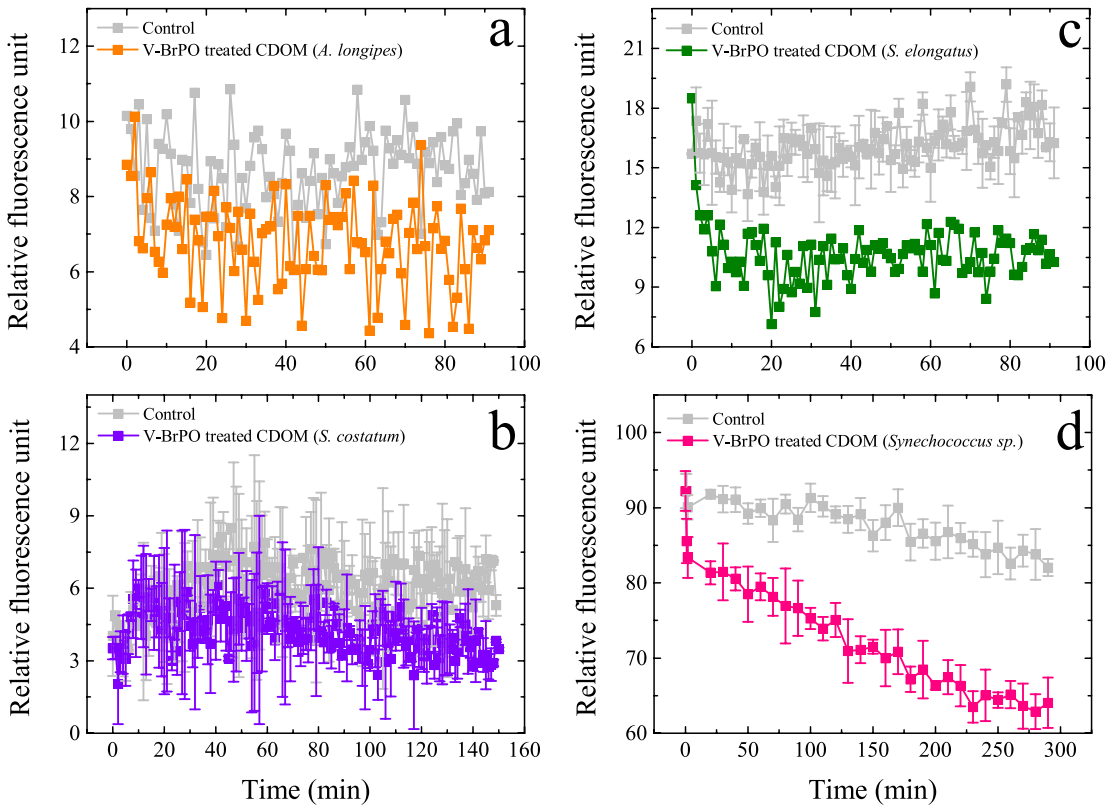

Figure 7-2. Fluorescence of V-BrPO treated CDOM collected from (a) *Achnanthes longipes* (orange), (b) *Skeletonema costatum* (purple), (c) *Synechococcus elongates* (green), and (d) *Synechococcus sp.* (pink) as a function of time. Fluorescence of their controls is presented in grey symbols. Error bars indicate 1 standard deviation (± 1σ) of replicates, numbers of samples (*n*) were 3 and 2 for control and V-BrPO treated CDOM collected from phytoplankton cultures, respectively. Note the different time scales of *S. costatum* and *Synechococcus sp.*

7.4 Discussion

7.4.1 Bio-bleaching of CDOM

Here, I presented evidence of V-BrPO induced transformation of CDOM. $\%RFU_{reduced}$ for the lignin phenols exhibit such a pattern as: ferulic acid > syringaldehyde > vanillin. This order is consistent with their relative reactivity/stability in the environment [*Dittmar and Lara*, 2001; *Tareq et al.*, 2004]. CDOM collected from cyanobacteria cultures appeared to be more reactive to V-BrPO induced halogenation than CDOM collected from diatom cultures. This may be important for CDOM biogeochemistry on a global scale, as cyanobacteria are ubiquitous in the ocean [*Waterbury et al.*, 1979].

CDOM, a fraction of DOM is of particular interest to researchers due to its unique optical characteristics, which are important to processes that can affect biogeochemistry and the ecological health of the aquatic environment. CDOM strongly absorbs light in the visible and UV range, and thus plays a key role in controlling light penetration in the water column, as well as the quantity and quality of photosynthetic active radiation (PAR). The photoreactivity of CDOM leads to the formation of a variety of compounds, which can then influence aquatic biogeochemistry, carbon cycling, and atmospheric chemistry. These compounds include low-molecular-weight OM that can be assimilated by prokaryotes [*Benner and Biddanda*, 1998; *Blough and Del Vecchio*, 2002; *Kieber et al.*, 1990; *Mopper et al.*, 1991; *Moran et al.*, 2000; *Zepp et al.*, 1998; *Zepp et al.*, 2007], reactive species such

as H_2O_2 [*Zafiriou et al.*, 1984; *Zika et al.*, 1993], and different trace gases such as carbon monoxide (CO), carbon dioxide (CO_2), and carbonyl sulfide (COS) [*Miller and Zepp*, 1995; *Miller et al.*, 2002; *Mopper et al.*, 1991; *Stubbins et al.*, 2011; *Stubbins et al.*, 2008; *Valentine and Zepp*, 1993; *Weiss et al.*, 1995; *Zafiriou et al.*, 2003; *Zepp et al.*, 1998; *Zepp et al.*, 2007].

Lignin degradation contributes in part, to the formation of humic and fulvic acids, which comprise a large fraction of coastal CDOM, which has additional contributions from amino acids, peptides, nucleic acids, and many other low-molecular-weight OM [*Nelson and Siegel*, 2002]. CDOM absorption decreases drastically along the freshwater to marine gradient. A similar pattern for lignin-phenols was observed in surface waters from the lower river out through the Mississippi River Plume (MRP) [*Hernes and Benner*, 2003], as CDOM fluorescence in coastal waters usually correlated with lignin phenol contents [*Boyle et al.*, 2009; *Del Vecchio and Blough*, 2004]. Photo-oxidation (photo-bleaching) is the dominant degradation path for CDOM in surface water. Bacterial degradation also contributes to the loss of CDOM, but to lesser extent [*Coble*, 2007]. However, to our knowledge, alteration of and/or "bleaching" of CDOM via phytoplankton biochemistry (*e.g.* enzymes) has not been investigated in coastal waters.

Therefore, results in this study may provide new insights to CDOM degradation. This is potentially important to regions where solar radiation is spatially and temporally limited in the water column, such as the turbid coastal areas and polar regions. Change in CDOM optical properties also implies chemical structural change. A well-known paradigm of the terrestrially derived DOM, as the "lost" DOM from

terrestrial sources, is that the annual DOC discharged to the global ocean can be accounted for in the turnover time of all marine DOC; yet, various markers evidenced that only small amount of terrestrially derived DOC ended up in the global ocean [*Bianchi*, 2011]. Such a paradigm suggested the presence of effective loss mechanism(s). Therefore, bio-bleaching may be an important pathway for OM chemical alteration in addition to photo- and bacterial- oxidation, which may be an important process in determining the fate of the "lost" terrestrial DOM in coastal waters.

Besides direct transformation or degradation, compounds produced via bio-bleaching may affect marine carbon cycling due to changes in bioavailability. HOBr itself is a mild acid and it is known through fundamental organic chemistry to transform carbohydrates into acids, for example, aldose sugars into aldonic acids [*Varela*, 2003]. Amino acids are important DOM that cycle rapidly in the ocean as they are utilized by microbes [*Duan and Bianchi*, 2007; *Ittekkot and Zhang*, 1989; *Spitzy and Ittekkot*, 1991]. Aromatic amino acids, such as tyrosine and tryptophan, are important CDOM constituents in the aquatic environment [*Burdige et al.*, 2004; *Mopper and Schultz*, 1993; *Mopper et al.*, 1996]. These two compounds interfered with BrVSLS formation and supposedly formed haloacetic acids (HAA) instead [*Hong et al.*, 2009]. HAAs are relatively stable in the marine environment [*Hashimoto et al.*, 1998]. Therefore, upon halogenation, these amino acids may be turned into molecules that are not as bioavailable to the microbes. In fact, I hypothesize this may be a general pattern for most of the halogenated molecules, as halogenated substances tend to be toxic.

7.4.2 Impacts beyond CDOM

While results presented in this study only demonstrated V-BrPO alteration of CDOM, its impact on the bulk DOM pool is likely. Only a small fraction of $HOBr_{enz}$ ultimately yielded BrVSLS [*Hill and Manley*, 2009; *Lin and Manley*, 2012]. Therefore, the fate of the remainder $HOBr_{enz}$ is open for speculation. Results presented by *Liu et al.* [In prep] (see Chapter V) and this study clearly showed that $HOBr_{enz}$ has significant impact on the non-volatile organic molecules. Bromine bounded organic molecules were found in sinking particles throughout the water column, as well as in sediments [*Leri et al.*, 2010]. Therefore, halogenated organic compounds may be more abundant than what we know thus far. Alteration in chemical properties of organic matter (OM) due to halogenation may significantly influence OM degradation and preservation in sediments, hence is important to diagenesis [*Leri et al.*, 2010]. The OM may be 'stabilized' upon halogenation, as its toxicity may protect it from bacterial degradation in the sediment. V-BrPO is likely one of the important halogenation pathway in the marine environment, though more halogenation pathways are yet to be discovered.

7.5 Conclusion

In this study, I extended the scope of my research interests beyond trace gas and BrVSLS biogeochemistry and examined the impact of V-BrPO mediated halogenation on the carbon cycle in general. I demonstrated transformation of DOM

via V-BrPO mediated halogenation, although the global significance of such a DOM alteration pathway is still unknown. High concentrations of BrVSLS observed in the Artic coast were attributed to high levels of V-BrPO activity. As the Artic permafrost is starting to thaw and will discharge more labile DOM to the coast, V-BrPO mediated halogenation may be one of the important pathway to alter this pool of reactive DOM.

CHAPTER VIII

CONCLUSIONS

8.1 Result summary

Results from the field observations and laboratory experiments consistently suggest that $CHBr_3$ and CH_2Br_2 are derived from disparate sources. Better correlations between CH_2Br_2 and the biological proxies observed in the field support the idea of biologically mediated transformation of CH_2Br_2 from $CHBr_3$ [*Hughes et al.*, 2013]. The general correlation between CH_2Br_2 and $CHBr_3$ suggest such a transformation process is ubiquitous in the ocean, where $CHBr_3$ is produced. Such a finding challenges the long believed concept: CH_2Br_2 and $CHBr_3$ are derived from common sources. Such a contradiction may have important implications for modeling studies on CH_2Br_2 and $CHBr_3$ oceanic emissions and their global budgets, as various environmental forcing may affect the two BrVSLS differently.

Results from the field observations generally indicate that the presences of photosynthetic biomass are important for BrVSLS production. However, relationships between the two are not straightforward. BrVSLS are believed to form via V-BrPO mediated halogenation of DOM, in the presence of H_2O_2. To date, most of studies on BrVSLS sources focus on phytoplankton specificity to BrVSLS production; *i.e.* in relation to V-BrPO activity. Based on the field observations, I hypothesized that BrVSLS production is controlled by complex factors in the ecosystems. Therefore,

phytoplankton species specificity to BrVSLS or V-BrPO production is not sufficient to explain BrVSLS production variability and biogeochemistry in the ocean.

Hence, I examined effects of extracellular DOM composition in controlling BrVSLS production. Results from the laboratory studies show that $CHBr_3$, $CHClBr_2$, and $CHBrCl_2$ production is sensitive to DOM composition. Therefore, DOM specificity to BrVSLS production may be a plausible explanation for the observed variability in BrVSLS production, as DOM composition varied significantly in different environments. Phytoplankton produces V-BrPO, which provides an initial condition for halogenation to occur. However, as shown in the laboratory results, DOM composition, reactivity, and dynamics control how much BrVSLS are ultimately produced, assuming H_2O_2 is not a limiting factor.

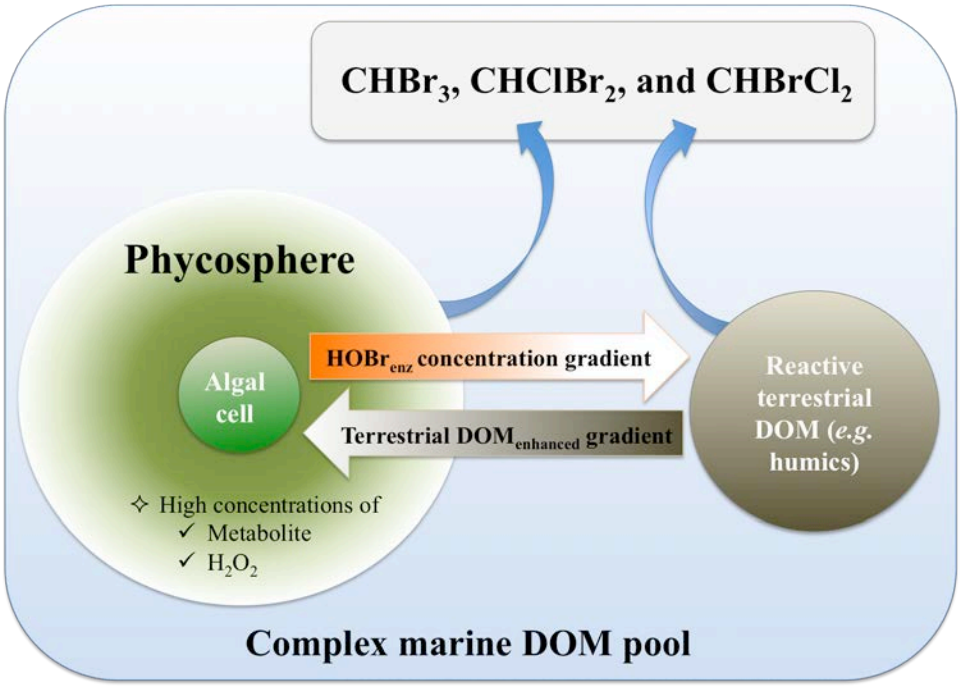

Figure 8-1. A conceptual model of BrVSLS production from within the phycosphere to the surrounding environment.

8.2 An outlook from a conceptual model

Based on the observed large-scale distributions of BrVSLS and laboratory results, a conceptual model of BrVSLS is proposed. I propose that a BrVSLS production "hot-spot" exists within the cell phycosphere (*i.e.* the micro-environment around the cell) (Figure 8-1). V-BrPO has been proposed as an extracellular enzyme bound to the cell surface [*Manley*, 2002]. Therefore, V-BrPO concentration is presumably higher within the phycosphere. Metabolites that served as $DOM_{enhanced}$, such as urea, glycolic acid, and alginic acid, along with photorespiration by-product such as H_2O_2 are at higher concentrations as they are being exuded by the cell. Such an environment provides ideal conditions for BrVSLS formation. Although

$DOM_{interfered}$ such as the amino acids will also exist at high concentrations in the phycosphere, it is possible that enough of V-BrPO and $DOM_{enhanced}$ can counteract the interferences. This conceptual model is supported by field observations that high BrVSLS concentrations are usually located in biologically active regions of the ocean. In the coastal ocean, reactive terrestrial DOM such as humics and fulvics may also enhance BrVSLS production in the phycosphere. Beyond the phycosphere, excess $HOBr_{enz}$ may diffuse further away and halogenate DOM in the surrounding waters. Along such a path, $HOBr_{enz}$ may convert to bromine chloride (BrCl) [*Sivey et al.*, 2013]. Although $HOBr_{enz}$ may be present at a lower concentration further away from the cell, it may encounter very reactive DOM in the coastal water, such as humic substances. Although BrCl's fate in seawater is elusive and it only occurs in minor abundance compare to HOBr, it is believed to be a more effective brominating agent than HOBr [*Sivey et al.*, 2013]. Therefore, there are mechanisms for BrVSLS to form away from the cell, although the magnitude will be highly dependent on fates of the reactive bromine species in seawater and reactivity of DOM. The fact that BrVSLS may be formed further away from the cell may be able to explain the complex relationships between the BrVSLS and chlorophyll *a*.

It should also be noted that pH within the phycosphere can be drastically different from the bulk medium, which is dependent on cell physiological state and carbon chemistry in seawater [*Dixon et al.*, 1989; *Flynn et al.*, 2012; *Kühn and Köhler-Rink*, 2008]. Such a pH difference from the surrounding environment may also affect the amounts of BrVSLS being produced (Figure 8-2).

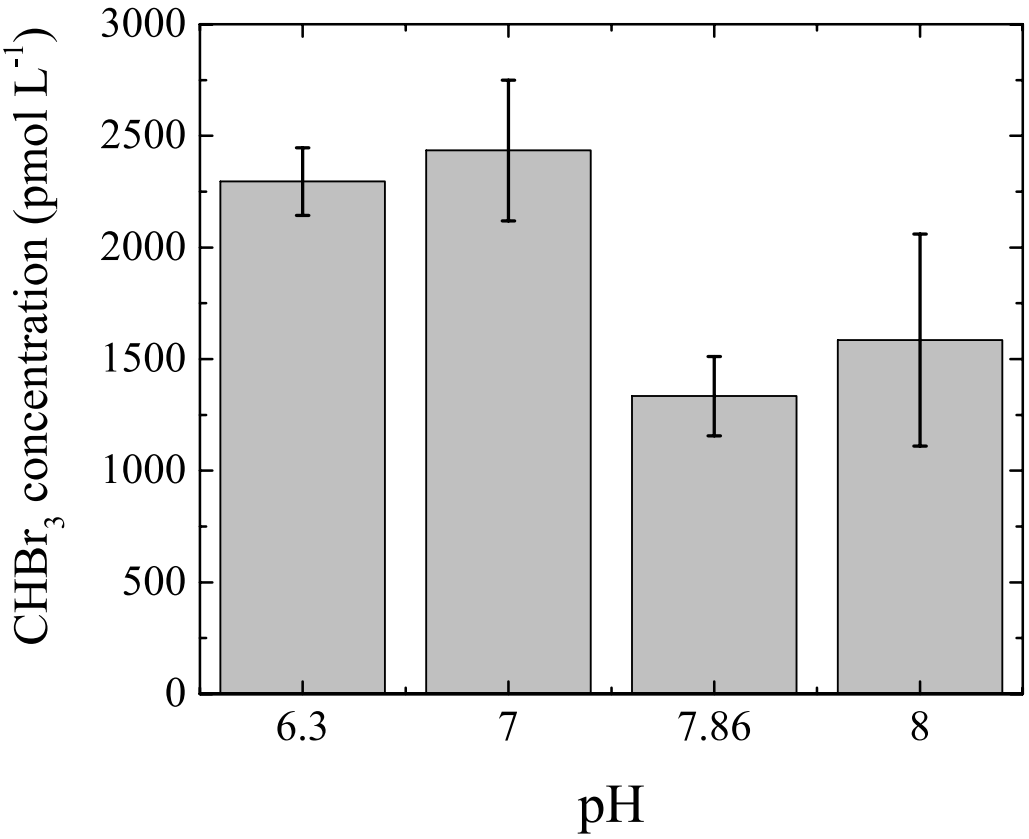

Figure 8-2. $CHBr_3$ concentrations observed from halogenated artificial seawater (HASW) buffered to different pHs.

8.3 Conclusions and future works

To conclude, global distributions of BrVSLS are controlled by complex environmental factors, such as those controlling HOBr fates in the ocean, as well as those controlling DOM dynamics. My conceptual model derived from the results of this dissertation suggests that most of the BrVSLS are produced in close proximity to the cell, but phytoplankton species specificity is probably not as important as long been believed. Moreover, a "life-after-death" concept was proposed by Manley and

colleagues (pers. comm. and *Wever and Van der Horst* [2013]). Basically, V-BrPO is a stable enzyme that can survive after drastic temperature and pH changes. Since $HOBr_{enz}$ produced via V-BrPO mediated processes is toxic, V-BrPO can potentially protect itself from microbial degradation. Therefore, V-BrPO can remain active and mediate halogenation even after cell death. Although this is merely a conceptual model as well, it also highlighted that the important factors of halogenation reactions are V-BrPO activity (*i.e.* $HOBr_{enz}$ supply) and DOM composition.

To better understand global BrVSLS distributions and the responses to climate change, researchers should go beyond observations and start to understand fundamental processes that control the production of BrVSLS. BrVSLS production should be studied in conjunction with DOM composition and production mechanisms of HOBr and/or V-BrPO in future studies. Identifying BrVSLS producers with traditional biomarkers, such as pigments, is probably not useful, unless better tools at molecular level are developed. Finally, although fully speculative, it is possible that photochemistry and ozone deposition in seawater can create reactive brominated species that can act as brominating agents. This may only be a minor pathway for DOM bromination, but provided a mechanism that is completely independent of phytoplankton.

REFERENCES

Abrahamsson, K., A. Lorén, A. Wulff, and S.-A. Wängberg (2004), Air–sea exchange of halocarbons: the influence of diurnal and regional variations and distribution of pigments, *Deep Sea Research Part II: Topical Studies in Oceanography*, *51*(22–24), 2789-2805.

Abrahamsson, K., K.-S. Choo, M. Pedersén, G. Johansson, and P. Snoeijs (2003), Effects of temperature on the production of hydrogen peroxide and volatile halocarbons by brackish-water algae, *Phytochemistry*, *64*(3), 725-734.

Acker, J. G., and G. Leptoukh (2007), Online analysis enhances use of NASA Earth science data, *Eos Trans. AGU*, *88*(2).

Aluwihare, L. I., and D. J. Repeta (1999), A comparison of the chemical characteristics of oceanic DOM and extracellular DOM produced by marine algae, *Marine Ecology Progress Series*, *186*, 105-117.

Aluwihare, L. I., D. J. Repeta, and R. F. Chen (1997), A major biopolymeric component to dissolved organic carbon in surface sea water, *Nature*, *387*(6629), 166-169.

Alves-de-Souza, C., M. T. González, and J. L. Iriarte (2008), Functional groups in marine phytoplankton assemblages dominated by diatoms in fjords of southern Chile, *Journal of Plankton Research*, *30*(11), 1233-1243.

Armstrong, F. A. J., C. R. Stearns, and J. D. H. Strickland (1967), The measurement of upwelling and subsequent biological process by means of the Technicon Autoanalyzer® and associated equipment, *Deep Sea Research and Oceanographic Abstracts*, *14*(3), 381-389.

Beggs, K. M. H., R. S. Summers, and D. M. McKnight (2009), Characterizing chlorine oxidation of dissolved organic matter and disinfection by-product formation with fluorescence spectroscopy and parallel factor analysis, *Journal of Geophysical Research: Biogeosciences*, *114*, G04001, doi:10.1029/2009JG001009.

Benner, R., and B. Biddanda (1998), Photochemical transformations of surface and deep marine dissolved organic matter: effects on bacterial growth, *Limnology and Oceanography*, *43*(6), 1373-1378.

Benner, R., J. D. Pakulski, M. McCarthy, J. I. Hedges, and P. G. Hatcher (1992), Bulk chemical characteristics of dissolved organic matter in the ocean, *Science*, *255*(5051), 1561-1564.

Berges, J. A., D. J. Franklin, and P. J. Harrison (2001), Evolution of an artificial seawater medium: improvements in enriched seawater, artificial water over the last two decades, *J Phycol*, *37*(6), 1138-1145.

Bernhardt, H., and A. Wilhelms (1967), The continuous determination of low level iron, soluble phosphate and total phosphate with the AutoAnalyzer, paper presented at Technicon Symposia, v. 1, p. 385-389.

Bianchi, T. S. (2011), The role of terrestrially derived organic carbon in the coastal ocean: A changing paradigm and the priming effect, *Proceedings of the National Academy of Sciences*, *108*(49), 19473-19481.

Bianchi, T. S., and E. A. Canuel (2011), *Chemical Biomarkers in Aquatic Ecosystems*, Princeton University Press, Princeton, New Jersey.

Blough, N. V., and R. Del Vecchio (2002), Chromophoric DOM in the coastal environment, in *Biogeochemistry of Marine Dissolved Organic Matter*, edited by D. A. Hansell and C. A. Carlson, pp. 509–546, Academic Press, San Diego, California.

Boyce, S. D., and J. F. Hornig (1983), Reaction pathways of trihalomethane formation from the halogenation of dihydroxyaromatic model compounds for humic acid, *Environ Sci Technol*, *17*(4), 202-211.

Boyle, E. S., N. Guerriero, A. Thiallet, R. D. Vecchio, and N. V. Blough (2009), Optical properties of humic substances and cdom: relation to structure, *Environ Sci Technol*, *43*(7), 2262-2268.

Brainerd, K. E., and M. C. Gregg (1995), Surface mixed and mixing layer depths, *Deep Sea Research Part I: Oceanographic Research Papers*, *42*(9), 1521-1543.

Burdige, D. J., S. W. Kline, and W. Chen (2004), Fluorescent dissolved organic matter in marine sediment pore waters, *Marine Chemistry*, *89*(1–4), 289-311.

Butler, A., and J. N. Carter-Franklin (2004), The role of vanadium bromoperoxidase in the biosynthesis of halogenated marine natural products, *Nat Prod Rep*, *21*(1), 180-188.

Butler, J. H., J. W. Elkins, C. M. Brunson, K. B. Egan, T. M. Thompson, T. J. Conway, and B. D. Hall (1988), Trace gases in and over the west Pacific and the east Indian Oceans during the El Niño–Southern Oscillation event of 1987*Rep.*, 104 pp, Natl. Oceanic and Atmos. Admin, Silver Spring, Md.

Butler, J. H., D. B. King, J. M. Lobert, S. A. Montzka, S. A. Yvon-Lewis, B. D. Hall, N. J. Warwick, D. J. Mondeel, M. Aydin, and J. W. Elkins (2007), Oceanic distributions and emissions of short-lived halocarbons, *Global Biogeochem Cy*, *21*(1).

Campbell, L. (2001), Flow cytometric analysis of autotrophic picoplankton, in *Methods in Microbiology*, edited by H. P. John, pp. 317-343, Academic Press.

Carpenter, L. J. (2003), Iodine in the marine boundary layer, *Chem Rev*, *103*(12), 4953-4962.

Carpenter, L. J., and P. S. Liss (2000), On temperate sources of bromoform and other reactive organic bromine gases, *J Geophys Res-Atmos*, *105*(D16), 20539-20547.

Carpenter, L. J., D. J. Wevill, C. J. Palmer, and J. Michels (2007a), Depth profiles of volatile iodine and bromine-containing halocarbons in coastal Antarctic waters, *Marine Chemistry*, *103*(3-4), 227-236.

Carpenter, L. J., C. E. Jones, R. M. Dunk, K. E. Hornsby, and J. Woeltjen (2009), Air-sea fluxes of biogenic bromine from the tropical and North Atlantic Ocean, *Atmos Chem Phys*, *9*(5), 1805-1816.

Carpenter, L. J., D. J. Wevill, J. R. Hopkins, R. M. Dunk, C. E. Jones, K. E. Hornsby, and J. B. McQuaid (2007b), Bromoform in tropical Atlantic air from 25 degrees N to 25 degrees S, *Geophys Res Lett*, *34*(11).

Chen, N., T. S. Bianchi, and J. M. Bland (2003), Implications for the role of pre- versus post-depositional transformation of chlorophyll-a in the Lower Mississippi River and Louisiana shelf, *Marine Chemistry*, *81*(1-2), 37-55.

Chuck, A. L., S. M. Turner, and P. S. Liss (2005), Oceanic distributions and air-sea fluxes of biogenic halocarbons in the open ocean, *J. Geophys. Res.*, *110*(C10), C10022.

Class, T., and K. Ballschmiter (1988), Chemistry of organic traces in air, *J Atmos Chem*, *6*(1), 35-46.

Coble, P. G. (2007), Marine optical biogeochemistry: the chemistry of ocean color, *Chem Rev*, *107*(2), 402-418.

Colomb, A., N. Yassaa, J. Williams, I. Peeken, and K. Lochte (2008), Screening volatile organic compounds (VOCs) emissions from five marine phytoplankton species by head space gas chromatography/mass spectrometry (HS-GC/MS), *Journal of environmental monitoring : JEM*, *10*(3), 325-330.

Cooper, W. J., R. G. Zika, R. G. Petasne, and J. M. C. Plane (1988), Photochemical formation of hydrogen peroxide in natural waters exposed to sunlight, *Environ Sci Technol*, *22*(10), 1156-1160.

Deboer, E., M. G. M. Tromp, H. Plat, G. E. Krenn, and R. Wever (1986), Vanadium(V) as an essential element for haloperoxidase activity in marine brown-algae - purification and characterization of a vanadium(V)-containing bromoperoxidase from *Laminaria-Saccharina*, *Biochim Biophys Acta*, *872*(1-2), 104-115.

Del Vecchio, R., and N. V. Blough (2004), On the origin of the optical properties of humic substances, *Environ Sci Technol*, *38*(14), 3885-3891.

Dewulf, J., D. Drijvers, and H. Van Langenhove (1995), Measurement of Henry's law constant as function of temperature and salinity for the low temperature range, *Atmos Environ*, *29*(3), 323-331.

Dittmar, T., and R. J. Lara (2001), Molecular evidence for lignin degradation in sulfate-reducing mangrove sediments (Amazônia, Brazil), *Geochim Cosmochim Ac*, *65*(9), 1417-1428.

Dixon, G. K., C. Brownlee, and M. J. Merrett (1989), Measurement of internal pH in the coccolithophoreEmiliania huxleyi using 2′,7′-bis-(2-carboxyethyl)-5(and-6)carboxyfluorescein acetoxymethylester and digital imaging microscopy, *Planta*, *178*(4), 443-449.

Dorf, M., A. Butz, C. Camy-Peyret, M. P. Chipperfield, L. Kritten, and K. Pfeilsticker (2008), Bromine in the tropical troposphere and stratosphere as derived from balloon-borne BrO observations, *Atmos. Chem. Phys.*, *8*(23), 7265-7271.

Duan, S., and T. S. Bianchi (2007), Particulate and dissolved amino acids in the lower Mississippi and Pearl Rivers (USA), *Marine Chemistry*, *107*(2), 214-229.

Dvortsov, V. L., M. A. Geller, S. Solomon, S. M. Schauffler, E. L. Atlas, and D. R. Blake (1999), Rethinking reactive halogen budgets in the midlatitude lower stratosphere, *Geophys Res Lett*, *26*(12), 1699-1702.

Ekdahl, A., M. Pedersén, and K. Abrahamsson (1998), A study of the diurnal variation of biogenic volatile halocarbons, *Marine Chemistry*, *63*(1–2), 1-8.

Erickson, D. J., III (1993), A Stability Dependent Theory For Air-Sea Gas Exchange, *J. Geophys. Res.*, *98*(C5), 8471-8488.

Fariña, J. M., A. T. Palma, and F. P. Ojeda (2008), Food webs and the dynamics of marine reefs, in *Food webs and the dynamics of marine reefs*, edited by T. McClanahan and G. Branch, pp. 79 - 107, Oxford University Press, Oxford; New York.

Flynn, K. J., J. C. Blackford, M. E. Baird, J. A. Raven, D. R. Clark, J. Beardall, C. Brownlee, H. Fabian, and G. L. Wheeler (2012), Changes in pH at the exterior surface of plankton with ocean acidification, *Nature Clim. Change*, *2*(7), 510-513.

Fogelqvist, E., and M. Krysell (1991), Naturally and anthropogenically produced bromoform in the Kattegatt, a semienclosed oceanic basin, *J Atmos Chem*, *13*(4), 315-324.

Garcia, R. R., and S. Solomon (1994), A new numerical model of the middle atmosphere: 2. Ozone and related species, *Journal of Geophysical Research: Atmospheres*, *99*(D6), 12937-12951.

Geen, C. E. (1992), Selected marine sources and sink of bromoform and other low molecular weight organobromines, Master Thesis thesis, Dalhousie University, Halifax, Nova Scotia.

Goodwin, K. D., W. J. North, and M. E. Lidstrom (1997), Production of bromoform and dibromomethane by Giant Kelp: Factors affecting release and comparison to anthropogenic bromine sources, *Limnology and Oceanography*, *42*(8), 1725-1734.

Goodwin, K. D., J. K. Schaefer, and R. S. Oremland (1998), Bacterial oxidation of dibromomethane and methyl bromide in natural waters and enrichment cultures, *Appl. Environ. Microbiol.*, *64*(12), 4629-4636.

Granum, E., S. l. Kirkvold, and S. M. Myklestad (2002), Cellular and extracellular production of carbohydrates and amino acids by the marine diatom Skeletonema costatum: diel variations and effects of N depletion, *Marine Ecology Progress Series*, *242*, 83-94.

Gribble, G. W. (2010), Naturally occurring organohalogen compounds - a comprehensive update, *Progress in the Chemistry of Organic Natural Products*, *91*, 349-365.

Grodsky, S. A., J. A. Carton, and C. R. McClain (2008), Variability of upwelling and chlorophyll in the equatorial Atlantic, *Geophys Res Lett*, *35*(3).

Gschwend, P. M., and J. K. MacFarlane (1986), Polybromomethanes, in *Organic Marine Geochemistry*, edited, pp. 314-322, American Chemical Society.

Guillard, R. R. L., and P. E. Hargraves (1993), Stichochrysis immobilis is a diatom, not a chrysophyte, *Phycologia*, *32*(3), 234-236.

Guo, L., C. H. Coleman Jr, and P. H. Santschi (1994), The distribution of colloidal and dissolved organic carbon in the Gulf of Mexico, *Marine Chemistry*, *45*(1-2), 105-119.

Hansell, D. A., C. A. Carlson, and Y. Suzuki (2002), Dissolved organic carbon export with North Pacific Intermediate Water formation, *Global Biogeochem. Cycles*, *16*(1), 1007.

Hartin, C. A., R. A. Fine, B. M. Sloyan, L. D. Talley, T. K. Chereskin, and J. Happell (2011), Formation rates of Subantarctic mode water and Antarctic intermediate water within the South Pacific, *Deep Sea Research Part I: Oceanographic Research Papers*, *58*(5), 524-534.

Harwood, J. E., and A. L. Kühn (1970), A colorimetric method for ammonia in natural waters, *Water Res*, *4*(12), 805-811.

Hashimoto, S., T. Azuma, and A. Otsuki (1998), Distribution, sources, and stability of haloacetic acids in Tokyo Bay, Japan, *Environmental Toxicology and Chemistry*, *17*(5), 798-805.

Hayduk, W., and H. Laudie (1974), Prediction of diffusion-coefficients for nonelectrolytes in dilute aqueous-solutions, *Aiche J*, *20*(3), 611-615.

Hense, I., and B. Quack (2009), Modelling the vertical distribution of bromoform in the upper water column of the tropical Atlantic Ocean, *Biogeosciences*, *6*(4), 535-544.

Hernes, P. J., and R. Benner (2003), Photochemical and microbial degradation of dissolved lignin phenols: Implications for the fate of terrigenous dissolved organic matter in marine environments, *J. Geophys. Res.*, *108*(C9), 3291.

Hill, V. L., and S. L. Manley (2009), Release of reactive bromine and iodine from diatoms and its possible role in halogen transfer in polar and tropical oceans, *Limnology and Oceanography*, *54*(3), 812-822.

Hong, H., M. Wong, and Y. Liang (2009), Amino acids as precursors of trihalomethane and haloacetic acid formation during chlorination, *Archives of Environmental Contamination and Toxicology*, *56*(4), 638-645.

Hossaini, R., M. P. Chipperfield, W. Feng, T. J. Breider, E. Atlas, S. A. Montzka, B. R. Miller, F. Moore, and J. Elkins (2012a), The contribution of natural and anthropogenic very short-lived species to stratospheric bromine, *Atmos. Chem. Phys.*, *12*(1), 371-380.

Hossaini, R., M. P. Chipperfield, S. Dhomse, C. Ordóñez, A. Saiz-Lopez et al. (2012b), Modelling future changes to the stratospheric source gas injection of biogenic bromocarbons, *Geophys Res Lett*, *39*(20), L20813.

Hughes, C., D. J. Franklin, and G. Malin (2011), Iodomethane production by two important marine cyanobacteria: *Prochlorococcus marinus* (CCMP 2389) and *Synechococcus sp*. (CCMP 2370), *Marine Chemistry*, *125*(1–4), 19-25.

Hughes, C., M. Johnson, R. Utting, S. Turner, G. Malin, A. Clarke, and P. S. Liss (2013), Microbial control of bromocarbon concentrations in coastal waters of the western Antarctic Peninsula, *Marine Chemistry*, *151*(0), 35-46.

Hughes, C., A. L. Chuck, H. Rossetti, P. J. Mann, S. M. Turner, A. Clarke, R. Chance, and P. S. Liss (2009), Seasonal cycle of seawater bromoform and dibromomethane concentrations in a coastal bay on the western Antarctic Peninsula, *Global Biogeochem Cy*, *23*.

Hurrell, J. W., et al. (2006), Atlantic Climate Variability and Predictability: A CLIVAR Perspective, *Journal of Climate*, *19*(20), 5100-5121.

Ittekkot, V., and S. Zhang (1989), Pattern of particulate nitrogen transport in world rivers, *Global Biogeochem Cy*, *3*(4), 383-391.

Jeffrey, S. W., S. W. Wright, and M. Zapata (2011), Microalgal classes and their sigature pigments, in *Phytoplankton Pigments - Characterization,*

chemotaxonomy, and applications in oceanography, edited by S. Roy, C. A. Llewellyn, E. S. Egeland and G. Johnsen, pp. 3 - 77, Cambridge University Press, New York.

Jin, Z., T. P. Charlock, W. L. Smith, and K. Rutledge (2004), A parameterization of ocean surface albedo, *Geophys Res Lett*, *31*(22), L22301.

Johnson, J. E. (1999), Evaluation of a seawater equilibrator for shipboard analysis of dissolved oceanic trace gases, *Analytica Chimica Acta*, *395*(1–2), 119-132.

Johnson, T. L., B. Palenik, and B. Brahamsha (2011), Characterization of a Functional Vanadium-Dependent Bromoperoxidase in the Marine Cyanobacterium Synechococcus Sp. Cc93111, *J Phycol*, *47*(4), 792-801.

Jones, C. E., and L. J. Carpenter (2005), Solar photolysis of CH_2I_2, CH_2ICI, and CH_2IBr in water, saltwater, and seawater, *Environ Sci Technol*, *39*(16), 6130-6137.

Jones, C. E., K. E. Hornsby, R. M. Dunk, R. J. Leigh, and L. J. Carpenter (2009), Coastal measurements of short-lived reactive iodocarbons and bromocarbons at Roscoff, Brittany during the RHaMBLe campaign, *Atmos. Chem. Phys.*, *9*(22), 8757-8769.

Karlsson, A., N. Auer, D. Schulz-Bull, and K. Abrahamsson (2008), Cyanobacterial blooms in the Baltic — A source of halocarbons, *Marine Chemistry*, *110*(3-4), 129-139.

Keller, M. D., R. C. Selvin, W. Claus, and R. R. L. Guillard (1987), Media for the culture of oceanic ultraphytoplankton1,2, *J Phycol*, *23*(4), 633-638.

Kieber, R. J., X. Zhou, and K. Mopper (1990), Formation of carbonyl compounds from UV-induced photodegradation of humic substances in natural waters: fate of riverine carbon in the sea, *Limnology and Oceanography*, *35*(7), 1503-1515.

King, D. B., J. H. Butler, S. A. Montzka, S. A. Yvon-Lewis, and J. W. Elkins (2000), Implications of methyl bromide supersaturations in the temperate North Atlantic Ocean, *J. Geophys. Res.*, *105*(D15), 19763-19769.

Kirk, J. T. O. (1994), *Light and Photosynthesis in Aquatic Ecosystems*, Cambridge Univ. Press, New York.

Kühn, S., and S. Köhler-Rink (2008), pH effect on the susceptibility to parasitoid infection in the marine diatom Coscinodiscus spp. (Bacillariophyceae), *Mar. Biol.*, *154*(1), 109-116.

Kujawinski, E. B. (2010), The impact of microbial metabolism on marine dissolved organic matter, *Annual Review of Marine Science*, *3*(1), 567-599.

Kurylo, M. J., and J. M. Rodriguez (1999), Short-lived ozone related compounds, in *Scientific Assessment of Ozone Depletion, 1998*, edited, pp. 2.1–2.56, Natl. Oceanic and Atmos. Admin., Washington, D. C.

Lapointe, B. E., P. J. Barile, and W. R. Matzie (2004), Anthropogenic nutrient enrichment of seagrass and coral reef communities in the Lower Florida Keys: discrimination of local versus regional nitrogen sources, *Journal of Experimental Marine Biology and Ecology*, *308*(1), 23-58.

Lapointe, B. E., P. J. Barile, M. M. Littler, and D. S. Littler (2005), Macroalgal blooms on southeast Florida coral reefs: II. Cross-shelf discrimination of

nitrogen sources indicates widespread assimilation of sewage nitrogen, *Harmful Algae*, *4*(6), 1106-1122.

Laturnus, F. (1996), Volatile halocarbons released from Arctic macroalgae, *Marine Chemistry*, *55*(3–4), 359-366.

Laturnus, F. (2001), Marine macroalgae in polar regions as natural sources for volatile organohalogens, *Environ Sci Pollut R*, *8*(2), 103-108.

Laturnus, F., C. Wiencke, and H. Klöser (1996), Antarctic macroalgae — Sources of volatile halogenated organic compounds, *Marine Environmental Research*, *41*(2), 169-181.

Law, K. S., and W. T. Sturges (2007), Halogenated very short-lived substances, in *Scientific Assessment of Ozone Depletion: 2006, Global Ozone Research and Monitoring Project - Report No. 50*, edited, World Meteorological Organization, Geneva, Switzerland.

Leboulanger, C., L. Oriol, H. Jupin, and C. Desolas-gros (1997), Diel variability of glycolate in the eastern tropical Atlantic Ocean, *Deep Sea Research Part I: Oceanographic Research Papers*, *44*(12), 2131-2139.

Leboulanger, C., L. Serve, L. Comellas, and H. Jupin (1998a), Determination of glycolic acid released from marine phytoplankton by post-derivatization gas chromatography-mass spectrometry, *Phytochemical Analysis*, *9*(1), 5-9.

Leboulanger, C., V. Martin-Jézéquel, C. Descolas-Gros, A. Sciandra, and H. J. Jupin (1998b), photorespiration in continuous culture of dunaliella tertiolecta (chlorophyta): relationships between serine, glycine, and extracellular glycolate, *J Phycol*, *34*(4), 651-654.

Leri, A. C., J. A. Hakala, M. A. Marcus, A. Lanzirotti, C. M. Reddy, and S. C. B. Myneni (2010), Natural organobromine in marine sediments: New evidence of biogeochemical Br cycling, *Global Biogeochem. Cycles*, *24*(4), GB4017.

Liang, Q., R. S. Stolarski, S. R. Kawa, J. E. Nielsen, A. R. Douglass, J. M. Rodriguez, D. R. Blake, E. L. Atlas, and L. E. Ott (2010), Finding the missing stratospheric Bry: a global modeling study of CHBr3 and CH2Br2, *Atmos. Chem. Phys.*, *10*(5), 2269-2286.

Lin, C. Y. (2011), The Role of Dissolved Organic Matter in the Formation of Polybromomethanes by Marine Algae, 90 pp, California State University, Long Beach, Long Beach, California.

Lin, C. Y., and S. L. Manley (2012), Bromoform production from seawater treated with bromoperoxidase, *Limnology and Oceanography*, *57*(6), 1857 - 1866.

Liu, Y., S. A. Yvon-Lewis, L. Hu, J. E. Salisbury, and J. E. O'Hern (2011), $CHBr_3$, CH_2Br_2, and $CHClBr_2$ in U.S. coastal waters during the Gulf of Mexico and East Coast Carbon cruise, *J Geophys Res*, *116*(C10).

Liu, Y., S. A. Yvon-Lewis, D. C. O. Thornton, L. Campbell, and T. S. Bianchi (2013), Spatial distribution of brominated very short-lived substances in the Eastern Pacific, *Journal of Geophysical Research: Oceans*, 118, doi:10.1002/jgrc.20183..

Liu, Y., D. C. O. Thornton, S. A. Yvon-Lewis, T. S. Bianchi, and M. R. Shields (In prep), DOM drives brominated very short-lived substances production variability and chemical speciation of brominated trihalomethane.

Liu, Y., S. A. Yvon-Lewis, L. Hu, D. C. O. Thornton, T. S. Bianchi, L. Campbell, and R. W. Smith (Submitted), Spatial and temporal distributions of bromoform and dibromomethane in the Atlantic basin, and their relationship with photosynethic biomass.

Lobert, J., J. Butler, S. Yvon, S. Montzka, R. Myers, A. Clarke, and J. Elkins (1996), Blast 94: Bromine Latitudinal Air/Sea Transect, 1994, Report on oceanic measurements of methyl bromide and other compounds*Rep.*, Environ. Res. Lab, Natl. Oceanic and Atmos, Boulder, Colorado.

Lüning, K. (1990), Temperate and polar seaweed vegetation of the southern hemisphere, in *Seaweeds: Their Environment, Biogeography and Eco-physiology*, edited by C. Yarish and H. Kirkman, pp. 235 - 274, Wiley, New York.

Mabey, W., and T. Mill (1978), Critical review of hydrolysis of organic compounds in water under environmental conditions, *Journal of Physical and Chemical Reference Data*, *7*(2), 383-415.

Manley, S. L. (2002), Phytogenesis of halomethanes: A product ofselection or a metabolic accident?, *Biogeochemistry*, *60*(2), 163-180.

Manley, S. L., and P. E. Barbero (2001), Physiological constraints on bromoform (CHBr3) production by Ulva lactuca (Chlorophyta), *Limnology and Oceanography*, *46*(6), 1392-1399.

Manley, S. L., K. Goodwin, and W. J. North (1992), Laboratory production of bromoform, methylene bromide, and methyl-iodide by macroalgae and

distribution in nearshore southern california waters, *Limnology and Oceanography*, *37*(8), 1652 - 1659.

Mattson, E., A. Karlsson, J. W. O. Smith, and K. Abrahamsson (2012), The relationship between biophysical variables and halocarbon distributions in the waters of the Amundsen and Ross Seas, Antarctica, *Marine Chemistry*, *140–141*(0), 1-9.

McCarthy, M., J. Hedges, and R. Benner (1996), Major biochemical composition of dissolved high molecular weight organic matter in seawater, *Marine Chemistry*, *55*(3–4), 281-297.

McElroy, M. B., R. J. Salawitch, S. C. Wofsy, and J. A. Logan (1986), Reductions of Antarctic ozone due to synergistic interactions of chlorine and bromine, *Nature*, *321*(6072), 759-762.

McLachlan, J. (1985), Macroalgae (seaweeds): industrial resources and their utilization, *Plant Soil*, *89*(1-3), 137-157.

Miller, W. L., and R. G. Zepp (1995), Photochemical production of dissolved inorganic carbon from terrestrial organic matter: Significance to the oceanic organic carbon cycle, *Geophys. Res. Lett.*, *22*(4), 417-420.

Miller, W. L., M. A. Moran, W. M. Sheldon, R. G. Zepp, and S. Opsahl (2002), Determination of apparent quantum yield spectra for the formation of biologically labile photoproducts, *Limnology and Oceanography*, *47*(2), 343-352.

Millero, F. J. (1974), Seawater as a multicomponent electrolyte solution, in *The Sea*, edited by E. D. Goldberg, pp. 3-80, Wiley, New York, NY.

Millero, F. J., and A. Poisson (1981), International one-atmosphere equation of state of seawater, *Deep Sea Research Part A. Oceanographic Research Papers*, *28*(6), 625-629.

Montzka, S. A., and S. Reimann (2011), Ozone-Depleting Substances (ODSs) and Related Chemicals, in *Scientific Assessment of Ozone Depletion: 2010, Global Ozone Research and Monitoring Project, Report No. 52*, edited, World Meteorological Organization, Geneva, Switzerland.

Moore, R. M. (2003), Marine sources of volatile organohalogens, in *Natural Production of Organohalogen Compounds*, edited by G. Gribble, pp. 56-56, Springer Berlin / Heidelberg.

Moore, R. M., and R. Tokarczyk (1993), Volatile biogenic halocarbons in the Northwest Atlantic, *Global Biogeochem Cy*, *7*(1), 195-210.

Moore, R. M., C. E. Geen, and V. K. Tait (1995a), Determination of Henry's Law constants for a suite of naturally occurring halogenated methanes in seawater, *Chemosphere*, *30*(6), 1183-1191.

Moore, R. M., M. Webb, R. Tokarczyk, and R. Wever (1996), Bromoperoxidase and iodoperoxidase enzymes and production of halogenated methanes in marine diatom cultures, *J Geophys Res-Oceans*, *101*(C9), 20899-20908.

Moore, R. M., R. Tokarczyk, V. K. Tait, M. Poulin, and C. Geen (1995b), Marine phytoplankton as a natural source of volatile organohalogens, *Environ Chem*, *1*, 283-294.

Mopper, K., and C. A. Schultz (1993), Fluorescence as a possible tool for studying the nature and water column distribution of DOC components, *Marine Chemistry*, *41*(1-3), 229-238.

Mopper, K., Z. Feng, S. B. Bentjen, and R. F. Chen (1996), Effects of cross-flow filtration on the absorption and fluorescence properties of seawater, *Marine Chemistry*, *55*(1-2), 53-74.

Mopper, K., X. Zhou, R. J. Kieber, D. J. Kieber, R. J. Sikorski, and R. D. Jones (1991), Photochemical degradation of dissolved organic carbon and its impact on the oceanic carbon cycle, *Nature*, *353*(6339), 60-62.

Moran, M. A., W. M. Sheldon, Jr., and R. G. Zepp (2000), Carbon loss and optical property changes during long-term photochemical and biological degradation of estuarine dissolved organic matter, *Limnology and Oceanography*, *45*(6), 1254-1264.

Nelson, N. B., and D. A. Siegel (2002), Chromophoric DOM in the open ocean, in *Biogeochemistry of Marine Dissolved Organic Matter*, edited by D. A. Hansell and C. A. Carlson, pp. 547–578, Academic Press, San Diego, California.

Nielsen, J. E., and A. R. Douglass (2001), A simulation of bromoform's contribution to stratospheric bromine, *Journal of Geophysical Research: Atmospheres*, *106*(D8), 8089-8100.

Nieuwenhuijsen, M. J., M. B. Toledano, N. E. Eaton, J. Fawell, and P. Elliott (2000), Chlorination disinfection byproducts in water and their association with adverse reproductive outcomes: a review, *Occupational and Environmental Medicine*, *57*(2), 73-85.

Nightingale, P. D., G. Malin, C. S. Law, A. J. Watson, P. S. Liss, M. I. Liddicoat, J. Boutin, and R. C. Upstill-Goddard (2000), In situ evaluation of air-sea gas exchange parameterizations using novel conservative and volatile tracers, *Global Biogeochem Cy*, *14*(1), 373-387.

Ohsawa, N., Y. Ogata, N. Okada, and N. Itoh (2001), Physiological function of bromoperoxidase in the red marine alga, *Corallina pilulifera*: production of bromoform as an allelochemical and the simultaneous elimination of hydrogen peroxide, *Phytochemistry*, *58*(5), 683-692.

Oliver, B. G., and E. M. Thurman (1983), Influence of aquatic humic substance properties on trihalomethane potential, *Water Chlorination: Environmental Impact and Health Effects*, *4*.

Ordóñez, C., J. F. Lamarque, S. Tilmes, D. E. Kinnison, E. L. Atlas, D. R. Blake, G. Sousa Santos, G. Brasseur, and A. Saiz-Lopez (2011), Bromine and iodine chemistry in a global chemistry-climate model: description and evaluation of very short-lived oceanic sources, *Atmos. Chem. Phys. Discuss.*, *11*(10), 27421-27474.

Ortiz-Bermudez, P., E. Srebotnik, and K. E. Hammel (2003), Chlorination and Cleavage of Lignin Structures by Fungal Chloroperoxidases, *Appl. Environ. Microbiol.*, *69*(8), 5015-5018.

Ortiz-Bermúdez, P., K. C. Hirth, E. Srebotnik, and K. E. Hammel (2007), Chlorination of lignin by ubiquitous fungi has a likely role in global organochlorine production, *Proceedings of the National Academy of Sciences*, *104*(10), 3895-3900.

Palma, M., E. Quiroga, V. A. Gallardo, W. Arntz, D. Gerdes, W. Schneider, and D. Hebbeln (2005), Macrobenthic animal assemblages of the continental margin off Chile (22° to 42°S), *Journal of the Marine Biological Association of the United Kingdom*, *85*(02), 233-245.

Pickard, G. L. (1990), *Descriptive physical oceanography :an introduction /by George L. Pickard and William J. Emery*, Pergamon Press, Oxford ;New York.

Quack, B., and D. W. R. Wallace (2003), Air-sea flux of bromoform: Controls, rates, and implications, *Global Biogeochem. Cycles*, *17*(1), 1023.

Quack, B., I. Peeken, G. Petrick, and K. Nachtigall (2007a), Oceanic distribution and sources of bromoform and dibromomethane in the Mauritanian upwelling, *J. Geophys. Res.*, *112*(C10), C10006.

Quack, B., E. Atlas, G. Petrick, and D. W. R. Wallace (2007b), Bromoform and dibromomethane above the Mauritanian upwelling: Atmospheric distributions and oceanic emissions, *J. Geophys. Res.*, *112*(D9), D09312.

Quack, B., E. Atlas, G. Petrick, V. Stroud, S. Schauffler, and D. W. R. Wallace (2004), Oceanic bromoform sources for the tropical atmosphere, *Geophys. Res. Lett.*, *31*(23), L23S05.

Raimund, S., B. Quack, Y. Bozec, M. Vernet, V. Rossi, V. Garcon, Y. Morel, and P. Morin (2011), Sources of short-lived bromocarbons in the Iberian upwelling system, *Biogeosciences*, *8*(6), 1551-1564.

Ram, N. M., Y. G. Mussalli, and C. Winston (1990), Total Trihalomethane Formation during targeted and conventional chlorination of seawater for biofouling

control, *Research Journal of the Water Pollution Control Federation*, *62*(6), 789-795.

Reckhow, D. A., P. C. Singer, and R. L. Malcolm (1990), Chlorination of humic materials: byproduct formation and chemical interpretations, *Environ Sci Technol*, *24*(11), 1655-1664.

Redeker, K. R., S. Meinardi, D. Blake, and R. Sass (2003), Gaseous emissions from flooded rice paddy agriculture, *J Geophys Res-Atmos*, *108*(D13).

Remsen, C. C. (1971), The distribution of urea in coastal and oceanic waters, *Limnology and Oceanography*, *16*(5), 732-740.

Ríos, C., W. Arntz, D. Gerdes, E. Mutschke, and A. Montiel (2007), Spatial and temporal variability of the benthic assemblages associated to the holdfasts of the kelp *Macrocystis pyrifera* in the Straits of Magellan, Chile, *Polar Biology*, *31*(1), 89-100.

Rook, J. J. (1974), Formation of haloforms during chlorination of natural waters, *Journal of water treatment examination*, *23* (2).

Rook, J. J. (1976), Haloforms in Drinking-Water, *J Am Water Works Ass*, *68*(3), 168-172.

Roy, R. (2010), Short-term variability in halocarbons in relation to phytoplankton pigments in coastal waters of the central eastern Arabian Sea, *Estuarine, Coastal and Shelf Science*, *88*(3), 311-321.

Roy, R., A. Pratihary, G. Narvenkar, S. Mochemadkar, M. Gauns, and S. W. A. Naqvi (2011), The relationship between volatile halocarbons and phytoplankton

pigments during a Trichodesmium bloom in the coastal eastern Arabian Sea, *Estuarine, Coastal and Shelf Science*.

Rush, C., A. Willetts, G. Davies, Z. Dauter, H. Watson, and J. Littlechild (1995), Purification, crystallisation and preliminary X-ray analysis of the vanadium-dependent haloperoxidase from Corallina officinalis, *Febs Lett*, *359*(2–3), 244-246.

Salawitch, R. J. (2006), Atmospheric chemistry: Biogenic bromine, *Nature*, *439*(7074), 275-277.

Sandy, M., J. N. Carter-Franklin, J. D. Martin, and A. Butler (2011), Vanadium bromoperoxidase from *Delisea pulchra*: enzyme-catalyzed formation of bromofuranone and attendant disruption of quorum sensing, *Chem Commun*, *47*(44), 12086-12088.

Sarmiento, J. L., and N. Gruber (2006), *Ocean biogeochemical dynamics /Jorge L. Sarmiento and Nicolas Gruber*, Princeton University Press, Princeton, N.J.

Schall, C., K. G. Heumann, and G. O. Kirst (1997), Biogenic volatile organoiodine and organobromine hydrocarbons in the Atlantic Ocean from 42°N to 72°S, *Fresenius' Journal of Analytical Chemistry*, *359*(3), 298-305.

Schmidtko, S., and G. C. Johnson (2011), Multidecadal warming and shoaling of Antarctic Intermediate Water*, *Journal of Climate*, *25*(1), 207-221.

Searles, R. B. (1984), Seaweed biogeography of the mid-Atlantic coast of the United States, *Helgolander Meeresunters*, *38*(2), 259-271.

Sinnhuber, B. M., and I. Folkins (2006), Estimating the contribution of bromoform to stratospheric bromine and its relation to dehydration in the tropical tropopause layer, *Atmos. Chem. Phys.*, *6*(12), 4755-4761.

Sinnhuber, B. M., et al. (2002), Comparison of measurements and model calculations of stratospheric bromine monoxide, *Journal of Geophysical Research: Atmospheres*, *107*(D19), 4398.

Sivey, J. D., J. S. Arey, P. R. Tentscher, and A. L. Roberts (2013), Reactivity of BrCl, Br_2, BrOCl, Br_2O, and HOBr toward dimethenamid in solutions of bromide + aqueous free chlorine, *Environ Sci Technol*, *47*(3), 1330-1338.

Soedjak, H. S., and A. Butler (1990), Chlorination catalyzed by vanadium bromoperoxidase, *Inorg Chem*, *29*(25), 5015-5017.

Solomon, S., D. Wuebbles, I. Isaksen, J. Kiehl, M. Lal, P. Simon, and N. Sze (1995), Ozone depletion potentials, global warming potentials, and future chlorine/bromine loading, in *Scientific assessment of ozone depletion: 1994, Global Ozone Research and Monitoring Project, Report No. 37*, edited, Geneva, Switzerland.

Spitzy, A., and V. Ittekkot (1991), Dissolved and particulate organic matter in rivers, *Ocean margin processes in global change. Report, Dahlem workshop, Berlin, 1990*, 5-17.

Stubbins, A., C. S. Law, G. Uher, and R. C. Upstill-Goddard (2011), Carbon monoxide apparent quantum yields and photoproduction in the Tyne estuary, *Biogeosciences*, *8*(3), 703-713.

Stubbins, A., V. Hubbard, G. Uher, C. S. Law, R. C. Upstill-Goddard, G. R. Aiken, and K. Mopper (2008), Relating carbon monoxide photoproduction to dissolved organic matter functionality, *Environ Sci Technol*, *42*(9), 3271-3276.

Sturges, W. T., G. F. Cota, and P. T. Buckley (1992), Bromoform emission from arctic ice algae, *Nature*, *358*(6388), 660-662.

Sturges, W. T., C. W. Sullivan, R. C. Schnell, L. E. Heidt, and W. H. Pollock (1993), Bromoalkane production by Antarctic ice algae, *Tellus B*, *45*(2), 120-126.

Sweeney, C., E. Gloor, A. R. Jacobson, R. M. Key, G. McKinley, J. L. Sarmiento, and R. Wanninkhof (2007), Constraining global air-sea gas exchange for CO2 with recent bomb 14C measurements, *Global Biogeochem Cy*, *21*(2).

Talley, L. D. (1997), North Pacific Intermediate Water Transports in the mixed water region, *Journal of Physical Oceanography*, *27*(8), 1795-1803.

Tareq, S. M., N. Tanaka, and K. Ohta (2004), Biomarker signature in tropical wetland: lignin phenol vegetation index (LPVI) and its implications for reconstructing the paleoenvironment, *Sci Total Environ*, *324*(1–3), 91-103.

Theiler, R., C. J.C., H. L.P., and S. J.F., JEROME F. (1978), Halohydrocarbon synthesis by bromoperoxidase, *Science*, *202*(4372), 1094-1096.

Tokarczyk, R., and R. M. Moore (1994), Production of volatile organohalogens by phytoplankton cultures, *Geophys Res Lett*, *21*(4), 285-288.

Valentine, R. L., and R. G. Zepp (1993), Formation of carbon monoxide from the photodegradation of terrestrial dissolved organic carbon in natural waters, *Environ Sci Technol*, *27*(2), 409-412.

Varela, O. (2003), Oxidative reactions and degradations of sugars and polysaccharides, in *Advances in Carbohydrate Chemistry and Biochemistry*, edited, pp. 307-369, Academic Press.

Vaulot, D. (1989), processing software for flow cytometric data, *CYTOPC*, *Signal Noise 2:8.*

Vinson, J. A., X. Su, L. Zubik, and P. Bose (2001), Phenol antioxidant quantity and quality in foods: Fruits, *Journal of Agricultural and Food Chemistry*, *49*(11), 5315-5321.

Vogel, T. M., C. S. Criddle, and P. L. McCarty (1987), ES Critical Reviews: Transformations of halogenated aliphatic compounds, *Environ Sci Technol*, *21*(8), 722-736.

von Glasow, R., R. von Kuhlmann, M. G. Lawrence, U. Platt, and P. J. Crutzen (2004), Impact of reactive bromine chemistry in the troposphere, *Atmos. Chem. Phys.*, *4*(11/12), 2481-2497.

Wamsley, P. R., et al. (1998), Distribution of halon-1211 in the upper troposphere and lower stratosphere and the 1994 total bromine budget, *J Geophys Res-Atmos*, *103*(D1), 1513-1526.

Wanninkhof, R. (1992), Relationship between wind speed and gas exchange over the ocean, *J. Geophys. Res.*, *97*(C5), 7373-7382.

Warwick, N. J., J. A. Pyle, G. D. Carver, X. Yang, N. H. Savage, F. M. O'Connor, and R. A. Cox (2006), Global modeling of biogenic bromocarbons, *J Geophys Res*, *111*(D24).

Washington, J. W. (1995), Hydrolysis rates of dissolved volatile organic compounds: principles, temperature effects and literature review, *Ground Water*, *33*(3), 415-424.

Watanabe, Y. W., K. Harada, and K. Ishikawa (1994), Chlorofluorocarbons in the central North Pacific and southward spreading time of North Pacific intermediate water, *J. Geophys. Res.*, *99*(C12), 25195-25213.

Waterbury, J. B., S. W. Watson, R. R. L. Guillard, and L. E. Brand (1979), Widespread occurrence of a unicellular, marine, planktonic, cyanobacterium, *Nature*, *277*(5694), 293-294.

Weiss, P. S., S. S. Andrews, J. E. Johnson, and O. C. Zafiriou (1995), Photoproduction of carbonyl sulfide in South Pacific Ocean waters as a function of irradiation wavelength, *Geophys. Res. Lett.*, *22*(3), 215-218.

Weiss, R. F., and B. A. Price (1980), Nitrous oxide solubility in water and seawater, *Marine Chemistry*, *8*(4), 347-359.

Wever, R. (2012), Structure and function of vanadium haloperoxidases, *Vanadium*, edited by H. Michibata, pp. 95-125, Springer Netherlands.

Wever, R., and M. A. Van der Horst (2013), The role of vanadium haloperoxidases in the formation of volatile brominated compounds and their impact on the environment, *Dalton Transactions*.

Wever, R., M. G. M. Tromp, B. E. Krenn, A. Marjani, and M. Van Tol (1991), Brominating activity of the seaweed *Ascophyllum nodosum*: impact on the biosphere, *Environ Sci Technol*, *25*(3), 446-449.

Wever, R., M. G. M. Tromp, J. W. P. M. Vanschijndel, E. Vollenbroek, R. L. Olsen, and E. Fogelqvist (1993), Bromoperoxidases - Their role in the formation of hobr and bromoform by seaweeds, *Biogeochemistry of Global Change*, 811-824.

Winter, J. M., and B. S. Moore (2009), Exploring the chemistry and biology of vanadium-dependent haloperoxidases, *J Biol Chem*, *284*(28), 18577-18581.

WMO (2003), Scientific Assessment of Ozone Depletion: 2002, Global Ozone Res. Monit. Proj. Rep. 47*Rep.*, World Meteorological Organization Geneva, Switzerland.

WMO (2007), Scientific Assessment of Ozone Depletion: 2006, Global Ozone Res. Monit. Proj. Rep. 50*Rep.*, World Meteorological Organization Geneva, Switzerland.

Wright, S. W., and S. Jeffrey (2006), Pigment markers for phytoplankton production in *marine organic matter: Biomarkers, Isotopes and DNA*, edited by J. Volkman, pp. 71-104, Springer Berlin / Heidelberg, Berlin / Heidelberg.

Wright, S. W., S. W. Jeffrey, R. F. C. Mantoura, C. A. Llewellyn, T. Bjornland, D. Repeta, and N. Welschmeyer (1991), Improved HPLC method for the analysis of chlorophylls and carotenoids from marine-phytoplankton, *Mar Ecol-Prog Ser*, *77*(2-3), 183-196.

Yang, X., R. A. Cox, N. J. Warwick, J. A. Pyle, G. D. Carver, F. M. O'Connor, and N. H. Savage (2005), Tropospheric bromine chemistry and its impacts on ozone: A model study, *Journal of Geophysical Research: Atmospheres*, *110*(D23), D23311.

Yokouchi, Y., et al. (2005), Correlations and emission ratios among bromoform, dibromochloromethane, and dibromomethane in the atmosphere, *J. Geophys. Res.*, *110*(D23), D23309.

Yvon-Lewis, S. A., K. D.B., T. R., G. K.D., S. E.S., and B. J.H. (2004), Methyl bromide and methyl chloride in the Southern Ocean, *J Geophys Res*, *109*(C2).

Zafiriou, O. C., S. S. Andrews, and W. Wang (2003), Concordant estimates of oceanic carbon monoxide source and sink processes in the Pacific yield a balanced global "blue-water"; CO budget, *Global Biogeochem. Cycles*, *17*(1), 1015.

Zafiriou, O. C., J. Joussot-Dubien, R. G. Zepp, and R. G. Zika (1984), Photochemistry of natural waters, *Environ Sci Technol*, *18*(12), 358A-371A.

Zehr, J. P., and B. B. Ward (2002), Nitrogen Cycling in the Ocean: New Perspectives on Processes and Paradigms, *Appl. Environ. Microbiol.*, *68*(3), 1015-1024.

Zepp, R. G., T. V. Callaghan, and D. J. Erickson (1998), Effects of enhanced solar ultraviolet radiation on biogeochemical cycles, *Journal of Photochemistry and Photobiology B: Biology*, *46*(1–3), 69-82.

Zepp, R. G., D. J. Erickson Iii, N. D. Paul, and B. Sulzberger (2007), Interactive effects of solar UV radiation and climate change on biogeochemical cycling, *Photochemical & Photobiological Sciences*, *6*(3).

Zhou, Y., R. K. Varner, R. S. Russo, O. W. Wingenter, K. B. Haase, R. Talbot, and B. C. Sive (2005), Coastal water source of short-lived halocarbons in New England, *Journal of Geophysical Research: Atmospheres*, *110*(D21), D21302.

Zhou, Y., H. T. Mao, R. S. Russo, D. R. Blake, O. W. Wingenter, K. B. Haase, J. Ambrose, R. K. Varner, R. Talbot, and B. C. Sive (2008), Bromoform and

dibromomethane measurements in the seacoast region of New Hampshire, 2002-2004, *J Geophys Res-Atmos*, *113*(D8).

Zika, R. G., P. J. Milne, and O. C. Zafiriou (1993), Photochemical Studies of the Eastern Caribbean: An Introductory Overview, *J. Geophys. Res.*, *98*(C2), 2223-2232.

APPENDIX

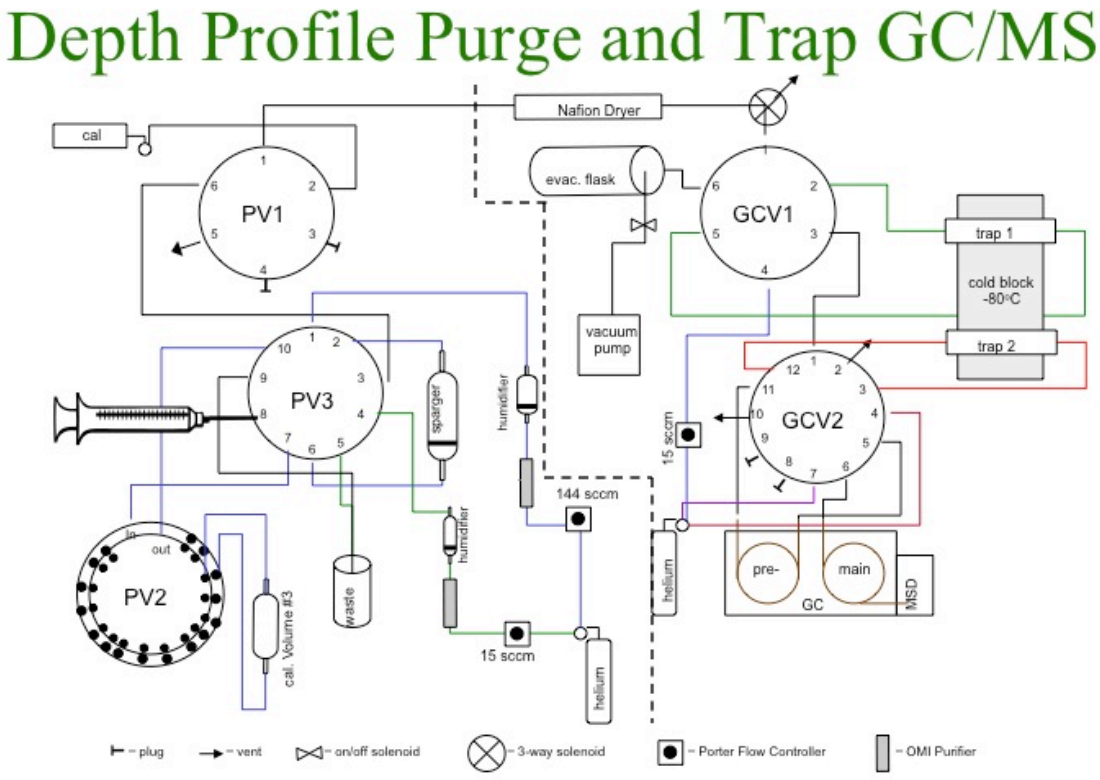

Figure A-1. Schematic of the purge and trap analytical system, used for depth profile and V-BrPO treated DOM studies.

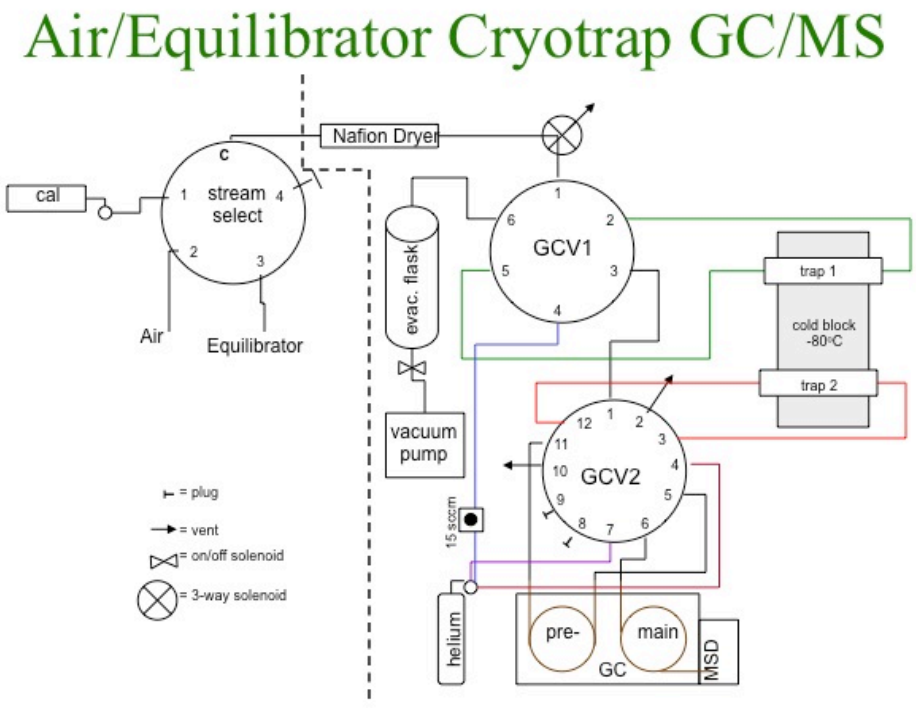

Figure A-2. Schematic of the stream select analytical system, used for continues air and equilibrator measurements and phytoplankton culture studies.